2014-02-12

Recovery Time between Multiple Mild Photothrombotic Strokes Affects Brain Damage

Deng, Qinbo

UNIVERSITY OF CALGARY

Recovery Time between Multiple Mild Photothrombotic Strokes Affects Brain Damage

by

Qinbo Deng

A THESIS

SUBMITTED TO THE FACULTY OF GRADUATE STUDIES

IN PARTIAL FULFILMENT OF THE REQUIREMENTS FOR THE

DEGREE OF MASTER OF SCIENCE

DEPARTMENT OF NEUROSCIENCE

CALGARY, ALBERTA

JANUARY, 2014

Abstract

Prior to stroke, patients often experience a transient ischemic attack (TIA) or minor stroke with a high recurrence within the first week. The initial episode of ischemia, traditionally considered to causing little permanent damage to brain, is poorly understood for its role in subsequent ischemic events. We hypothesized that despite functional recovery following TIA/minor stroke, there can be sparse tissue damage that alters the brain response to a secondary mild stroke, with the final tissue fate being dependent on the recovery time between recurrent strokes.

Thus, the first objective of this thesis was to establish a rat model of TIA/minor stroke using modifications of a phothothrombotic (PT) occlusion of the cerebral microvasculature. The effect of varied light intensities and illumination durations were examined on the severity of stroke. Multiple sequences (T2, Apparent Diffusion Coefficient (ADC), Perfusion Weighted Imaging) of Magnetic Resonance Imaging (MRI) were performed to evaluate the tissue damage. We found that a 5-min illumination at approximate 35,000 Lux of light intensity was optimal to produce a mild tissue damage associated with a transient ischemia measured by Laser-Doppler Flowmetry. The T2 signatures measured at 24h were good predictors of graded ischemic injury confirmed by histology. Compared with ADC measures, T2 provided a better diagnosis of mild damage (scattered necrosis).

The second objective was to use this modified PT model to produce a recurrent stroke and to investigate if the outcome differed depending on the interval between insults – i.e. 1day, 2days, 3days and 1week. Using this novel model, we demonstrated that a mild recurrent stroke produced more deleterious injury with acute intervals (1 day

to 3 day) than a subacute one (1week). This enhancement of damage was characterized by an increase of T2 and a decrease of perfusion. In contrast, the 1week interval produced tissue damage similar to a single mild stroke, associated with similar changes of MR. Together, our finding revealed a temporal change of brain susceptibility to ischemia, implying the importance of early treatment after TIA/minor stroke for reduction of damage with stroke recurrence.

Acknowledgements

First, I would like to express my sincere gratitude and respect to my supervisor Dr. Ursula I. Tuor for her continuous support and for her encouragement during the period of my master's study. I thank her greatly for her original suggestions for this project, for her patience and guidance of writing the thesis, and, for her dedicated attitude towards academic research. Dr. Tuor has been a wonderful mentor for my research and my personal life. I could not be the person I currently am without her. I am so grateful and happy for the opportunity of working in this lab for the past two years. The things I learned from her will provide treasures for my future life.

Besides my supervisor, my sincere thanks go to my thesis committee, Dr. Grant Gordon and Dr. Richard Dyck, for their insightful comments and suggestions for the completion of this thesis.

This thesis contains a large body of MRI result. Tadeusz Foniok, David Rushforth, and former staff Dave Kirk, who are the experienced staffs in Experimental Imaging Center (EIC) at university, would be given the most credits for their outstanding and professional work on MRI scans.

I would also like to thank Min Qiao, who taught me a lot about surgery and experiments. She was always kind and patient regarding my questions and was always there when I needed help. She is one of the greatest persons I've worked with. Working with her has been an unforgettable journey and memory. Her passion and enthusiasm helped me through the toughest times of research. My thanks also go to Zonghang Zhao and my fellow lab members Melissa Morgonv and Manasi Sule. I appreciate all of you for your help and all the fun we have had together.

I am also thankful to all of my friends that I made in Calgary: Yingjie Liu, Luyao Xiu and Jeanie Quanch and many others that I cannot all mention. Their company excited me and brought sparkles to my life in Calgary.

Last but not least, my sincere gratitude goes to my family, both in Calgary and in China: my cousin Lin, my brother in-law Alden and aunt Xiulu for their help from all aspects; my new-born niece, Alexis, for the happiness she brought to me; my parents in China, for their deepest love and enormous confidence in me. I hope I am worth your pride. Finally, I would particularly thank my grandparents who were the initial driving force for me to receive a better education in Canada. My grandma's last wish was for me to pursue study abroad. Unfortunately she forever left me just one week after I arrived in Canada without a chance to see me achieve the goal.

I will always remember everyone I mentioned above, because without you, I am a lesser person.

Dedication

This master thesis is dedicated to my dearest grandma and my mother, who has suffered sickness during the past weeks yet strongly comforted me and encouraged me to complete this work. I wish this piece of work to be a precious gift for her.

Table of Contents

List of Tables

List of Figures and Illustrations

List of Symbols, Abbreviations and Nomenclature

Symbol	Definition
TIA	Transient Ischemic Attack
MRI	Magnetic Resonance Imaging
9.4T	9.4 Telsa
PT	Photothrombosis
MCAO	Middle Cerebral Artery Occlusion
CCAO	Common Carotid Artery Occlusion
RF	Radiofrequency
T2	T2 Relaxation Time
M_o	Magnetization
B	Magnetic Field
ω_0	Larmar Frequency
T2WI	T_2-weighted Imaging
DWI	Diffusion-weighted Imaging
ADC	Apparent Diffusion Coefficient
PWI	Perfusion-weighted Imaging
ROI	Region of Interest
TE	Echo Time
TR	Repetition Time
H&E	Haematoxylin and Eosin staining
CBF	Cerebral Blood Flow
BBB	Blood Brain Barrier
ATP	Adenosine triphosphate
NMDA	N-methyl-D-aspartate
EPO	Erythropoietin
VEGF	Vascular Endothelial Growth Factor
Na^+	Sodium Iron
K^+	Potassium Iron
a1	Area 1
a2	Area 2
a3	Area 3
i.v.	intravenous
m.c.	Middle Caudate level
p.c.	Post Caudate level
ant hp	Anterior Hippocampus level
hp	Hippocampus level

Chapter One: Introduction

1.1 Ischemic Stroke

Every year, stroke affects nearly 800,000 people in the United States [1], killing approximately 150,000 according to the American Heart Association [2]. Strokes are categorized as haemorrhagic or ischemic/occlusive, with up to 85% of strokes being ischemic in adults whereas 55% are ischemic in children [3]. An ischemic stroke occurs as a result of a feeding artery to the brain being occluded for a certain period of time. Since the supply of oxygen and glucose to the brain is impaired due to occlusion, neuronal dysfunction begins. After stroke onset, the immediate response is the cessation of neuronal electrical activity [4]. Along with electrical failure, the cell lacks energy substrates and develops hypoxemia, leading to the depletion of cellular adenosine triphosphate (ATP), a major source of energy utilized in normal brain function [5]. As a result, the membrane potentials cannot be maintained and a depolarization of neurons occurs, which then triggers the release of glutamate into the extracellular space. The increase in glutamate is fatal to the cell, referred to as "excitotoxicity". This is because the high levels of extracellular glutamate activate amino-3-hydroxy-5-methyl-4-isoxazole propionic acid (AMPA), N-methyl-D-aspartate (NMDA), and kainite receptors [6-8], leading to an influx of sodium and calcium ions. Water passively flows into the cell, leading to brain edema and exacerbating the tissue damage. Elevated intracellular calcium results in the activation of proteolytic enzymes, leading to the development of oxygen free radicals that disrupt mitochondrial membranes and promote tissue injury. A downstream cascade of events that include lipolysis and

proteolysis are triggered which contribute to the ensuing cell death in the form of necrosis or apoptosis [9, 10].

Adjacent to the ischemic core is a region of compromised blood flow and suppressed protein synthesis, called the "penumbra" first described by Astrup [11]. The penumbral area is thought of as either tissue-at-risk or salvageable tissue depending on whether timely reperfusion or therapeutic intervention can be exerted. Though reperfusion can rescue the structural and functional integrity of the penumbra, several studies have demonstrated the presence of selective neuronal necrosis in this area that cannot be detected by conventional Magnetic Resonance Image (MRI) techniques because the ischemia is very brief that the affected tissue does not develop into infarction [12, 13]. The temporal evolution of cell death in the penumbra is complicated and highly dynamic based on the magnitude and duration of ischemia before reperfusion. In an early study in monkeys, tissue with a milder degree of hypoperfusion had a therapeutic window of 3 hours before necrosis occurred, whereas a severe degree of hypoperfusion preserved the brain from necrosis after only 2 hours of ischemia [14]. A complete cessation of flow irreversibly affected tissue producing an infarct within 25 min of stroke onset [15]. However, complete deprivation of flow is uncommon in focal ischemia since collateral blood flow can contribute to partial preservation of the affected region [16].

1.1.1 Blood Flow Thresholds for Neuronal Disturbance

Normal CBF in the cortex is approximately 50 mL/100 g brain tissue/min. After the onset of stroke, the blood flow deprivation occurs in a graded fashion (Figure 1.1.1). In the core region, the blood flow can drop to less than 10mL/100g/min where irreversible damage occurs. In the peri-infarct or penumbral region, a moderate reduction

of blood flow (<20 mL/100g/min) is present. Cerebral dysfunction occurs but with a possibility for recovery following the resumption of blood flow [11]. Tissue outside the penumbra with a mild hypoperfusion is considered not at risk of infarction [17]. Electrical activity is one of the first impaired functions as a result of CBF decline [18]. Protein synthesis inhibition occurs when the flow drops below 50% of baseline [19, 20]. The extent of protein inhibition is related to the magnitude and duration of ischemia, and as much as 80% of protein synthesis can be blocked [21]. In contrast, ATP depletion is least sensitive to perfusion impairment, occurring when blood flow declines to 20%. Thus, the different thresholds for various biochemical and molecular processes lead to the concept of the "silent neuron". That is, the neuron is functionally inactive with structural preservation.

Figure 1.1.1 Diagram of CBF threshold for specific functional and biochemical events.

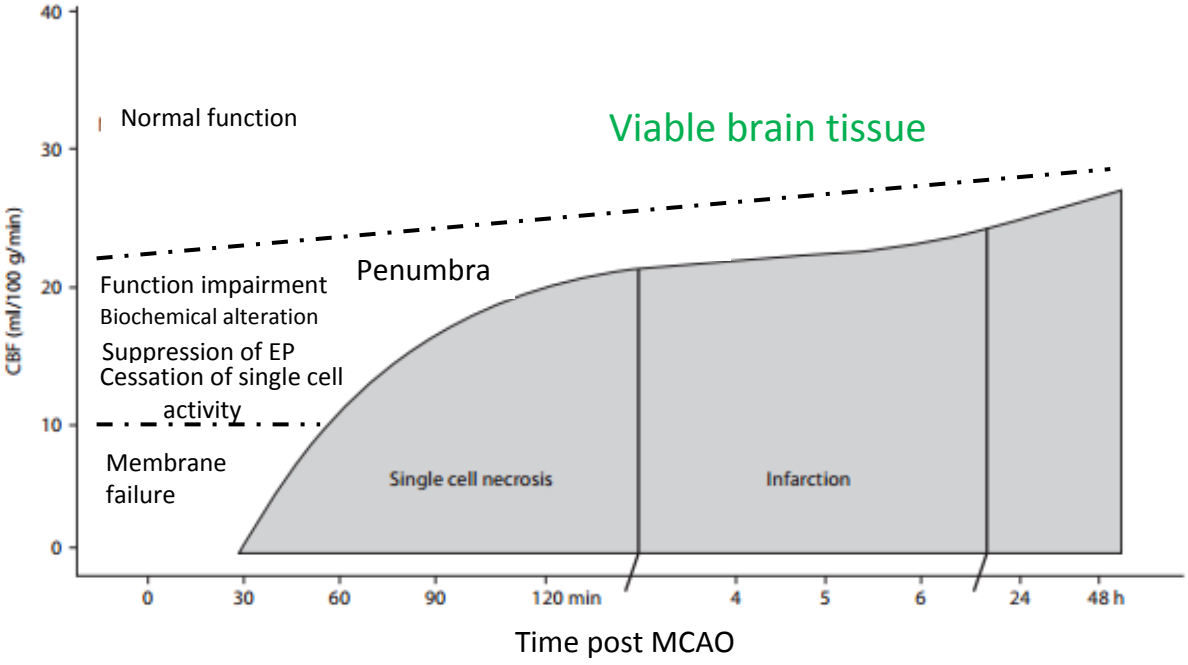

Neuronal disturbance begins as the flow drops below a certain level (dashed line). Two thresholds are represented: there is functional and electrical impairment occurring as CBF <20ml/100g/min, and there are structural alterations as CBF <10ml/100g/min. Prolonged ischemia with mild hypoperfusion or severe CBF impairment with short duration can switch the penumbra into infarct (Modified from Heiss [15] with permission). EP: Evoked Potential.

1.1.2 Necrosis and Apoptosis

Histologically, there are two forms of cell death based on morphological assessments [22]. One is necrosis, which is characterized by an appearance of pyknosis of the nucleus and breakdown of cellular membranes and cellular organelles. Necrosis is a common feature of neuronal death in cerebral ischemic stroke. Another pattern of death is apoptosis, first described by John Kerr and associates [23]. The typical apoptotic changes are characterized by membrane blebbing, chromatin condensation, and an apoptotic appearance of the cell body (the cell is compartmentalized into several vesicles). Unlike necrosis, apoptotic cell death can be seen during the entire lifetime of living creatures. The apoptotic pathway is an ordered or “programmed” process inside the cell. So it is considered as cell suicide or cell autonomous defense not to influence the neighbour cells, differing from the necrotic process which is associated with a post-ischemic inflammatory response.

There is evidence that the fate of a cell is determined by the availability of a residual supply of ATP post ischemia [24]. This is because the ischemia-induced apoptotic signaling is an energy dependent process initiated by the activation of certain regulatory

proteins that control the apoptosis pathway, such as caspases, cytochrome c and apoptosis-inducing factor (AIF) [25].

Apoptosis is most often seen in the ischemic penumbra because the blood flow in this region is able to maintain the energy demand for those "cell death or injurious proteins" to initiate apoptotic signaling. Thus, therapeutic intervention, such as thrombolytic agents, for reperfusion of tissue which can prevent the growth of infarction and cellular necrosis, may not stop the cell death in the form of apoptosis, i.e. a "delayed selective neuronal loss". Apoptosis is accompanied by activation of caspases (mainly caspase-3) [26]. With the inhibition of caspase-3, the pathway of apoptosis can be halted in the penumbra, and this provides an explanation of the salvageable nature of this region.

In the ischemic core, if the blood supply is severely diminished leading to a malfunction of K^+/Na^+ pumps and a lack of ATP being supplied to the neurons, then neurons undergo the process of necrosis [27, 28]. Twenty four hours following a 30 min complete occlusion of a middle cerebral artery branch supplying the barrel cortex, there are a large number of necrotic cells in the ischemic cortex which continue to increase in number and reach a peak at 3d post insult [28].

Along with the occurrence of the depletion and restoration of cerebral blood flow, the corresponding cell death may shift from apoptosis to necrosis with the worsening of CBF or from necrosis to apoptosis when the CBF is restored. Thus, in individual neurons, the neuronal injury can present a mixed form, termed a "hybrid cell death" with both an apoptotic and necrotic appearance [28].

1.1.3 Recovery

Studies from experimental and clinical stroke reveal that the ischemic injury, which initially occupies a large territory associated with functional disorders, is followed by a stage of recovery that occurs either spontaneously or with training [29-37]. An early and highly cited study in monkeys with middle cerebral artery occlusion (MCAO) [38] revealed that even after one hour of complete ischemia, functional integrity was able to recover. A similar observation was seen in the rat with photochemically induced cortical stroke, which showed functional recovery at 7days post stroke [30]. The reversibility of neurological deficits is believed to be attributed to the collateral flow or recanalization of the occluded vessel, by which neuronal function and metabolism is preserved and neuronal loss is avoided. During the acute phase after stroke onset, the protective and recovery strategies associated with reperfusion emphasized neuroprotection by stabilization of membrane potentials that can be achieved by administration of γ -aminobutyric acid (GABA) receptor agonists [39, 40], by maintenance of ionic gradients and tissue haemostasis achieved by restoration of energy supplies such as glucose and ATP [41], and by administration of compounds that scavenge free radicals [42, 43] in order to prevent secondary reperfusion damage (Figure 1.1.3).

Ischemic damage of the brain also triggers inflammatory responses contributing to the worsening of tissue injury [41]. Administration of anti-inflammation agents can reduce the pace of damaging events. In the long-term, the reestablishment of structure post-ischemia requires neurogenesis [44, 45], axonal sprouting [46], and angiogenesis [31, 47] (Figure 1.1.3). These processes rely on the involvement of various growth factors to promote tissue repair [37, 45, 48, 49]. For example, the glial cell line-derived factor is a neurotrophic

factor found to increase neuronal proliferation post focal ischemia in adult rats [50]. The expression of this growth factor is enhanced in the region adjacent to the photochemically induced infarction and this enhancement is accompanied by the improvement of paralysis [30]. Exogenous infusion of epidermal growth factor (EGF) and erythropoietin (EPO) has shown to be beneficial in the recovery of motor and behavioral function at chronic time after stroke [47, 51]. This is because EGF and EPO stimulate differentiation of neuronal precursors in the subventricular zone and promote migration of the differentiated neurons towards damaged area. EPO can also up-regulates the expression of vascular endothelial growth factor (VEGF) [47], which play a big role in angiogenesis, reconstruction of microvasculature network so as to reduce infarct volume [47, 52, 53].

The capacity for recovery depends on the initial magnitude and duration of ischemia. Ischemic damage from incomplete ischemia and/or with a short duration is less and often delayed than that from a permanent ischemia and/or an ischemia with a long duration [54, 13, 55, 56] (Figure 1.1.1). A study of graded spinal cord ischemia using a photochemical occlusion in rat [57] showed a mild ischemia along with mild histological deficits had an ability to regain normal function over time, whereas in rats with severe spinal cord ischemia there was no improvement of their paralysis. After a 2 h long period of distal MCAO, even reperfusion failed to rescue the penumbra from infarction [58].

Figure 1.1.3 Diagram representing cellular responses after stroke onset.

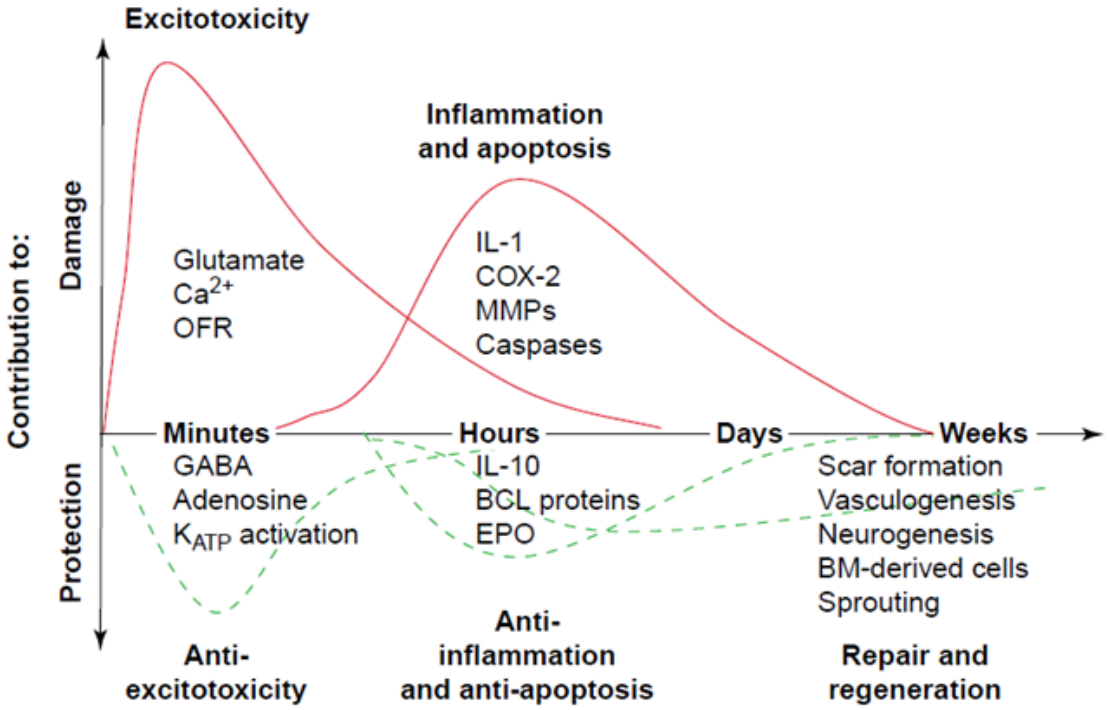

The time-course of damage after stroke shows two waves of damaging mechanisms (excitotoxicity and inflammatory activation, respectively, red lines). At chronic times after stroke onset, tissue repair occurs to regain normal function. There is evidence for several protective pathways counteracting the two waves of injury (green color). Specific molecules for each mechanism are addressed. Abbreviations: OFR, oxygen free radicals; IL, interleukin; MMPs, matrix metalloproteinase; COX-2, cyclooxygenase 2; EPO, erythropoietin; BM, bone marrow. (Adapted from Dirnagl [41] with permission).

1.2 Transient Ischemic Attack (TIA) or Minor Stroke

A transient ischemic attack is an ischemic stroke with transient symptoms resulting in neurological recovery within 24 hours. This classic definition of transient ischemic attack emphasizes only the duration of the sudden neurological deficit to be less than 24 hours. However, the extent of the brain damage associated with such clinical

symptoms can vary from a complete tissue recovery to a mature infarction (silent infarct) depending on the duration and/or severity of the ischemia. Even minutes of severe ischemia can produce an acute infarct. Thus, a revised definition has been suggested based on the tissue level, referring to a TIA as "a brief episode of neurological dysfunction caused by focal brain or retinal ischemia, with clinical symptoms typically lasting less than one hour, and without evidence of acute infarction" [59]. This definition uses diffusion-weighted imaging as a diagnosis to differentiate transient ischemia from infarct; however, it is still unclear to what extent the tissue is fully recovered after a TIA. Indeed, from clinical assessments it is difficult to differentiate a TIA from a minor stroke and thus both are often grouped together in clinical studies.

In Alberta, 68.2 people per 100,000 population experience a TIA every year [60]. The short-term risk of TIA is a recurrent stroke [1]. Patients often have one or more TIAs prior to their devastating one. According to community based studies, the incidence of stroke recurrence is reported as 2.5% at 2days [61], 2.6-7% at 7days [62-64], 12% at one month [65] and 6%-14% within 90 days [66, 67].

Little is known regarding how the initial ischemic episode affects the second stroke. It is possible that tissue that has recovered less completely is more vulnerable to subsequent ischemia than tissue that is well recovered. In a multicenter cohort sutdy that recruited 3,206 patients, the tissue-postive patients with abnomal DWI had a higer rate of recurrence at 7days (7.1%) than tissue-negative patients with normal DWI (0.4%) [64]. Using an NIHSS (National Institute of Health Stroke Scale) or ABCD(2) score system to assess the severity after TIA, patients with higher scores were at risk of early recurrence of stroke accompanied by worsening of symptoms [68, 69].

The recurrent lesions either at day 7 or day 30 are more likely to develop in the region of perfusion deficits after the intial TIA/minor stroke [70]. So far, most of the recurrent stroke studies are based on clinical observations. Experiemental evidence is lacking regarding what the damage will be when a second stroke occurs at different time points following an initial TIA/minor stroke. An important question is how an initial TIA/minor stroke will impact the severity of a subsequent ischemic insult? Is it a time-dependent process? This project is designed to throw light on these questions by developing and using a novel model of recurrent stroke.

1.3 Experimental TIA/mild Stroke Models

Compared to the extensive clinical reports of TIA, strikingly few experimental models have been proposed regarding the production of TIA/mild stroke. Although complete functional recovery is a general impression in human TIA patients, unknown is the true extent of tissue recovery clinically. The damage on a tissue or cellular level is hard to assess due to a lack of sufficiently sensitive measures for detecting mild injury *in vivo*. This uncertainty also provides difficulties with respect to the histological criteria for modelling TIA. The nature of the short-lived symptoms and rapid recovery following TIA/mild stroke is considered to be the result of re-establishing cerebral blood flow. Therefore a model of transient occlusion of the cerebral artery, for example transient MCAO with manipulation of the duration of ischemia, provides a promising method for TIA induction. In a previous study from our laboratory, a transient occlusion of MCA for 30 min was produced, resulting in scattered necrosis within the affected territory [12]. In the clinic, TIA symptoms can only last a few minutes, however, most of the reported experimental MCAO studies do not employ such relatively brief durations of ischemia.

MCAO, either temporally or permanently, has been extensively used in stroke modeling. Occlusion methods include intraluminal ligation [71], microclip occlusion or electrocoagulation of the cerebral branch via craniotomy [12], and embolus injection [72, 73]. These methods are all invasive and are accompanied by undesirable side effects. For example, using a filament to produce occlusion of the proximal MCA by inserting it in the carotid artery also involves transection of external carotid artery (ECA). This can damage masticatory muscles supplied by collaterals of the ECA, subsequently impeding eating and increasing mortality of experimental animals. Moreover, this model can interfere in behavioral tests (e.g. balance beam test, cylinder test) because it disables animals' movements. Although MCAO via craniotomy is free of these shortcomings, there are other disadvantages. First it requires occlusion of the distal MCA that directly lies upon the brain; and this is difficult to produce without some surgical manipulation and potential injury to the brain. Second, a hole in the skull and dura needs to be made to expose the MCA, which increases the risk of infection. More importantly, this method is technically difficult hampering its general utility. Finally, without modifications, MCAO produces a large cortical infarction whereas small transient infarcts are more common in patients with TIA or minor stroke.

A less invasive and easier to produce model of cerebral ischemia that results in mild injury is needed. A promising alternative is a photochemically-based occlusion method, which was pioneered by Waston and his colleagues in 1985 [74]. Ischemic stroke with this method is produced by evoking vascular occlusion with a light-dye interaction that generates reactive single oxygen species that initiates peroxidation of endothelial membrane, causing vasoconstriction and stimulates platelet aggregation and white

thrombosis formation at the surface of damaged endothelial cell [75-77] (Figure 1.3). One of the advantages of this method lies in its flexibility regarding selection of cortical location to produce an infarct experimentally. Also, this model is less invasive than MCAO and the mortality is low due to that it does not require manipulation of muscles and parenchyma as light can penetrate through intact skull. Furthermore, the lesion size produced with this model is less variable than MCAO [78].

Figure 1.3 The process and mechanisms of the photochemical approach to produce an ischemic stroke.

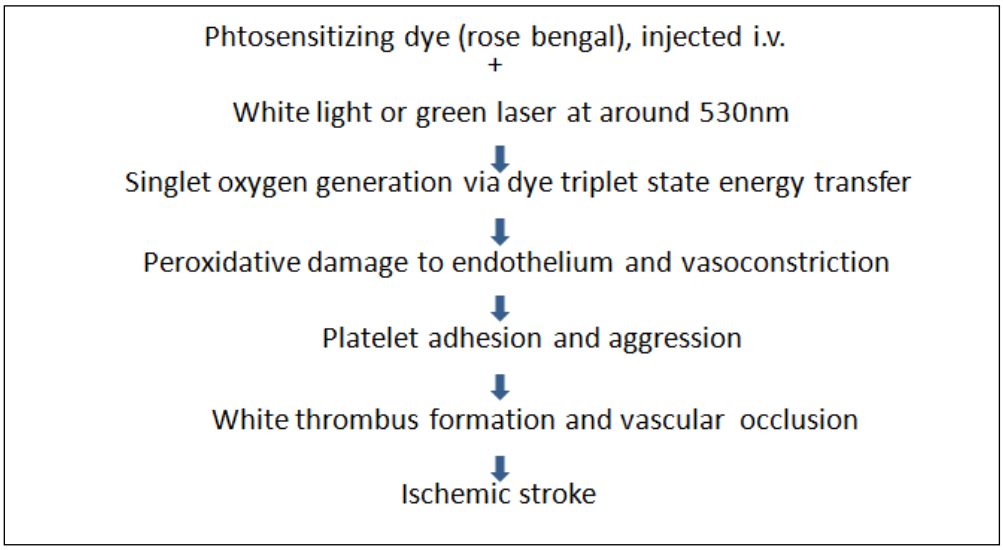

Administration of intravenous Rose Bengal under light illumination at a specific wavelength (normally around 530nm to 560nm) produces the single oxygen species within the illuminated vessels which damages the endothelium followed by vasoconstriction, platelet aggregation and production of thrombi. Eventually, ischemic stroke is induced.

Studies have shown that the severity of photothrombotic stroke can be varied by adjusting light type, light intensity, duration of illumination, dye concentration and skull

thickness (Table 1.3). In the original experiment, photothrombosis was conducted in rat cortex illuminated for 20 min using a xenon arc lamp (0.64W/cm^2) filtered at 560nm This resulted in the production of an infarct thorough the cortex. The technology was then improved by replacing the heat-emitting xenon light with cold white light such as a halogen lamp or laser (Table 1.3). When Boquillon [79] used graded light intensities to illuminate mouse cortex, the ischemic lesion increased with increased light intensity. The infarct size in the mouse already covered the entire width of the cortex when using a power level of 0.16W/cm^2 under 3min illumination. Boquillon suggested that the lesser skull thickness of a mouse probably allowed light to reach the cortex with less loss of its power therefore resulting in greater damage, compared to that in the rat. The close relationship between light intensity and lesion size has also been shown in rats. Alaverdashvili [80] produced a mild, moderate and severe stroke with power levels of 78,000 Lux, 140,000 Lux and 170,000 Lux respectively, where twice the light intensity approximately doubled the infarct volume. Also, the size of tissue damage corresponded to the behavioral deficits score. Pevsner [81] reported that illumination by a minimal beam intensity (0.1W/cm^2) for 30min could produce a small infarct that only damaged the superior layer of the cortex. Most of previous studies using photothrombosis in rats chose a duration of illumination around 10-30min which produced a well-defined infarct restricted to the cortex area. The quantitative relationship between illumination duration and lesion severity, however, is not well studied and whether conditions can be optimized to consistently produce a ***mild*** insult with regions of mild ischemic damage in rats is not known.

I anticipated that the highly adjustable nature of photothrombosis is capable of producing a TIA/minor stroke. In our previous work, 30 min of MCAO resulted in scattered neuronal loss that did not produce changes in MR images. We considered this degree of ischemic injury to be mild [12]. With photochemically induced cerebral occlusion, I expected that a similar mild ischemic injury could be produced. Although photothrombosis produces a relatively smaller cortical infarct compared to the MCAO model, the outcome of traditional photothrombotic stroke is a severe local infarct which is often accompanied by functional and behavioural disorders. Therefore, the first aim of this project was to produce a TIA/minor stroke by modifying the photothrombosis method and then to develop a recurrent mild stroke by combining two mild phothothrombosis insults.

Table 1.3 Summary of previous studies using the PT model.

Reference	Animal Species	Light Source	Power Level	Intensity Level	Diameter of Light	Skull Preparation	Rose Bengal	Duration of Exposurement	Post-damage Measurement time point	Severity of Damage
Watson, 1985	Wistar rat (male, 250-320g)	xenon arc lamp at 560nm		0.64 (W/cm2)	60nm through a 75mm focal lenth		7.5mg/ml, 0.133ml/100mg	20 min	30min, 1/5/15 days	30min, superficial cortex vessels traceable decrease; 5 days, a well-confined infarct surrouded by macrophages was observed
Grome, 1988	SD rat (male, 300-350g)	xenon arc lamp at 570nm	75mW		3mm through fiber optic		5mg	15 min	1/4/24/72/168 h	4h: 32ul of infarct volume, 2.2% increase in water content
Schroeter, 2000	Wistar (male, 280-320g)	cold light	not mentioned			4mm anterior to bregma and 4 mm lateral to midline		20 min	3/7/14 days	ADC: 3 days, 72%; 7 days, 102%; 14 days, 123% of contralateral side; 3 days, infarct core embraced by phagocytes and glial activation area
Pevsner, 2001	SD rat (female, 200-300g)	halogen lamp	150W	0.1	5mm through fiber optic	3mm incision over the frontoparietal area	20mg	30 min	55-360 min	Infartion: T2, 2.31; Histology, 4.2 mm; transitional zone: 2.00mm T2; 1.7 mm histo
Alaverdashuili, 2008	Long-Evan rat (young female, 90-100 days)	light bulb	150W	mild, 78000 lx; moderate, 140000lx; severe, 1700001x	5 mm *3 mm shaped from the fiberoptic buddle of 5 mm diameter	1.5mm anterior to bregma and 2.5mm lateral to midline	10mg/kg	20 min	24 h; 1 to 21 days	mild, 2.84±0.58 mm3; moderate, 6.16±1.08 mm3; severe, 9.86±0.89 mm3
Nowicka, 2008	Wistar rat (male, 250-280g)	cold light			1.5 mm through fiber optic	4.5mm posterior to bregma and 4 mm lateral to midline	0.4ml, 10mg/ml	20 min	4h, 1/4/7/28/60 days	GFAP increased both in farction zone and hippocampus at 1day, expanding in amygdala at 4 days; microglial response was restricted in lesion core
Dyck, 2004	neonatal mice (7 day)	green laser light at 532nm	20mW		rectangular (1.7mm x 2.4mm); circular (2mm)	medial frontal cortex/primary somatosensory cortex irradiation	50mg/kg	MFC: 40/60/80 s; somatosensory cortex: 40s	48h	well-confined infarct in targeted tissue area
Jin, 2010	SD rat (200-250g)	cold white light	not mentioned		4 mm aperure	2.5 mm posterior to bregma and 3 mm lateral to midline	20mg/kg	20 min	1d-5d	large cortical infarct; motor deficit
Horinouchi, 2007	Wistar rat (200-250g)	green light at 560nm	Moritex, Japan		not mentioned	intact skull; 4mm posterior and 6mm lateral	20mg/kg	20 min	1d-14d	large infarct extended to subcortex region; motor deficit
Dietrich, 1994	Wistar Rat (male, 250-300g)	xenon arc lamp at 560nm	not mentioned			4.3mm posterior to bregma and 2.5 mm alteral to midline	not mentioned	7 min	mins to hours	CBF declined within 3h; cortical spreading depression lasted 3h
Ikeda, 2013	Wistar Rat (male, 8 week age)	halogen lamp at 533nm	not mentioned		fiber optic of 10 mm diameter	sensorimotor area	20mg/kg	20 min	1d-7d	large infarct; severe motor dyfuntion
Boquillon, 1990	Swiss Mice (male, 25-30g)	argon laser Innova 90 at 562nm	2/5/10/20 mW	0.064/0.16/0.32 /0.64, respectively	2mm through fiberoptic	a midline head incision	10mg/kg	3 min	4/24/72 h	5mW power level caused unilateral entire cortex infarction

Using the PT model, a large cortical infarct was the normal outcome which was also associated with different degrees of neurological deficit (See references [30, 74, 79-87]). Therefore, modifications were needed to produce a mild stroke.

1.4 Repetitive Ischemia and models

Animal models being widely used for repetitive stroke are repetitive focal ischemia produced by MCAOs [88, 89], multiple global ischemia produced by repetitive common carotid artery occlusions(CCAOs) [90-92] or their combination [93], for their reproducibility of infarct volume. Less frequently used models contain an initial thromboemolic stroke followed by another thromboembolic event or global ischemia, and hypoxia-ischemia procedures [94-96]. Currently, most of the repetitive ischemic studies are in the context of "ischemic preconditioning" or "ischemic tolerance". That is, a very brief ischemia that is non-lethal can give the brain a "stress" and is therefore protective to the subsequent ischemic attack [97-99]. In these studies, the initial ischemia lasted only minutes similar to the definition of TIA, conferring tolerance or protection to the subsequent prolonged ischemia. Varying time intervals between multiple ischemia from minutes to days alike the short-term incidence of recurrent stroke, ischemic preconditioning occurred both rapidly and chronically through different protecting cascades [88-90, 92, 93, 100]. However in clinic, more often is the case of a worsened symptom, not tolerance, in recurrent stroke followed by TIA. The reasons remain unknown, but potential explanations may be 1) All of these models produce a relatively larger affected territory than a true TIA; 2) Other risk factors are often involved in recurrent stroke; 3) Experimental tolerance studies often induce hypothermia treatment or other "just-right stimulus" as preconditioning which are hard to achieved in human practice; 4) The ischemic tissue does not have complete recovery following TIA as expected, altering the response of brain to subsequent ischemia.

In contrast to ischemic tolerance, there were reports showing exacerbation of tissue damage followed by repetitive ischemia. Pioneered by Mrsulja [101], a serial studies of triple repetitive ischemia of 5min duration each using bilateral occlusion of CCA in gerbils, had demonstrated that although each alone produced very little damage, there was an enhanced cumulative tissue damage greater than a single insult of either 5min or 15min duration [102-105]. This enhancement was most pronounced with a 1h interval between multiple ischemic attacks. The cumulative effect was dependent on the duration of ischemia and the interval between them. A 3h interval had more severe damage than 48h [106], However, these studies did not investigate the interaction between multiple episodes with prolonged intervals (i.e., up to 1week). Enhancement of injury was also demonstrated in our previous studies using a combination of transient MCAO of either 30min or 40min with a 3day interval between them [12], while the same duration of 30min was reported in other studies to provide a preconditioning neuroprotection to a subsequent ischemia in several other studies [88, 89].

In summary, these studies of repetitive ischemia offer limited knowledge of how a first mild ischemic insult influences a subsequent ischemic event. Thus, more study is required to determine how recovery time after a first mild ischemic insult affects damage produced by a second mild insult.

1.5 Magnetic Resonance Imaging (MRI)

1.5.1 Basic Principles of MRI

Magnetic Resonance Imaging is a promising technology that has been widely used in diagnosis and evaluation of various diseases. The ability to image properties of tissue lies in the fact that there is a high abundance of water and fat in the human body

and the protons in water can be manipulated within a strong magnetic field using radiofrequency pulses (RF) that can be coded and imaged by MRI software.

The hydrogen nucleus contains a single proton with a positive charge. It orbits around the axis and this results in a net spin of 1/2, which produces a small magnetic field, called a "magnetic moment". In nature, these magnetic moments are randomly oriented because the earth's magnetic field (approximately $0.5x10^{-5}$ Telsa(T)) is too small to affect their alignment. However, when the body is exposed to a strong magnetic field (B_0) (i.e., a 9.4T MR system that produces a magnetic field 180,000 times greater than that of earth's magnetic field), these magnetic moments align either parallel or anti-parallel to B_0, producing a net "magnetization" (M_0). Since the moments are not fully aligned along the direction of B_0 (defined as z-axis), they experience a turning force (torque); as a result, These magnetic moments precess about B_0 at Larmor frequency (ω_0), which is directly proportional to B_o:

$$\omega_0 = \gamma B_{0,}$$

where γ is the nuclei specific gyromagnetic ratio. The hydrogen-specific processional frequency (ω_0) is in the range of the radiofrequency.

The net magnetization (M_0) of hydrogen nuclei in the direction of B_0 is small compared to the main magnetic field. For the purpose of imaging, M_0 must be measured in another direction, which can be achieved by adding an additional magnetic field (B_1) through a transmitter coil. B_1 is first applied perpendicularly to B_o (x-y plane). Once its frequency is tuned at the Larmar frequency, B_1 perturbs the alignment of the macroscopic spin magnetization into x-y plane (also called transverse plane). The B_1 field is thus called a radiofrequency pulse. The spins absorb the electromagnetic energy and flip from

their low-energy orientation to a high-energy orientation. After the removal of RF, there is a return of spin magnetization to thermo equilibrium (original state along B_0 direction) based on two processes called a longitudinal (T1) and transverse (T2) relaxation.

T1 relaxation, also referred to spin-lattice relaxation, measures the time of net magnetization to lose its 37% of energy to surrounding environment.

Unlike T1 relaxation, the transverse relaxation (T2) is caused by the de-phasing of spins coherence in x-y or transverse plane. The transverse relaxation measures the time it takes for the transverse magnetization (M_{xy}) to go from an excited phase back to its thermo equilibrium phase. The time constant that characterizes it called T2. The M_{xy} relaxation is rapid and is not in pace among spins due to the local field inhomogeneity, resulting in a loss of MR signal to be recorded. To deal with this, an 180^o RF pulse is then applied at a certain time following the 90^o pulse. This 180^o RF refocuses the spins with an approximate 180^o rearrangement. As a result, the once slow decaying spins are now ahead of the fast ones. Because the direction of relaxation is not changed, they begin to decay towards the starting axis, generating an echo with an increased MR signal that can be detected by a receiver coil. The time between 180^o pulses is called repetition time (TR), and the time between the application of RF and the middle of spin-echo is called echo time (TE).

M_{xy} decays in an exponential manner. To catch this ‘de-phasing’ phenomena, MR images are acquired at various TE after the application of each RF pulse. This produces a set of T2 weighted images at these different TE. The longer the ‘out-of-phasing’ process takes, the higher the T2 resulting in a brighter region on the T2 image. The protons of

water have free movement and take a longer time to normalize producing a higher T2 than tissue with structural integrity due to their macromoledular bonds.

Diffusion-weighted images (DWI) measures the microscopic random motion of water molecules. This diffusion property of water molecules can be restricted by biologic barriers in the brain tissue (for example, cellular organelles and cellular membranes). MR signal can be made sensitized to diffusion. After a 90^o pulse, all spin are in phase and they undergo diffusion. After an 180^o pulse, the water molecules that have free movement diffuse in the direction of the magnetic field gradient (G_{diff}), generating a phase shift directly relevant to the signal attenuation of the image in a measurable fashion. The diffusion gradient can be adjusted by the gradient amplitude, application time and the time between RF pulses, and is described as a b-factor (s/mm^2). The relationship between MR signal without diffusion (T2 signal) and MR signal followed by diffusion is calculated by:

$$S(TE)=S_0 \exp^{(-bD)},$$

where S_0 is the signal intensity without diffusion (b=0), and S(TE) is the signal intensity after diffusion at a given b value. D is the diffusion coefficient.

This equation can be adjusted as:

$$\frac{S(TE)}{S_0} = \exp(-b \cdot ADC)$$

D is replaced by an Apprent Diffusion Coefficient, ADC, indicating the water diffusion is not free in tissue, but rather hindered by the enviorment where the water is placed.

It shows that the value of ADC is dependent on the choice of b-factor value. At least two b factors are needed for the measurent of ADC, desribed as:

$$ADC=In[(S(TE)-S_o)/(b_1-b_2)]$$

Figure 1.5.1 Illustration of sequence pulses, T2, diffusion gradient and imaging process.

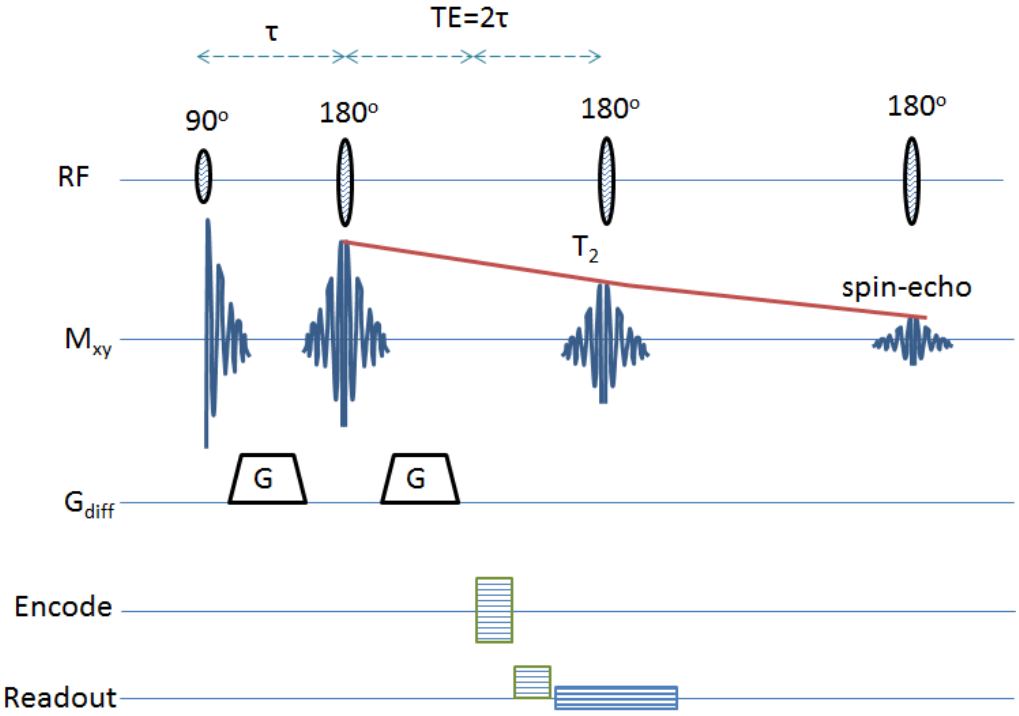

Perfusion-weighted images (PWI) provide an index of cerebral blood flow. Two techniques are commonly used in imaging cerebral perfusion [107, 108]. One is bolus-contrast tracking with which information of perfusion is generated by monitoring the passage of a non-diffusible contrast agent (e.g. gadolinium) through brain vessels. Another MR perfusion method is arterial spin labeling during which the arterial blood is tagged with a radiofrequency pulse and the perfusion status is available as more labelled blood flows through regions with high compared to low flow.

1.5.2 MRI Utility in Ischemic Stroke

Based on the idea of the T2 relaxation of pathologically abnormal tissue being different from normal tissue, T2 weighted imaging provides a tool for the diagnosis of stroke. The tissue in the region of an ischemic infarct has an increased blood-brain-barrier (BBB) permeability, leading to increased free water followed by vasogenic edema which then appears hyper-intense on T2-weighted imaging (T2WI) and these hyperintense areas of an increased T2 relaxation time.

DWI often provides early and accurate detection of a stroke infarct. This is because DWI measures the restricted water diffusion initiated by cytotoxic edema that is almost an immediate process after stroke onset. In the acute phase, a DWI abnormality appears as a hyper-intensity in the ischemic lesion that contrasts with normal tissue. It should be noted that hyper-intensities on diffusion images can be produced from either T2 related vasogenic edema (T2-shine through effect) or regions of authentic restriction of water diffusion caused by cytotoxic edema. To distinguish the two, the ADC map is produced, which maps the regions of restricted water diffusion as a dark area is very sensitive to the change of tissue microstructure. Acutely after a major stroke, T2-weighted images and DWI changes appear to be homogeneous and obvious because the border of infarct and non-infarct tissue is clear. However, what remains unclear is how T2WI and DWI diagnose mild ischemia, particularly if scattered necrosis is present and the majority of tissue structure is preserved.

Perfusion-weighted imaging (PWI) measures cerebral perfusion or blood flow. Regions of decreased cerebral perfusion appear less intense in PWI. In the acute phase of stroke, region of PWI abnormality appear larger in area than the area of DWI abnormality,

which has led to the concept of a DWI/PWI mismatch. The area of PWI deficit without a DWI abnormality has been believed to indicate the penumbra. Combinations of the two MR techniques have had clinical importance for the diagnosis of salvageable brain tissue as targets for medical intervention.

Despite substantial research on the MR imaging of a single stroke, our knowledge regarding the MR signatures in mild and recurrent stroke are extremely limited.

1.6 Research Purpose

To summarize, there is a large population every year that experiences TIA/minor stroke and these individuals have a high risk for stroke recurrence. Despite the importance of this health problem, our knowledge remains limited regarding the interaction between multiple episodes of TIA/minor stroke, that each alone produces minimal damage to the brain. A lack of animal models that mimic well TIA/minor stroke have hindered progress in this area. We lack basic information regarding how often there is complete tissue recovery after TIA and how an initial mild ischemic attack influences subsequent ischemic episodes. This project aims to expand our knowledge of pathological processes of recurrent stroke and the importance of varying the recovery intervals between the initial and second insult on outcomes as assessed using histology and MRI.

Chapter Two: Hypothesis and objectives

2.1 Hypothesis and Objectives

I hypothesize that the photothrombosis (PT) method with modification can produce an ischemic insult that can be repeated to model recurrent stroke; and, that damage produced by a recurrent insult can be enhanced by the initial ischemic event but the degree of enhancement depends on the timing between the two strokes.

Objective 1: Determine the conditions of the photothrombosis method that produces a transient ischemia and a mild cortical injury in rats. Specific aims were:

a) Identify the pharmacokinetics of Rose Bengal following i.v. injection.

b) Determine the Importance of Illumination Duration to Produce Mild Injury.

c) Determine the Importance of light intensity to Produce Mild Injury.

d) Investigate the correlation between histology and MRI signatures.

Objective 2: Produce a recurrent stroke with intervals between strokes of 1day, 2day, 3day and 1 week to determine whether damage due to recurrent mild stroke is greater with a shorter recovery time between insults.

2.2 Rational of Objective 1

The photothrombotic (PT) model produces ischemic damage based on the interaction between a photosensitive dye and light which eventually leads to thrombus formation and vascular occlusion. Therefore, light conditions should play a significant role in the severity of the induced ischemia. This objective investigated the impact of light intensity and duration of illumination on the severity of stroke measured by

quantitative MR changes and histological assessments. MRI scanning was performed at 24h after PT induction, because at this time point the MR change was pronounced and readily detected. Histological assessment was followed after two days after PT induction, allowing additional time for the development of neuronal damage.

Potential adverse effects of this model were considered and minimized prior to our recurrent stroke studies. For example, the heat generated by illumination was reduced by using a halogen lamp with two heat filters before light was transmitted through an optic fiber. Also, my pilot experiments showed that a shorter time period of illumination and overall experimental time was possible when the illuminated skull was evenly thinned so the skull was thinned in subsequent experiments.

2.2.1 Experimental Design of Objective 1

To study the relationship between illumination duration and ischemic damage, the duration of light illumination was varied for times of 15min, 10min, and 5min using a light intensity of 45,000 Lux measured by a lightmeter with a 3mm*3mm sensing area that matched the illuminated skull size.

To determine the impact of light intensity on the severity of damage, 4 graded light intensities were tested: 70,000, 60,000, 45,000, and 35,000 Lux respectively under 5min of illumination.

The concentration of photosensitive dye (Rose Bengal) used in the present study was chosen to be 10mg/kg. This is a minimal concentration reported in many previous studies with PT modeling (see Table 1.3). A low concentration was selected since my objective was to produce a mild photothrombotic stroke.

2.2.2 Experimental Flow Chart of Objective 1

Figure 2.2.2 Experimental flow chart of Objective 1

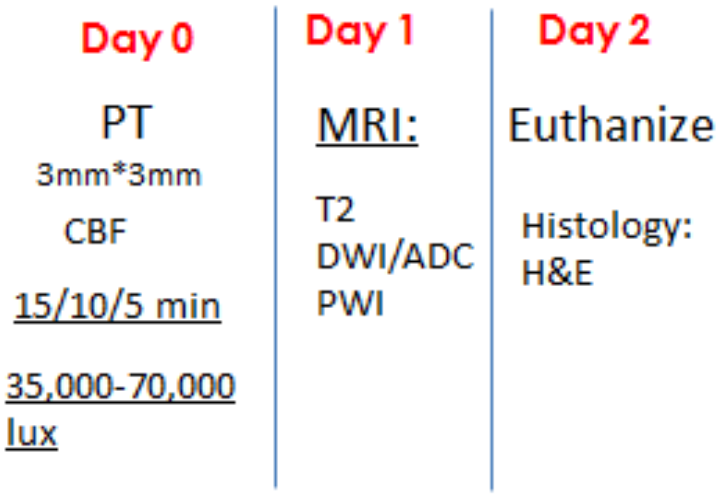

2.3 Rational of Objective 2

To control for potential changes in light conditions between the two illuminations, the illumination area was shifted to render a single illuminated site (area 3) at the 2nd PT in comparison with the single illuminated site at the 1st PT (area 1). If the light conditions were similar, then the damage within areas 1 and area 3 should be similar. To model recurrent stroke, the time intervals between PT were varied by 1day, 2d, 3day and 1week, to mimic the high incidence of recurrence within the first week after TIA clinically.

2.3.1 Experimental Design of Objective 2

Four interval groups were conducted with repeated PT surgery with varied time intervals mentioned above. Additionally, animals subjected to a single PT were sacrificed at 1d, 2d, 3d and 1wk to study the histological progress over time after ischemia.

2.3.2 Experimental Flow Chart of Objective 2

Figure 2.3.2(a) Experimental flow chart of recurrent PT induction.

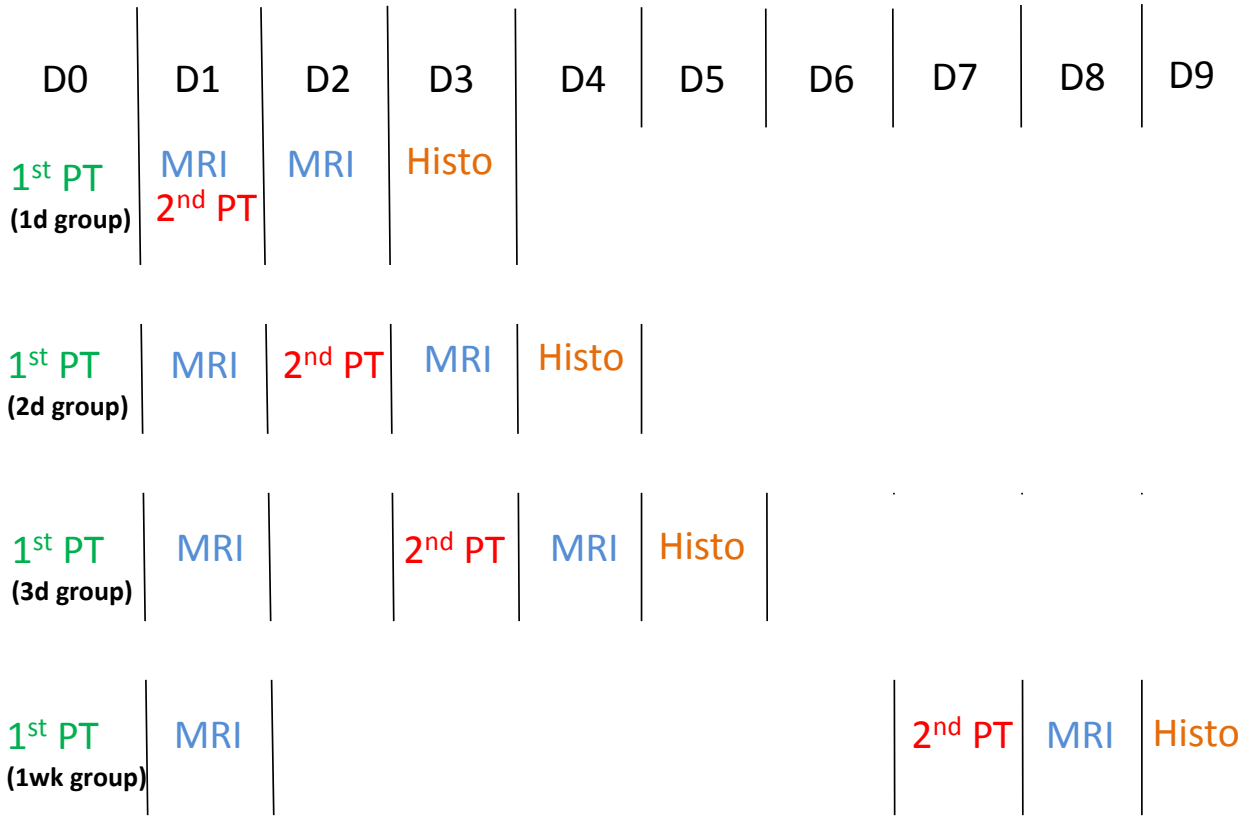

Figure 2.3.2(b) Experimental flow chart of histological study over time post to single PT.

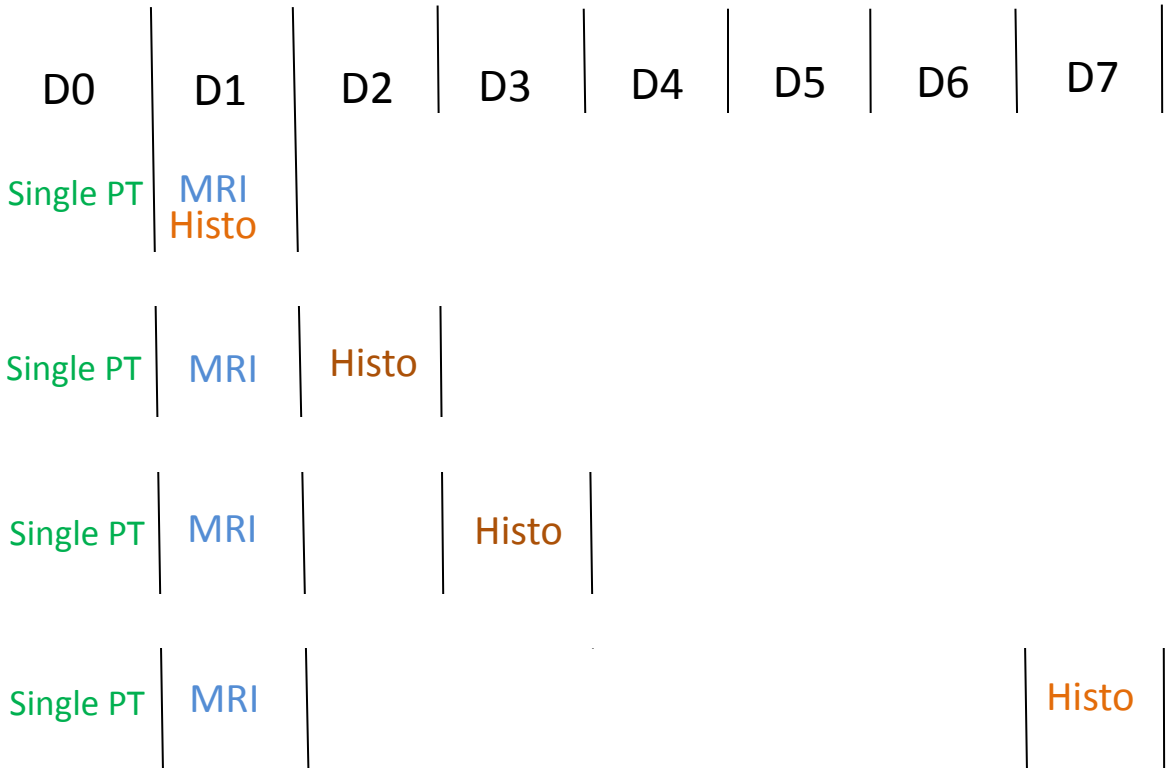

Chapter Three: Research method

3.1 Animals and Ethics

All experiments were approved by the University ethics committee (Protocol M11037). The experimental rats, male Wistars, were procured from Charles River, with weights between 160-190g on the delivery day. The animals were housed in the semi-clean room in the Animal Resource Center for at least five days before use. In the Rose Bengal pharmacokinetic study, the animals were surplus post-pregnancy Wistars weighing 350-400g. After each experiment, rats were kept in the laboratory overnight for monitoring recovery and physiology before their return to the rat half-way house. Water, food and clean cages were provided until the rat was sacrificed.

3.2 Pharmacokinetic Study of Rose Bengal

3.2.1 Preparation of Rose Bengal Solution

Rose Bengal powder (Sigma-Aldrich Company) was dissolved in distilled water, at a concentration of 10mg/ml. The solution was thoroughly mixed and filtered with an 80μm filter before use. The solution was kept in a brown tube and stored in a 4 ℃ fridge for future use. Each preparation contained 5 mL of Rose Bengal solution and was used within 2 months. After that a new solution was made to avoid possible loss of efficacy with storage.

3.2.2 Rose Bengal Plasma Sample Collections and Analysis

Rats (n=4) were anesthetized with isoflurane (2%) and the right femoral vein and artery were then cannulated for injecting Rose Bengal and collecting arterial blood samples, respectively. The injected volume (0.1ml/100g) of Rose Bengal (10mg/kg) was at a concentration of 10mg/ml. The same Rose Bengal was used to calibrate the

spectrophotometric measures. A pre-injection sample was collected as control. Timing was started once the injection was finished. Blood samples were collected at consecutive time points of 10, 20, 30, 40, 50 seconds and at 1, 2, 3, 5, 10, 15, 20, 25, 30 min, respectively. Blood samples were centrifuged immediately and plasma aliquots of each sample were taken for analysis.

3.2.3 Calibration Curve for Measuring Rose Bengal Concentration in Plasma

Rose Bengal concentrations in plasma were measured using a spectrophotometer. The standard curve was prepared using a stock Rose Bengal solution which was diluted with distilled water by 10, 20, 50, 100, 200, 500, 1000, 2000, 5000, and 10000 times. The corresponding absorption was immediately analyzed at a wavelength of 532nm and the mean absorption value of each dilution was measured in triplicate. A blank solution which contained only distilled water was also analyzed for zero adjustment. The calibration curve was calculated as S=aC+b. (C is the diluted concentration of Rose Bengal and S stands for the absorption value subtracted by the blank value). Plasma samples were measured in triplicate and the calibration curve was applied to determine the Rose Bengal concentration in plasma.

3.3 Photothrombosis Model

3.3.1 Light Source

The light unit used in this study was a halogen bulb combined with a tuning system that can offer 16 gradients of light intensity (NCL 150 unit, 20V/150W, Volpi). Two heat filters are added to the filter slot provided in the light unit to minimize the heat effect during illumination with 90% preservation of light power. The light was then

transmitted through a flexible fiber optic of 13mm diameter and 30cm length attached to the unit.

3.3.2 Single Photothrombosis (PT) Induction

Wistar rats were initially anesthetized with 5% isofluorane which was reduced and maintained at 2% during surgery. The fur over the right femoral vessels and skull were shaved and disinfected and surgery was performed using a no touch aseptic technique. Normothermia (rectal temperature of 37 ℃) during surgery was maintained using a sensor- controlled heating pad. The right femoral vein was cannulated with a PE-50 tube that had a stretched bevelled end to allow later injection of Rose Bengal. After cannulation, the rat was carefully flipped 180° to lie prone on the heating pad. The head was then fixed level using ear pins in a stereotactic frame. An approximate 3cm incision was made over the scalp along the midline and the skin was retracted back with suture thread to expose bregma and the midline. Blood from cranial muscle and bone was wiped clean with gauze and cold saline. An opaque foil mask with a 3mm*3mm opening was placed directly on the right side of skull, 0mm posterior to bregma and 1mm lateral to the midline. The mask prevented extraneous skull from being illuminated. The skull within the area to be illuminated was thinned evenly using a dental drill until the pial microvessels were visible under the microscope. The thinned area was somewhat larger than that to be illuminated, to ensure that the illumination field was flat and skull thickness was uniform. Regional cerebral blood flow (rCBF) within the illuminated region was measured prior to, during and post illumination using a Laser-Doppler flowmetry probe placed perpendicular to the skull. Rose Bengal (10mg/ml) prepared as above was injected intravenously (0.1ml/100g body

weight) 1min prior to illumination. The skull was illuminated using the white light as mentioned above. The light guide was placed 2.5 mm above and perpendicular the skull. The skull was illuminated for various times (5-15min). For durations of longer than 10 min, a 2nd Rose Bengal injection was given at 10 min. After PT, all surgical sites were cleaned and closed with 3-0 nylon sutures. Analgesic buprenorphine (0.03mg/kg) was administered afterwards and rectal temperature was monitored for 1 hour post to surgery (Figure 3.3.1).

3.3.3 Recurrent Photothrombosis (PT) Induction

The animals were subject to 5min of illumination duration under 35,000 Lux of light intensity as determined in Objective 1. The photothrombotic procedure was repeated using the same procedures except for a shift in the location of the illuminated area. In this set of experiments, the illumination site moved 1.5mm posterior, starting from 1.5mm from the bregma and 1mm lateral from midline. The skull was thinned again if regrowth of skull was observed. The skull was thinned such that the pial microvessels underneath the skull became clearly visible under microscope.

Figure 3.3.1 Schematic representative of illumination method for photothrombotic ischemia in the rat.

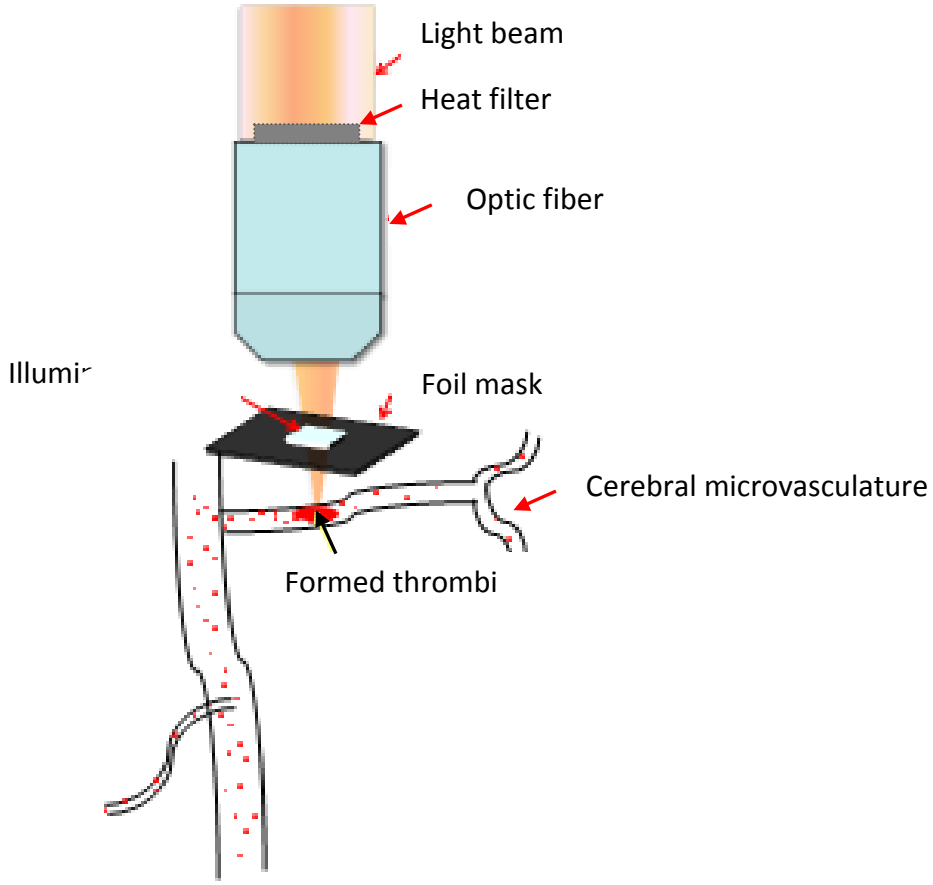

Figure 3.3.1 Schematic representation of illumination method for photothrombotic ischemia in the rat. A fibre optic source of white light was carefully positioned perpendicular to the illumination field. A foil tape with a square opening (3mm*3mm) was placed onto the thined skull to prevent illumination of extraneous tissue. During illumination, platelet thrombi form which adhered to the endothelial cell wall producing occlusion of microvessels.

Figure 3.3.2 Representative of location of recurrent PT in rat.

(a)

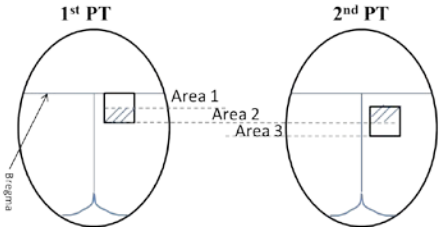

(b)

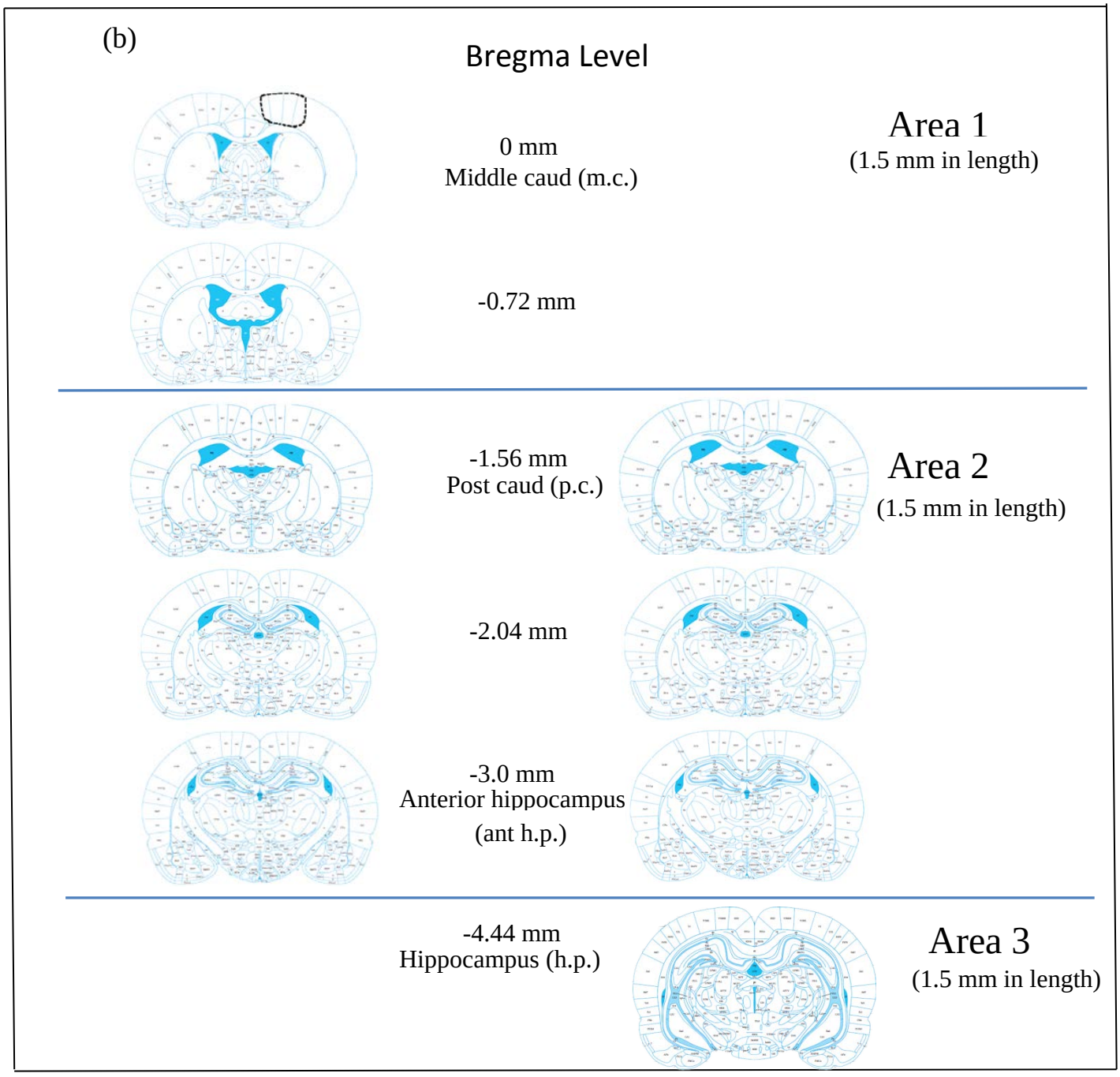

Figure 3.3.2 Representation of Locations of Recurrent PT (continued).

(a) The black open squares represent the illuminated area in the 1st PT and 2nd PT procedures. The illumination area was moved 1.5mm posterior between insults. This produced three distinct ischemic regions: Area 1 was a single PT area illuminated during the 1st PT; Area 2 was a double illuminated PT area analyzed in recurrent insults, and Area 3 was another single PT area illuminated during the 2nd PT. (b) Representative diagrams of the corresponding coronal slides covering the illuminated regions of 1st PT (left column) and 2nd PT (right column). Dashed square represents the location of illumination. The post caudate (p.c.) level was near the center of 1st illuminated area. The total length of illumination was 4.5mm (Adapted and modified from reference[109]).

3.4 MRI Scanning

MRI scanning was conducted in the Experimental Imaging Center at the University of Calgary. Twenty-four hours after surgery, MR scans were acquired using a 9.4T Bruker MR system. During the MR scan, animals were anesthetized with 2% isoflurane and body temperature was monitored and kept at 37℃ via an air heating feedback system. The animal was placed in a 35mm quadrature volume coil. Each scan contained a set of MR sequences including a multi-slice T2 map, apparent diffusion coefficient (ADC), a diffusion-weighted Imaging (DWI) map and a perfusion-weighted Imaging map (PWI). Details of the MR parameters used are provided in Table 3.4.

Table 3.4 Acquisition parameters for the various MRI sequences

Sequences	FOV (cm^2)	Matrix	Number of slices	Slice thickness (mm)	TE (ms)	TR (ms)	Number of b values
T2 multi-echo	3x3	128x96	20	0.7	10x32	7000	na
ADC	3x3	128x128	20	0.7	40	5000	5 b
Perfusion	3x3	128x128	1	1	13.3	3000	na

3.5 Histological Processing of Brain Sections

After a single PT, animals were deeply anesthetized with pentobarbital (120mg/kg, Intraperitoneal) and then perfused with cold phosphate-buffered saline (PBS, 1x) and fixed with 10% formalin. Animals were randomized to perfusion fixation at different times of 1day, 2day, 3day and 1week post-insult. For double PT, animals were killed and perfused 2days after the last MRI. The head was decapitated and immersed in 10% formalin overnight. The brain was removed from the skull and stored in 10% formalin

solution for about 5days before being embedded in paraffin. Semi-serial coronal sections (7 µm thick) were cut using a microtome at levels of the brain that included illuminated and non-illuminated levels. Sections were mounted onto glass slides coated with polylysine and then stained with haematoxylin and eosin.

3.6 Analysis Procedures

3.6.1 MR Quantification

MR images were inspected and it was apparent from these images that the PT lesion usually consisted of a maximal intensity 'core' region in the upper cortex and less intense peri-infarct regions in adjacent cortex. Thus, initially the regions of interest (ROI) selected for analysis were selected according to visualized differences in MR intensities on T2 images – designated infarct core and peri-infarct. MR values (T_2, ADC and PWI) were measured in these regions of interest (ROI) using locally available software (Marevisi, Institute for Biodiagnostics, NRC). The infarct volume was measured according to the hyperintense area in DWI or the brightest area in T_2 images. The volume of ischemic lesion was a sum of the hyperintense areas in each slice multiplied by slice thickness (0.7mm). The quantitative MR changes of each rat were measured in slices with maximal T2 changes. This level was often located in the center of the illumination field with coordinates of -1.4mm~2.1 from bregma.

Another set of ROIs were used for Objective 2 which investigated the effects of recurrent mild PT induction. MR measurements were conducted using three ROIs which were all similar in size and divided the illuminated cortex into three parts, described as an upper/core, middle/peri-infarct and lower/remote layers of cortex with the ROIs being named depending on whether the upper layer showed acute infarct (Figure 3.6.1). These

regions remained consistent between the first and second scanning sessions. In addition to ischemic regions, MR quantification of T2 and ADC was performed in unaffected control regions - a1, a2, and a3 for comparison.

A PWI scan was acquired in one coronal level (one slice) in rats subjected to either a single PT or a recurrent PT. The level used for PWI scanning was the one that showed biggest MR abnormality on T2 and DWI. This level was often in the center of the illumination field, at coordinates of -1.56mm bregma (area 2) on the representative coronal slice in Figure 3.3.2(b). For Single PT, area 2 was the illumination center. For recurrent PT, area 2 represented the double illuminated field. The PWI was measured in the region that had a visually apparent perfusion deficit presenting as a darker area of reduced signal intensity, compared to normal contralateral cerebral perfusion. Due to a large variation of absolute PWI and uncertainties in constants required for calculating absolute perfusion, PWI was converted to relative changes in flow as % of a non-ischemic control region. In all rats, the region selected for a control measure was remote from the illuminated ROI reflecting a mean of the three cortical layers.

Figure 3.6.1 Representative of ROI selection for MR measurement

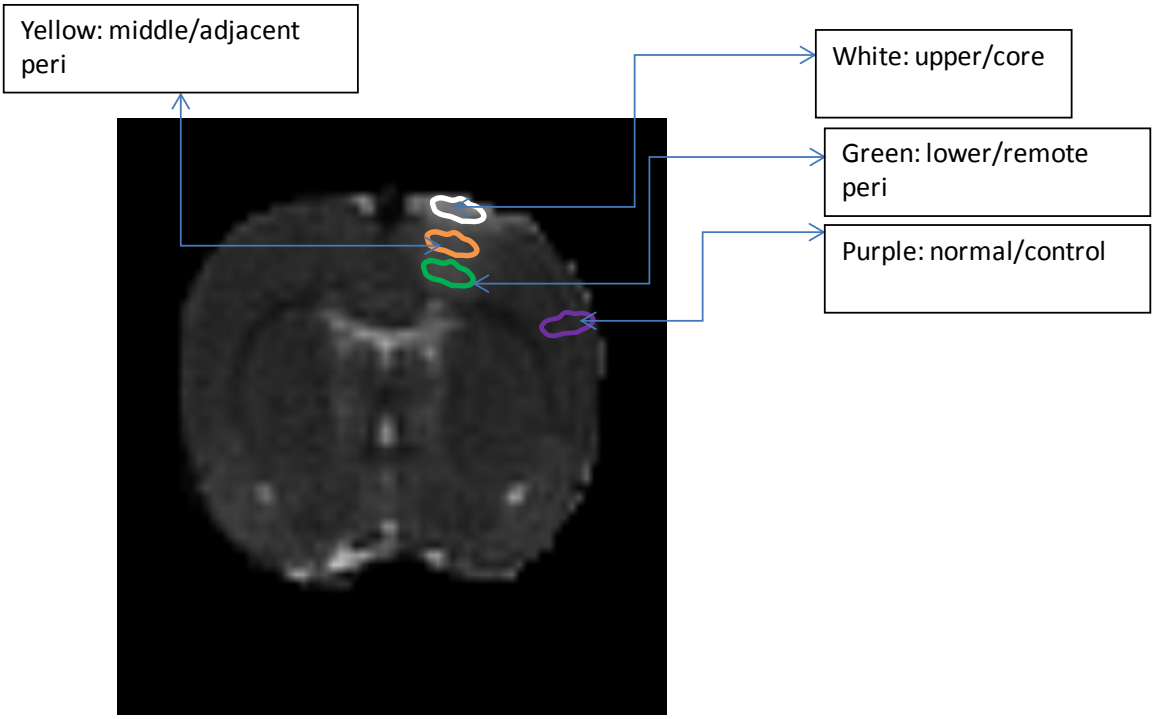

Figure 3.6.1 Representative of ROI selection for MR measurement. ROIs were drawn with similar size, dividing the illuminated cortex into three regions: upper/core (white), middle/adjacent peri (yellow) and lower/remote peri (green). A control ROI (purple) was chosen remote to the illuminated region. The representative slice was picked at bregma level (middle caudate level) from a T2 map.

3.6.2 Histological Assessments

Brain sections were stained with standard staining methods (Haematoxylin & Eosin) and the stained slides were observed under an Olympus microscope at 4-20x magnification. Representative photographs were acquired using image analysis software (Microbrightfield). The scoring criteria for damage assessment were: 0= no infarct; 1= scattered necrosis with preservation of structure; 2= incomplete infarct with more necrotic cells and tissue losing affinity to the dye; 3= complete infarct with pannecrosis and destruction of tissue morphology.

3.6.3 Statistical Analysis

All data are presented as the mean value ± SD. Differences between means were compared using a one-way analysis of variance (SigmaStat 3.5 version). Significance of differences between means within groups was compared using a Bonferroni test for a multiple comparison of means or a Student's paired t-test for two group comparison. A Mann-Whitney Rank Sum Test was used for histological score analysis and a Student's paired t-test was used for comparison of repeated measures. Differences were considered significant at $P<0.05$.

Chapter Four: Results

4.1 Pharmacokinetics of Rose Bengal following i.v injection

The Rose Bengal distributed rapidly after intravenous injection. Its plasma concentration in arterial blood samples reached a peak of 0.136 ± 0.01mg/ml quickly subsequently decreasing by 50% at 1 min after injection (Fig 4.1). However, the time taken to reach the peak varied slightly, with a range of 10 seconds to 30 seconds in individual rats producing variability in Rose Bengal concentration within the early minutes after injection (not shown on the graph). This may be due to sampling variability and variation in the speed of injection. Subsequently Rose Bengal was rapidly metabolised from the blood with approximately 95% of Rose Bengal being eliminated in the first 10 min. (Fig 4.1)

Based on this study, a one minute interval between the end of injection and the start of illumination was chosen for PT induction because at this time point the Rose Bengal concentration in blood was relatively stable yet not too small to lose its effect. Another implication was that if illumination time was longer than 10min, a second injection of Rose Bengal would be required to maintain an efficient level for the light-dye interaction.

Figure 4.1 Plots of Rose Bengal plasma concentration against time after injection. (n=4)

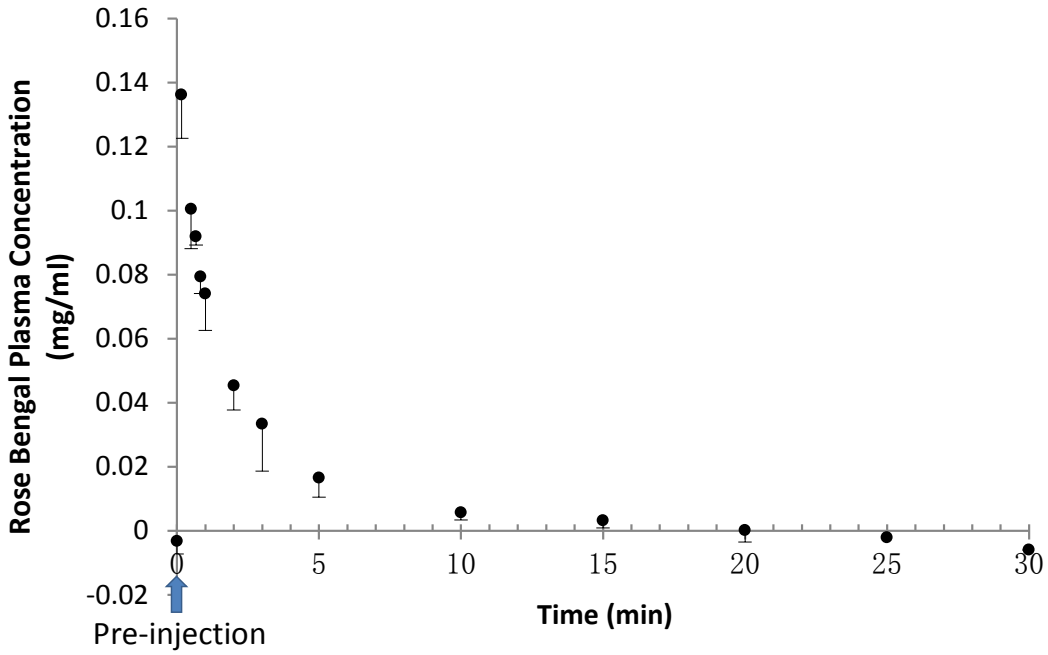

4.2 Objective 1: Single PT Induction

4.2.1 Effects of illumination duration on the severity of stroke

As the duration of the 45,000 Lux illumination decreased from 15min to 5min, so did the injury volume measured the on MR images (Fig 4.2.1a). At 24h, both T2 and DWI changes were pronounced with a clear border distinguishing the ischemic lesion from normal tissue. With 5min of light illumination at 45,000 Lux, a substantial region of core appeared in the upper layer of the illuminated cortex. With 15min of illumination, a lesion was apparent in the whole illuminated cortex and expanded to a small portion of the subcortical region and adjacent cortex. The region of T2 elevation corresponded well with that of the T2 and DWI hyperintensity with respect to the size and location of lesion. Haematoxylin and eosin stained slides showed a demarcated infarct with pannecrosis in the region where MR abnormalities were observed (Fig 4.2.1b).

The lesion volume (Fig 4.2.1c) measured from regions of brightest T2 signal decreased as the illumination duration decreased and there was a linear correlation between them (r^2=0.91). The cerebral blood flow measured with Laser-Doppler flowmetry (Fig 4.2.1d) showed that at 45,000 Lux there was a significant decrease in perfusion immediately post illumination. Perfusion was 51.5% ± 11.8% of pre-illumination baseline values following 10 min of illumination and at 58.03%±7.8% of baseline with 5 min illumination. Despite a significant change of infarct volume between 10 min and 5 min illumination, the decline of blood flow for these two was similar. The cerebral blood flow returned towards baseline with near full recovery within 30 min post illumination, indicating the ischemia produced by PT was at least partially transient. At 35,000 Lux, the time taken before the blood flow returned to baseline varied in individual

rats but it tended to return quickly (e.g. within 5 minutes) to near baseline (data not shown).

The major finding of this group of experiments was that there exists a good correlation between the duration of illumination and the produced lesion volume. Five min of illumination resulted in a small infarct core (4.89 ± 1.65 mm^3) located in the upper layer of illuminated cortex. The cerebral blood flow recovered relatively quickly after illumination. Considering that the aim was to develop a mild stroke using PT, in subsequent experiments we used a 5min illumination to further optimize the PT method for producing a mild insult.

Figure 4.2.1 Effects of illumination duration on the severity of stroke (n=9).

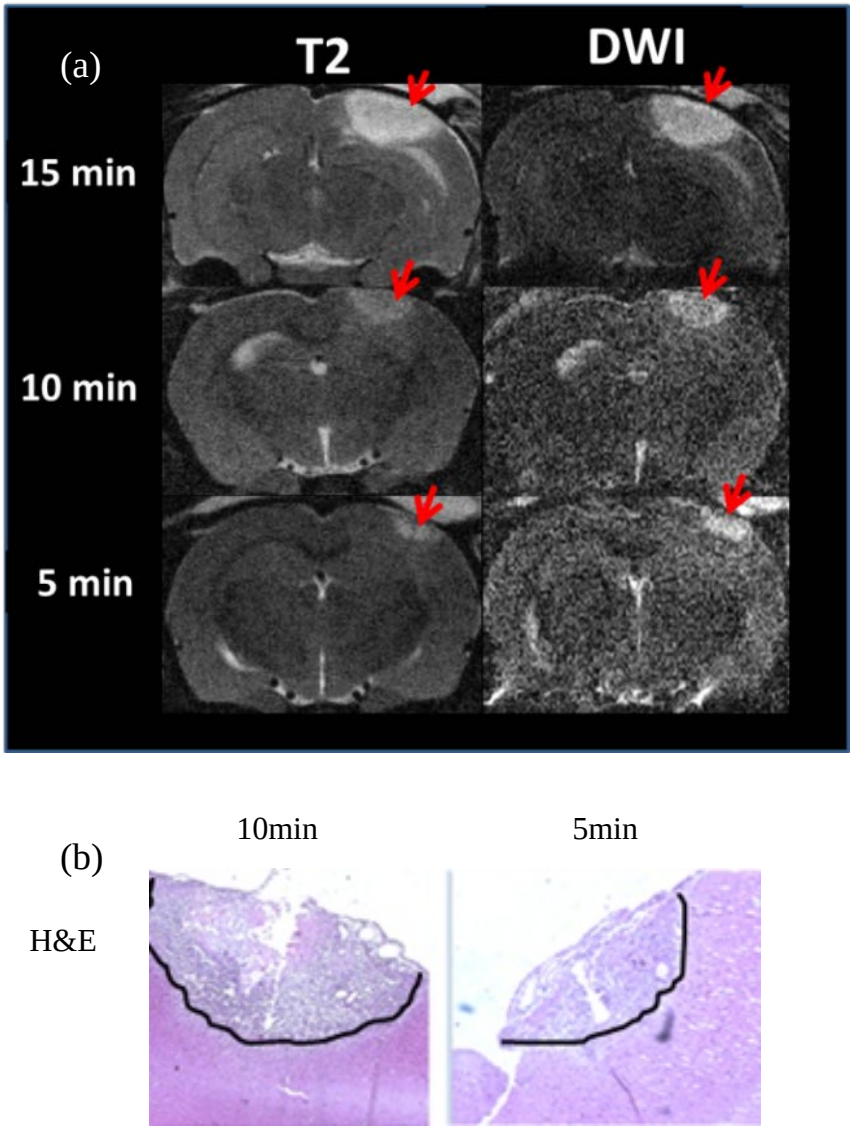

Figure 4.2.1 Effects of illumination duration on the severity of stroke (n=9). (a) Representative T2-weighted and diffusion-weighted images showed ischemic lesions had areas of hyperintensity (red arrows) after 15 min (n=1), 10 min (n=3) and 5 min (n=5) durations of illumination. (b) Representative micrographs of haematoxylin and eosin staining with10 and 5 min of illumination.

Figure 4.2.1 Effects of illumination duration on the severity of stroke (n=9)

(c)

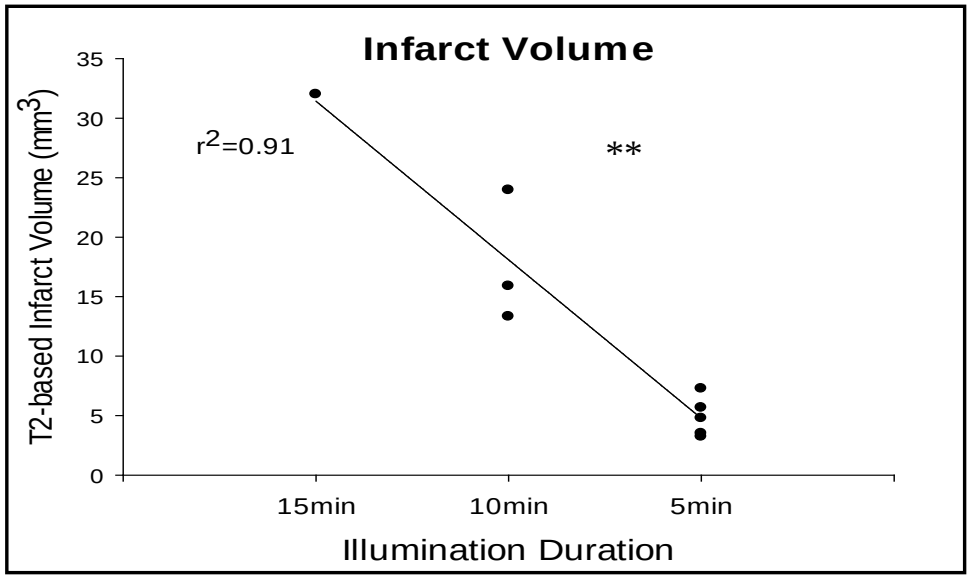

(d)

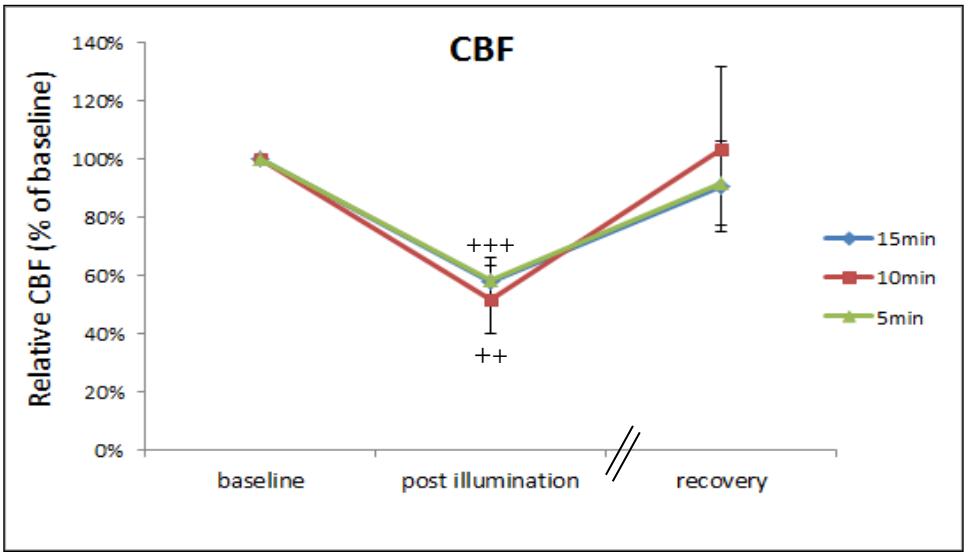

Figure 4.2.1 Effects of illumination duration on the severity of stroke (n=9). (c) Quantitative infarct volume measured from brightest regions of T2 map as illumination duration was varied (**p<0.01, 10min different from 5min, Paired Student's t-test). (d) Relative cerebral blood flow (% of baseline) measured with Laser-Doppler flowmetry prior to and post illumination in the different illumination duration groups. (++p<0.01, +++p<0.001 vs baseline, paired student t-test).

4.2.2 Effect of intensity of illumination on severity of ischemic damage detected with MRI

Four different groups light intensities with a duration of illumination of 5 min were studied in 5 rats per group. The intensity varied from a high light power (70,000 Lux) to a low light power (35,000 Lux). The lesion volume was measured from the brightest T2 region in T2 weighted images. Lesion volume decreased in tandem with the decrease of light intensity (Fig 4.1.2a) and there was a good correlation between them (r^2=0.81) under the conditions investigated. Furthermore, absolute T2 within the hyperintense area also decreased with decreases in light intensity resulting in a linear correlation between them (r^2=0.67). This indicated that as light power increased, the tissue damage was more severe. As the light intensity decreased from 45,000 Lux to 35, 000 Lux, the T2 relaxation time significantly decreased ($p<0.05$) whereas the T2-based lesion volume did not ($p>0.05$).

This study showed that the light intensity of approximate 35,000 Lux was able to produce a small lesion (3.92 ± 0.45 mm^3) with a mild T2 elevation (66.7 ± 11.1 ms). Thus, this light setting with a 5min duration of illumination was chosen for mild PT induction.

Figure 4.2.2 Correlation between light intensity and severity of ischemic damage assessed using MRI.

(a)

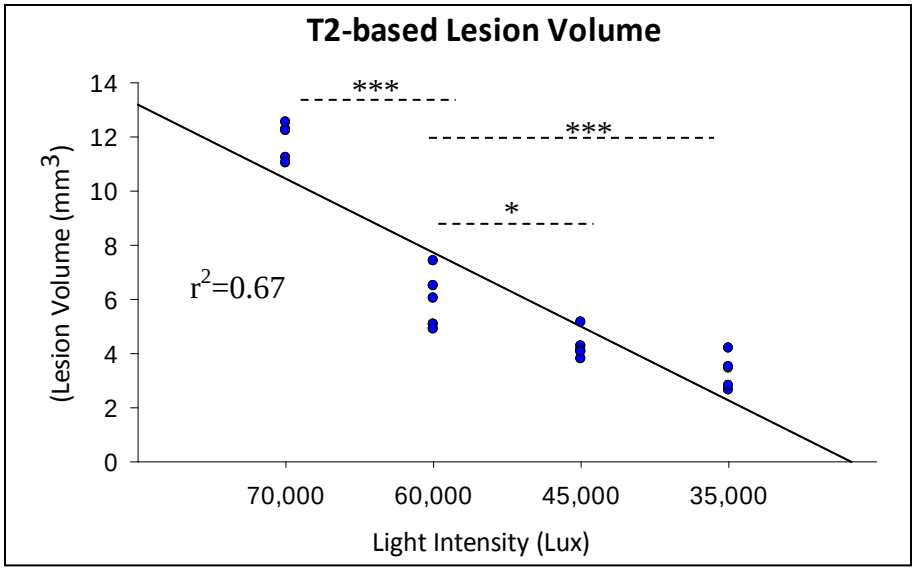

(b)

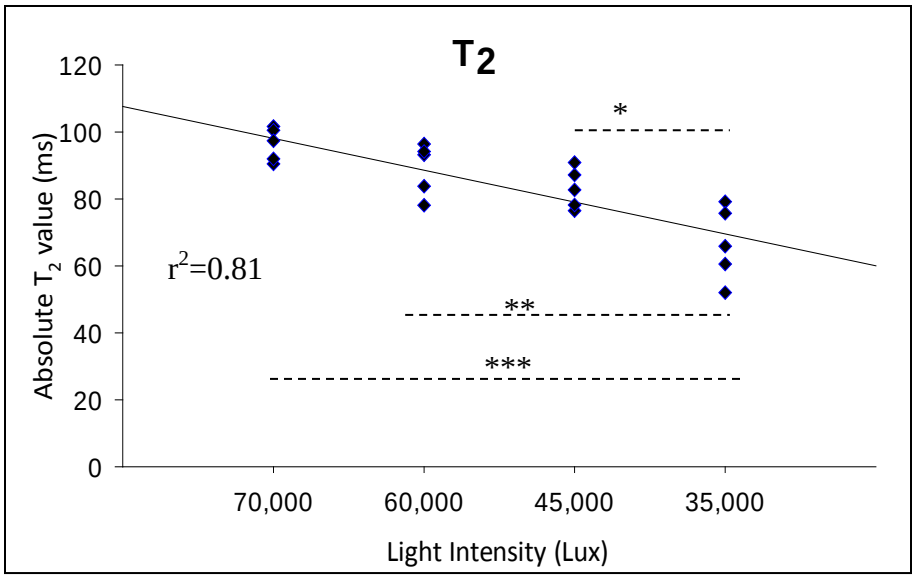

Figure 4.2.2 Correlation between light intensity and severity of ischemic damage assessed using MRI. Mean ±SD (n=5) lesion volumes measured from bright hyper-intense regions on T2-weighted images in (a) and mean T2 relaxation times in (b). (*p<0.05, **p<0.01, *** p<0.001, Differences significant, Bonferroni test)

4.2.3 Relationship between light intensity and cerebral perfusion measured by PWI.

Perfusion-weighted Images (PWI) were darkest in regions of infarct core and less dark in regions of peri-infarct. Visually, the area of greatest cerebral perfusion deficit matched that of brightest areas on T2 and diffusion image. In contrast, peri-infarct regions showed modest changes in perfusion and T2 that were not observed in diffusion-weighted images (Fig 4.2.3a). Quantification of relative PWI changes at 24h (Fig 4.2.3b) demonstrated that the PWI deficit in the region of infarct core was significantly greater than that of peri-infarct regions, and this difference was more pronounced with high light intensity ($p<0.01$) than low light intensity ($p<0.05$). The PWI in the core was less than 30% of control ($p<0.001$) at light intensities of over 60,000 Lux. In contrast, when the illumination light intensity was 35,000 Lux, cerebral perfusion in the core region was modestly diminished (79%±5% of control) and the peri-infarct region appeared to have fully recovered (111% ± 15% of control). This analysis of the PWI indicates that using conditions of 5min illumination at 35,000 Lux produces a relatively mild transient ischemia.

Figure 4.2.3 Relationship between light intensity and cerebral perfusion measured by PWI.

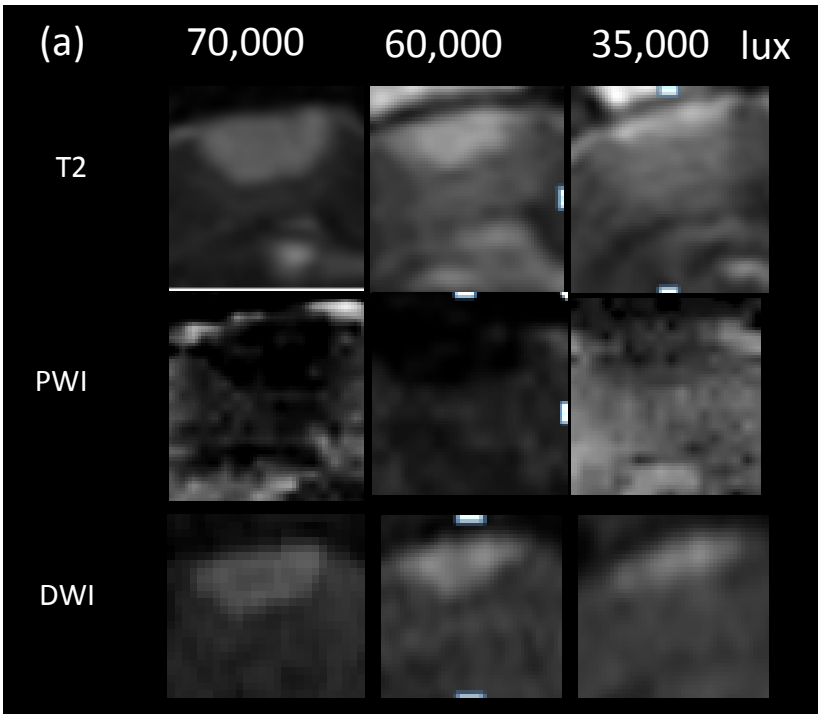

(b)

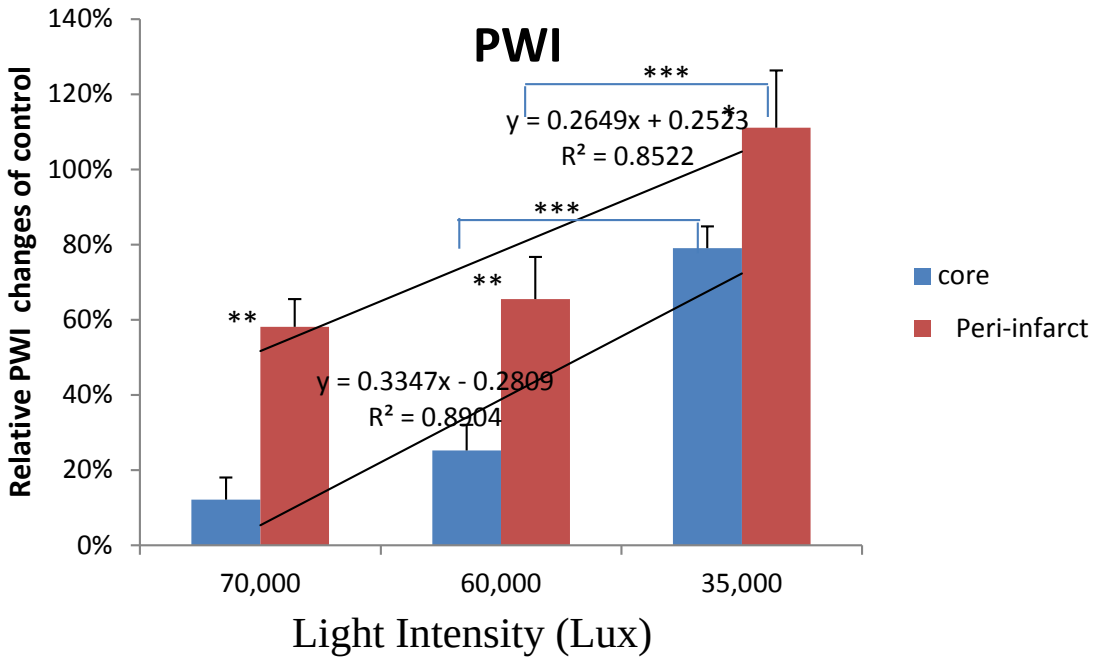

Figure 4.2.3 Relationship between light intensity and cerebral perfusion measured by PWI (continued).

(a) Representative T2, perfusion-weighted (PWI) and diffusion-weighted (DWI) images from animals illuminated at various light intensities for 5 min. (b) Mean±SD PWI changes in the core (upper cortex) and peri-infarct region. The change in perfusion was linear to the change of light intensity in both core and peri-infarct regions. (**p<0.01, ***p<0.001)

4.2.4 Different T2 values measured at 24h after PT were associated with different severities of ischemia.

The mean T2 value in normal brain was approximately 40ms. At 24 h after a single PT, there was a range of T2 changes observed. I divided the results into three groups with T2 of 50-70ms, 80-95ms, and >95ms resulting in 3 subgroups with T2 changes that were mild (57.48±6.35 ms, n=5), moderate (87.41±4.80 ms, n=4), and severe (100.03±2.97 ms, n=8), respectively. Histologically, at 2d post ischemia, the mild PT had a peri-infarct like lesion distributed uniformly in the illuminated area, consisting of selective necrosis. In addition, the tissue morphology was generally preserved compared to other groups. As T2 increased to 80ms, histologically the lesion consisted of an infarct in the superficial layer of cortex. Within the core infarct region, there were many dead cells. The core consisted of pale stained tissue with spongy vacuolated neutropil. Adjacent to the core was a less bright region of T2 similar to the mild PT group, where scattered neuronal loss was present. A complete infarct zone developed as T2 values reached above 100ms.

The good correspondence of histological severity of tissue damage with T2 values led us to conclude that T2 could be used as a non-invasive method to diagnose the severity of ischemic injury produced by PT.

Figure 4.2.4 T2 signatures reflect well the tissue damage.

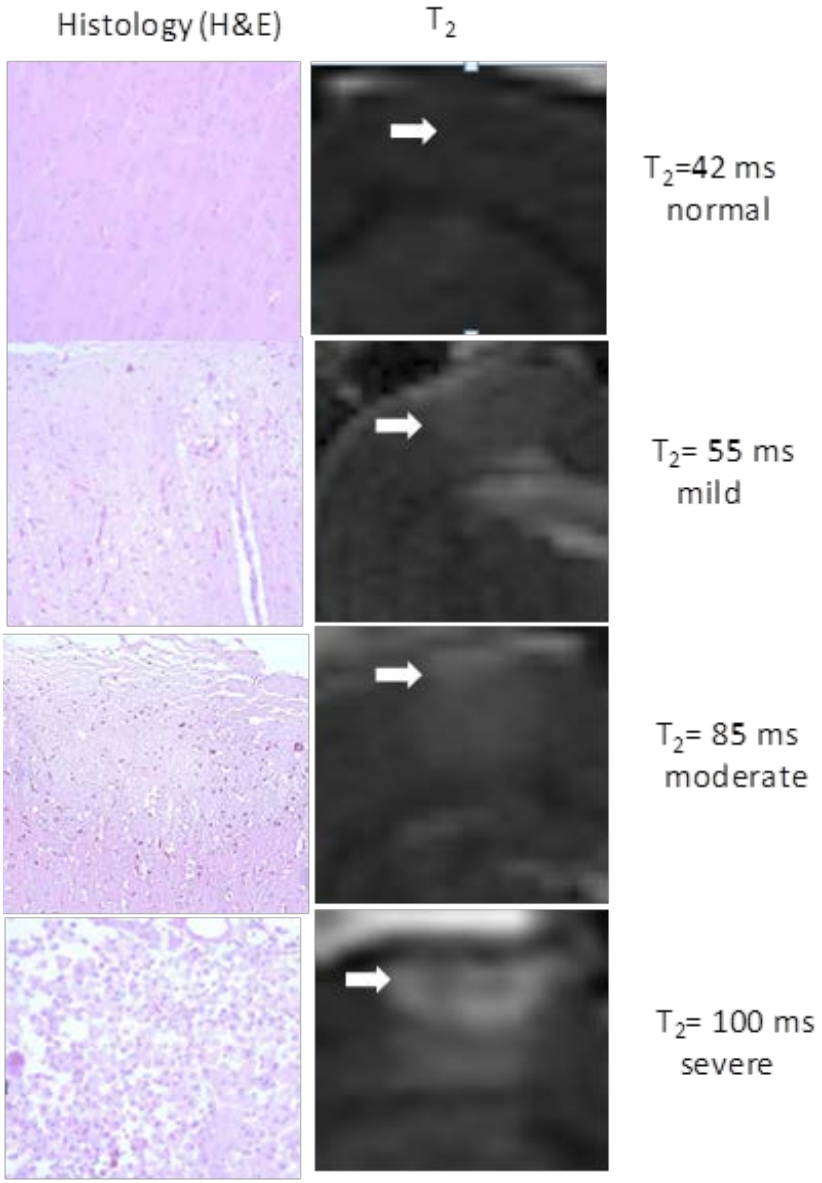

Figure 4.2.4 T2 signatures reflect well the tissue damage. The first column presents representative micrographs of the histology observed in coronal sections stained with H&E at various T2 values. The second column shows the corresponding T2 images with white arrows emphasizing the regions of T2 change.

4.2.5 MR signatures differ in different regions following PT induction (n=5).

Inspection of the T2 and DWI images with PT produced by illumination above 45,000 Lux for 5 min showed some qualitative differences in the areas of increased intensity changes in T2 and DWI images (Fig 4.2.5 a and b). These regions were referred to as a region of infarct core and a region of peri-infarct. Histological assessment (Fig 4.2.5c) showed that the regions of brightest intensity change reflected a core region with pannecrosis whereas peri-infarct regions with increased T2 had signs of scattered necrosis. Quantitative measures of T2 and ADC in core areas of maximal intensity change and peri-infarct regions (Fig 4.2.5d) indicated significant differences between the two. There was a significant ADC reduction in the infarct core ($p<0.05$ vs control) but not the peri-infarct region, whereas T2 was increased significantly in both core ($p<0.001$) and in the peri-infarct region ($p<0.001$). This indicated that T2 was better at detecting mild injury compared to ADC. Thus in the second objective of recurrent PT induction, T2 measurements were used as the major MRI criteria for selection of animals for recruitment and analysis.

Figure 4.2.5 Quantitative MR changes in regions of infarct core, peri-infarct and normal tissue.

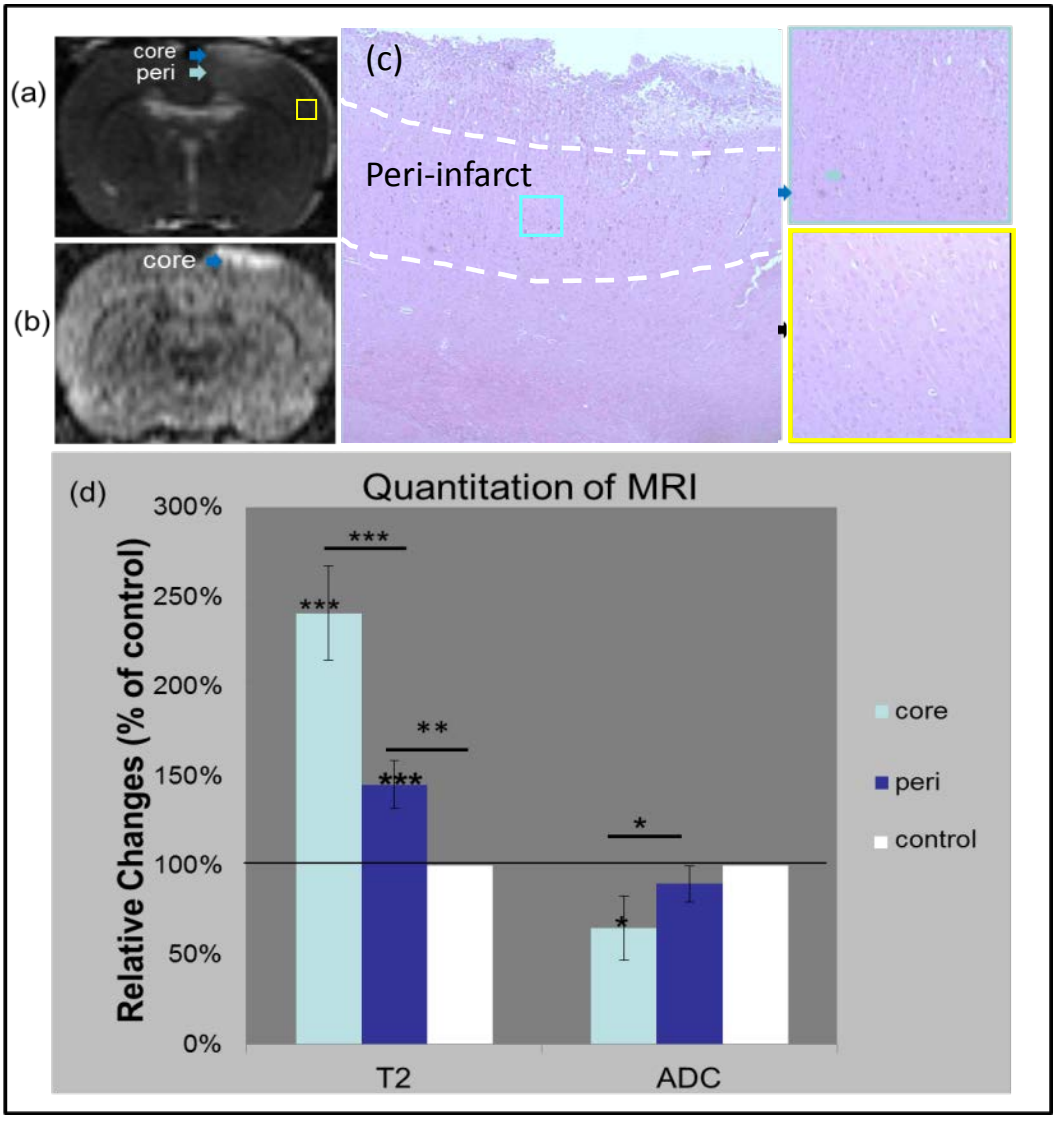

Figure 4.2.5 Quantitative MR changes in regions of infarct core, peri-infarct and normal tissue (continued).

(a) Representative T2-weighted image showing the intensity changes at 24h after PT in subregions of core (blue arrow), peri-infarct (green arrow) and normal tissue (yellow square). The corresponding representative DW image shows intensity changes in the PT area at 24h after PT (b). (c) Corresponding representative micrographs of brain sections stained by haematoxylin and eosin demonstrate different severities of tissue damage in the core and peri-infarct regions. (d) Mean $\pm$ SD MR changes measured in the core and peri-infarct regions (presented as % of control). (*$p<0.05$, **$p<0.01$, ***$p<0.001$, significantly different, Paired Student's t-test)

4.2.6 Summary and Conclusions of Objective 1

The results demonstrate that the PT model can be modified to produce mild ischemic brain injury: A thinned skull exposed to white light at 35,000 Lux of intensity for 5min was able to produce a mild injury consisting of a region of selective neuronal death and in some animals a small region of pannecrosis. Cerebral blood flow measured by Laser-Doppler flowmetry recovered quickly post illumination and at 24h flow measured with PWI progressed to a mild decline. Measures in the regions of interest indicate a mismatch between T2/PWI and diffusion-weighted imaging changes. The alterations in T2 and PWI were milder than those in the core and were considered representative of peri-infarct or penumbra. Despite DWI being largely used in acute stroke imaging to identify infarction, in the current study it was less sensitive in detecting peri-infarct compared to T2/PWI. T2 changes correlated well with histology in demarcating lesion volumes and in grading the severity of cell death. Thus, PT ischemic injury is best detected using T2 imaging and for Objective 2 we focussed on using T2 to assess the severity of damage after either the first or second insult.

4.3 Objective 2: Recurrent PT Induction

4.3.1 Animal subgroups and selection criteria for analysis

In parallel to recurrent PT experiments, control experiments were also performed. In 2 rats that experienced single sham surgery (saline injection plus illumination), the 24h MRI did not show abnormality. The T2 relaxation time was in normal range (approximate 41ms).

A total of 65 rats were used in recurrent PT experiments. Successful recurrent PT was produced in 39 animals and 36 of them were recruited for MRI and histological analysis. 9 animals died after surgery. In 10 animals there were no T2 lesions visible after recurrent PT and these were excluded. Table 4.3.1 lists the detailed selection criteria and mortality of subgroups. There was an increase of mortality as the time interval between two surgeries was shortened, which was potentially related to lung complications and the stress of multiple surgeries and anesthesia for MR imaging.

.

Table 4.3.1 Animal number of subgroups and selection criteria for analysis

	Initial Amount	No T2 lesion	a1≠a3	Abnormal MRI Map	Died (Mortality)	Successful Amount	Recruited For Analysis
1d group	16	5	0	0	4(25%)	7	6
2d group	17	1	3	0	2(11.7%)	11	10
3d group	18	4	0	1	2(11.1%)	11	10
1wk group	14	0	3	0	1(7.14%)	10	10
Total	65	10	6	1	9(13.8%)	39	36

a1=area 1(single illumination region at 1st PT); a3= area 3 (single illumination region at 2nd PT). Abnormal MRI Map may present as blurred images or abnormal T2 map.

4.3.2 Criteria of regrouping animals into two main cohorts.

For the 39 rats with a successful induction of recurrent PT, despite care with illumination parameters, the ischemic lesion produced was still somewhat variable. Some of the first PT insults were more severe than those that were clearly mild. Thus, using all the data with recurrent PT insults, I separated groups according to whether the first PT was mild (Initial-Mild cohort) or severe (Initial-Severe cohort). In the Initial-Mild group (Fig 4.3.2a), the T2 was modestly elevated uniformly in the upper, middle and lower layers of illuminated cortex (n=5 per subgroup). In the Initial-Severe group (Fig 4.3.2b), there was a small hyper-intense region located in the upper layer (infarct core) with a less hyper-intense region underneath (adjacent peri-infarct and remote peri-infarct). Each subgroup contained 5 animals except for the 1d subgroup that only had 1 rat recruited to the Initial-Severe group.

Figure 4.3.2 Representative T2 images post 1st and 2nd PT for the different subgroups of varied time intervals between two ischemic events for the Initial-Mild (a) and the Initial-Severe (b) cohorts.

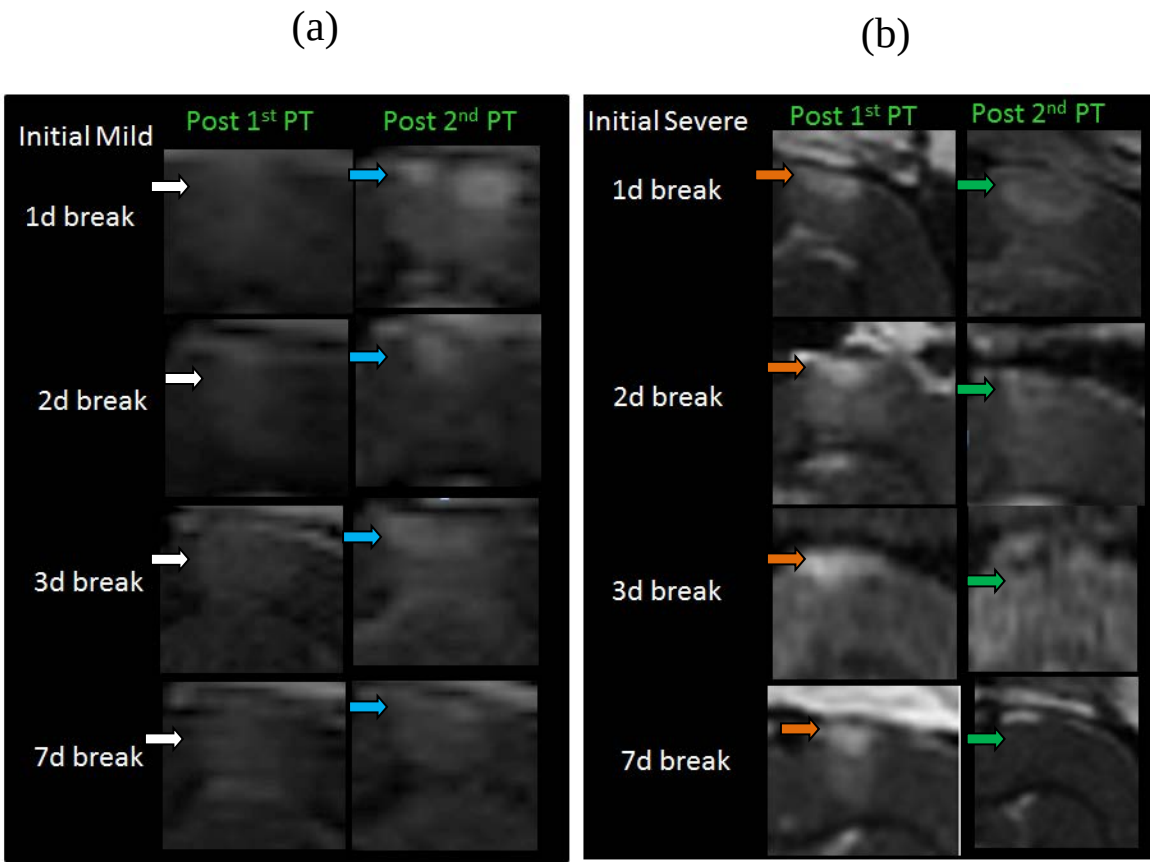

In the Initial-Mild (a) cohort, T2 had visually mild hyperintensities (white arrow) in the illuminated area of each subgroup. After a second PT induction, an enhanced T2 elevation was visually apparent in upper layer of cortex in each subgroup (blue arrow).

In the Initial-Severe (b) cohort, a T2 hyperintenisty was apparent in the upper layer (core, yellow arrow) of illuminated cortex. In this cohort, the hyper-intense T2 signal normalized visually regardless of whether a recurrent PT was produced (green arrow).

4.3.3 Body temperature recorded during and post the 1st and 2nd PT surgery

Animals were monitored carefully during and after surgery to maintain optimal ventilation and anesthesia level. The body temperature between groups before each illumination was similar (Table 4.3.3). The illumination of the cortex for 5min with approx. 35,000 Lux did not increase the rat's body temperature measured rectally. Rectal temperature after surgery was monitored for 1h and the measurement was normal at approx. 37℃, indicating a good recovery of the animals from the PT and surgery.

Table 4.3.3 Body temperatures measured by rectal probe at different time points in varied groups.

Temp (℃)		1st PT			2nd PT		
		before illumination	after illumination	post surgery	before illumination	after illumination	post surgery
Initial mild	1d group(n=5)	37.0±0.16	37.2±0.22	37.0±0.23	37.0±0.59	36.8±0.35	37.0±0.18
	2d group(n=5)	36.9±0.35	37.1±0.37	37.0±0.21	37.0±0.24	37.0±0.15	37.0±0.21
	3d group(n=5)	37.1±0.27	37.1±0.15	37.0±0.11	37.1±0.51	37.0±0.27	37.0±0.19
	1wk group(n=5)	37.0±0.27	37.1±0.29	37.0±0.19	37.0±0.18	37.1±0.22	37.0±0.21
Initial severe	1d group(n=1)	37.2	37.3	37	36.9	37.1	37.2
	2d group(n=5)	36.9±0.26	37.0±0.26	37.0±0.41	36.9±0.30	37.1±0.28	37.1±0.25
	3d group(n=5)	37.5±0.37	37.4±0.30	37.0±0.42	37.0±0.29	37.3±0.27	37.0±0.19
	1wk group(n=5)	37.0±0.41	37.1±0.34	36.9±0.10	37.2±0.25	37.2±0.13	37.0±0.21

Data presented as Mean ± SD. Mean body temperature was similar at the different time points for the different interval groups ($p>0.05$, multiple comparison using ANOVA followed by Bonferroni t-test).

4.3.4 Quantitative T2 changes in the Initial-Mild cohort

4.3.4.1 Comparison of absolute T2 changes after the 1st and 2nd PT

In this cohort, the T2 relaxation time at 24h after the 1st PT was significantly elevated ($p<0.05$ vs normal) in the upper layer of illuminated cortex. The mean T2 increased further following a 2nd PT ($p<0.01$ vs 1st PT) produced at an acute recovery time (1day to 3day) after the 1st PT. T2 values were also elevated in the middle and lower layers but to a lesser degree. With a more chronic interval between insults, the T2 elevation after the 2nd PT was modest in the upper and lower layers compared to the change after the 1st PT ($p>0.05$). It was noticed that the normal T2 value in brain not affected by PT had some variability, e.g. due to the potential variations of the animal, coil and MRI system. Thus, to control for such variations, in the next section, comparisons of T2 between groups was made using a normalized value of T2 where T2 was converted to a % of normal.

Figure 4.3.4.1 Absolute T2 values for different ROIs obtained after the 1st and 2nd PT in the different interval subgroups of the Initial-Mild cohort.

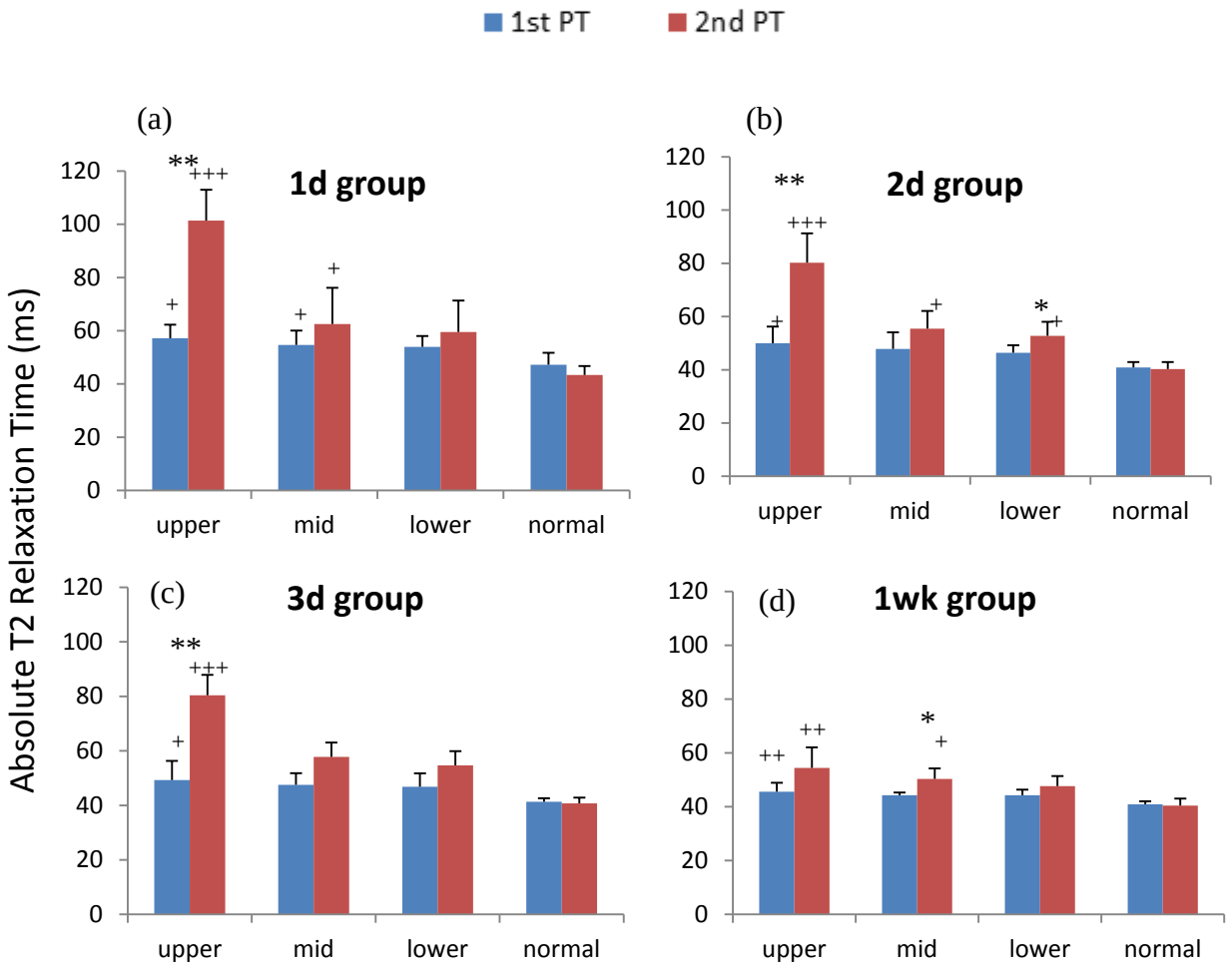

Figure 4.3.4.1 Absolute T2 values for different ROIs after the 1st and 2nd PT in the different interval subgroups of the Initial-Mild cohort (n=5 per group)**.** Representative absolute T2 changes at 24h after a 1st PT (blue column) and a 2nd PT (red column) for interval groups of 1day (a), 2day (b), 3day (c) and 1week (d) between insults (*p<0.05, **p<0.01, 1st different from 2nd, paired Student's t-test; +p<0.05, ++p<0.01, +++p<0.001 vs normal/control; Bonferroni t-test)

4.3.4.2 Comparison of relative T2 changes in different ROIs for the interval subgroups after a 1st and 2nd PT.

After the 1st PT induction, T2 elevations were modestly elevated to similar levels (less than 121% of control) ($p>0.05$) between groups in each layer. Following the second PT, the increase of T2 was more pronounced as the time interval between insults became shorter. In the upper layer, T2 changes with shorter intervals (1day to 3day) significantly exceeded those in the 7day interval group, which had the smallest T2 increase (134.9%± 20.3%). Although the T2 increase of the 1d interval group (234.3%±29.1%) was greater than that of 2d and 3d, these changes were not significant.

In the middle and lower cortical layers (peri-infarct), the T2 increases in each group were similar ($p>0.05$) and were less than in upper layer (infarct core). This indicated that there was a milder brain damage in the peri-infarct region than in the infarct core.

Figure 4.3.4.2 Relative T2 changes (% of normal) in different ROI after a 1st and 2nd PT for the different interval subgroups of the Initial-Mild cohort.

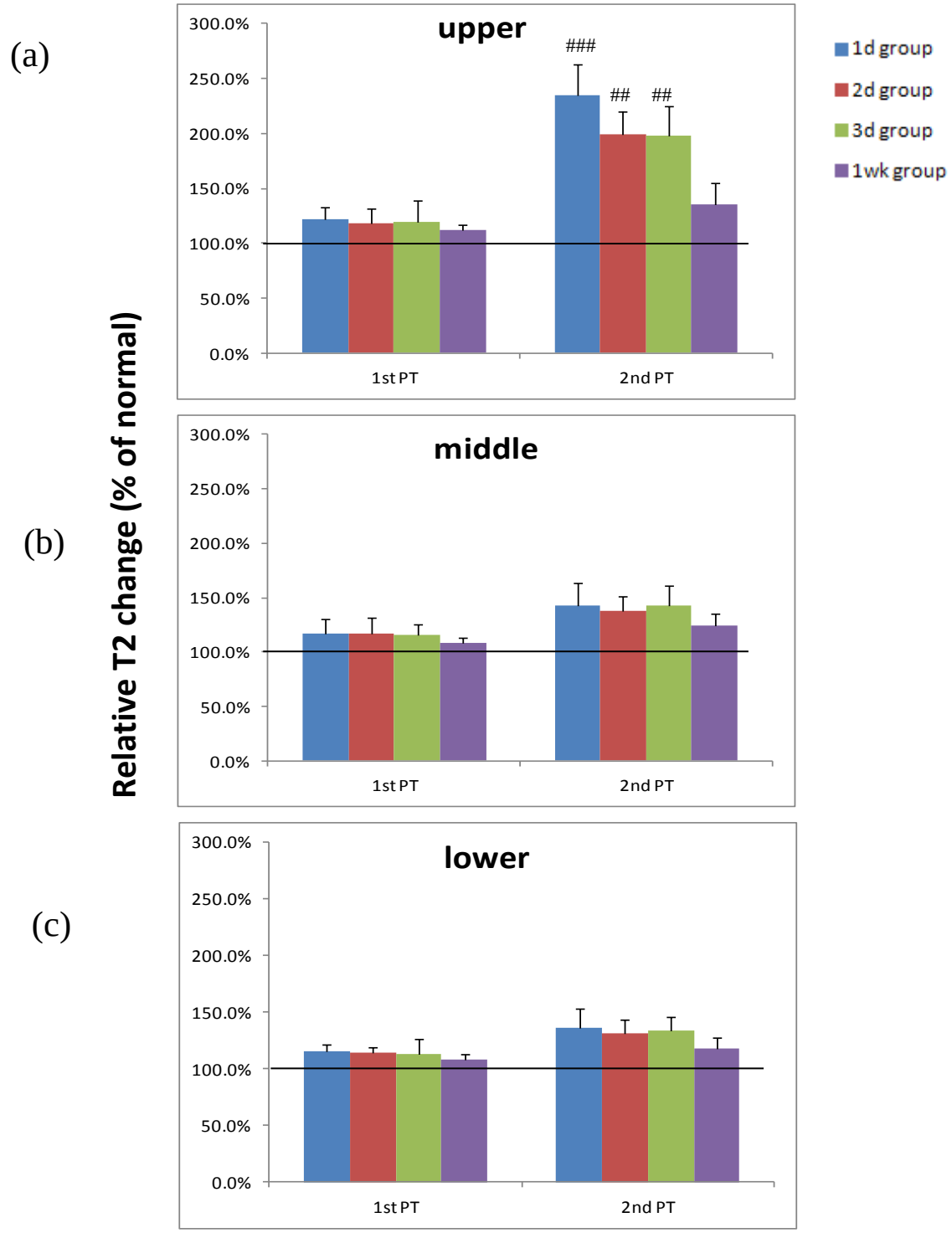

Figure 4.3.4.2 Relative T2 changes (% of normal) in different ROI after a 1st and 2nd PT for the different interval subgroups of the Initial-Mild cohort (continued). Mean±SD (n=5) T2 changes 24h after the 1st PT or 2nd PT in upper (a), middle (b) and lower(c) layers with varied time intervals between two episodes of mild ischemia. T2 increases between groups were similar ($p>0.05$) in each layer after the 1st PT but differed in the upper layer after the 2nd PT. In deeper layers, T2 increases were mild and not significantly different between groups (##$p<0.01$, ###$p<0.001$ different from 7d group, Bonferroni t-test).

4.3.4.3 Comparison of T2 changes in area 1 and area 3

Absolute T2 relaxation time measured in area 1 and area 3 in each interval subgroup were similar ($p>0.05$), indicating that the light conditions between the 2 PTs were consistent and the enhancement of T2 insults after the 2nd PT was not caused by potential variations of light intensity. Each group had 5 rats except the 3d interval group containing 4 rats.

Figure 4.3.4.3 Absolute T2 changes in area 1 and area 3 with varied time intervals for the Initial-Mild Cohort.

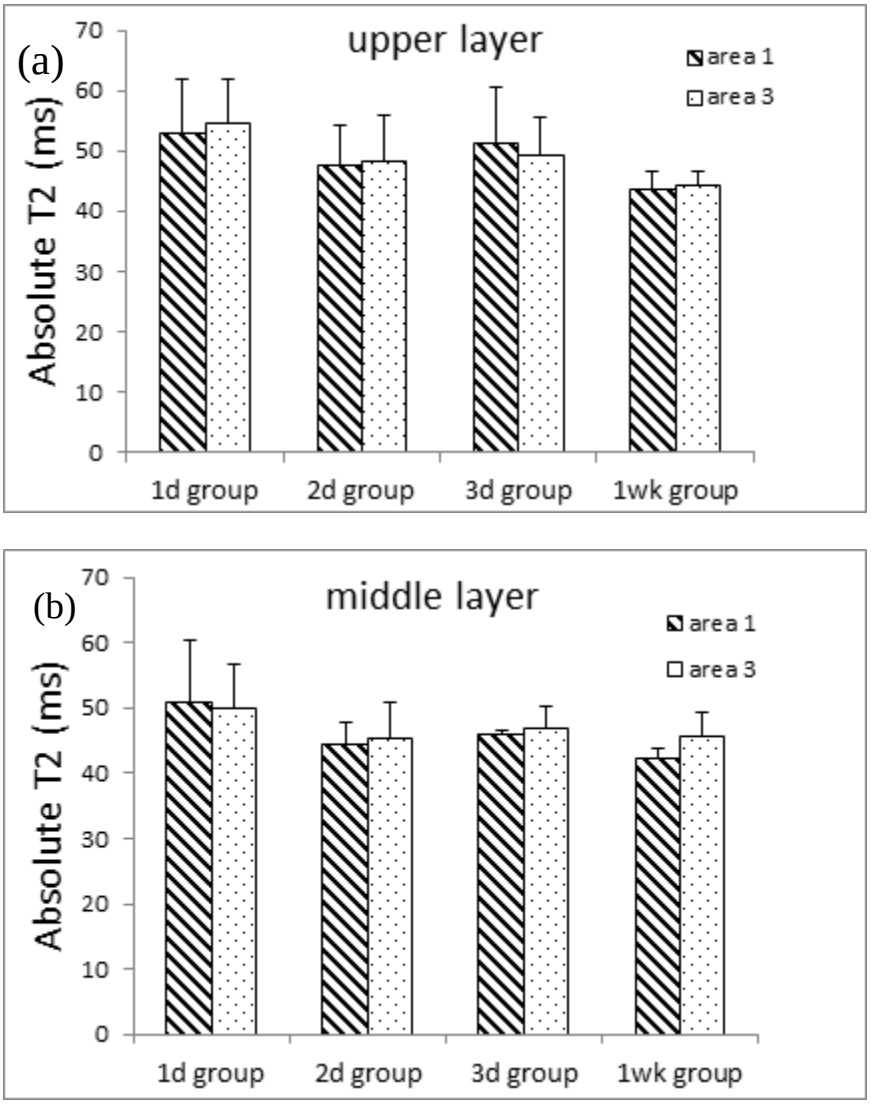

Figure 4.3.4.3 Absolute T2 changes in area 1 and area 3 with varied time intervals for the Initial-Mild cohort (continued).

Mean±SD (n= 4 or 5) T2 changes in the upper (a) and middle (b) layer of area 1 and area 3 for the various time interval groups. Difference of means between the two areas in each group were not significant ($p>0.05$, Paired Student's t-test).

4.3.5 Quantitative T2 changes in the Initial-Severe Cohort

4.3.5.1 Absolute T2 relaxation after a 1st and 2nd PT with various intervals between them.

Each interval group contained 5 rats except for the 1d group (n=1). Similar to the Initial-mild cohort, the normal control T2 values measured in non-illuminated cortex of all groups was similar between the 1st and 2nd PT. In the core region, the T2 relaxation time was markedly elevated after a 1st PT ($p<0.001$vs normal), whereas it was decreased after a 2nd PT (Fig 4.3.5.1). The decrease was more pronounced when the 2nd PT occurred at 1week ($p<0.01$) compared to at 2d or 3d ($p<0.05$) after the 1st insult. In the 2d interval group, the T2 value after a 2nd PT remained elevated compared to that in the normal control region ($p<0.01$ or $p<0.001$). Different from the other groups, T2 relaxation in the 1d group (n=1) had a further increase above 100ms in adjacent and remote peri-infarct regions, indicating an exacerbation of tissue damage in these regions.

Figure 4.3.5.1 Absolute T2 in the different ROI after a 1st or 2nd PT for the various interval groups of the Initial-Severe cohort.

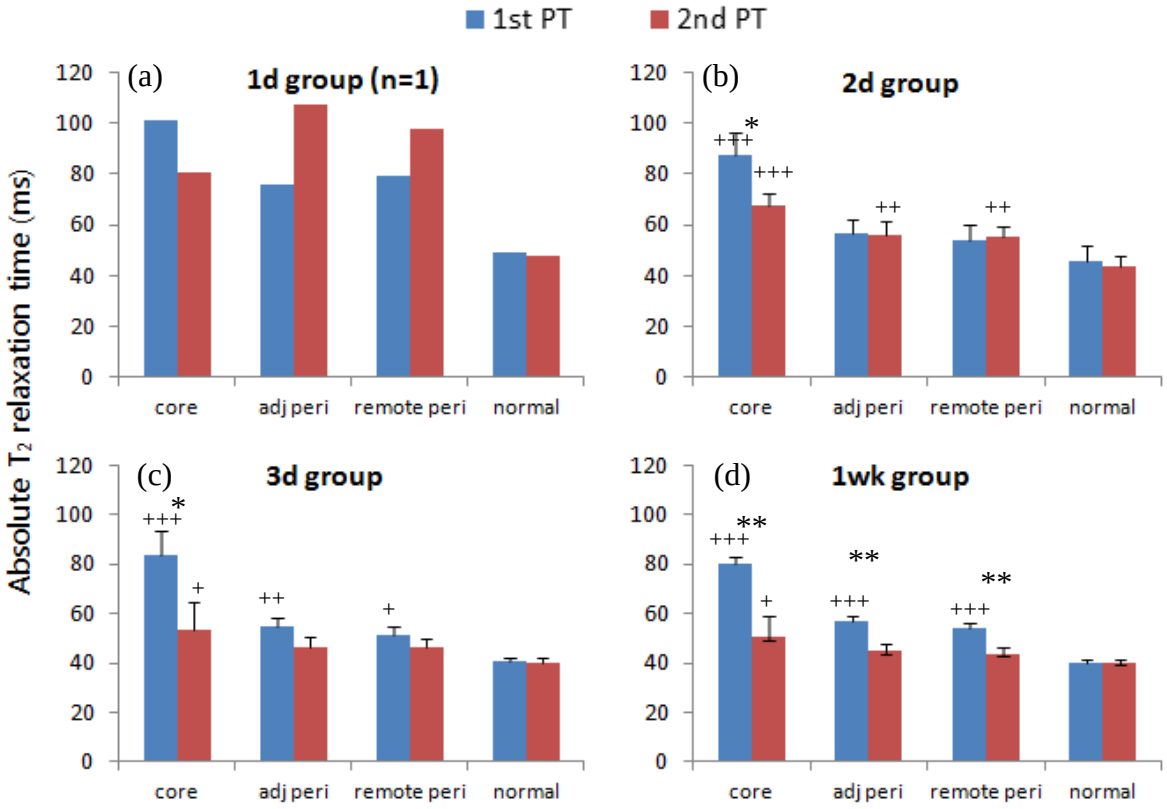

Figure 4.3.5.1 Absolute T2 in different ROI after a 1st and 2nd PT for the various time interval groups of the Initial-Severe Cohort. Shown are the T2 values in groups with 1day (a, n=1), 2day (b, n=5), 3day (c, n=5) and 1week (d, n=5) intervals between the 1st (red) and 2nd (blue) insult. (+p<0.05, ++p<0.01, +++p<0.001, different from normal control, Bonferroni t-test; *p<0.05, **p<0.01, 1st PT different from 2nd PT, Paired Student's t-test)

4.3.5.2 Quantification of relative T2 changes (% of normal control)

In this Initial-Severe cohort, the T2 elevation after the 1st PT was similar in the core region of the different interval groups, but differed in deeper cortex depending on the time between insults ($p<0.01$, 2d vs 1wk). T2 had the greatest increase in the core with means above 190% of control, followed by lesser increases in regions of peri-infarct (<145%) and remote-infarct (<140%).

Following a 2nd PT, the T2 for all interval groups declined towards the normal control level in the core region. Although T2 in 1week group had the biggest decrease, its change was not significant compared to the other interval groups ($p>0.05$). In the peri-infarct regions, where the first T2 elevation was mild, there was an increase of T2 in the 2d interval group ($p<0.05$ vs 1week). This suggested an enhancement of tissue damage in these regions.

The major finding of this section was that when the initial ischemia led to severe MR changes, a 2nd PT was unlikely to produce a further increase in T2. This suggests a potential for distinguishing severities of recurrent stroke in the clinic.

Figure 4.3.5.2 Relative T2 changes (% of normal) in the Initial-Severe Cohort.

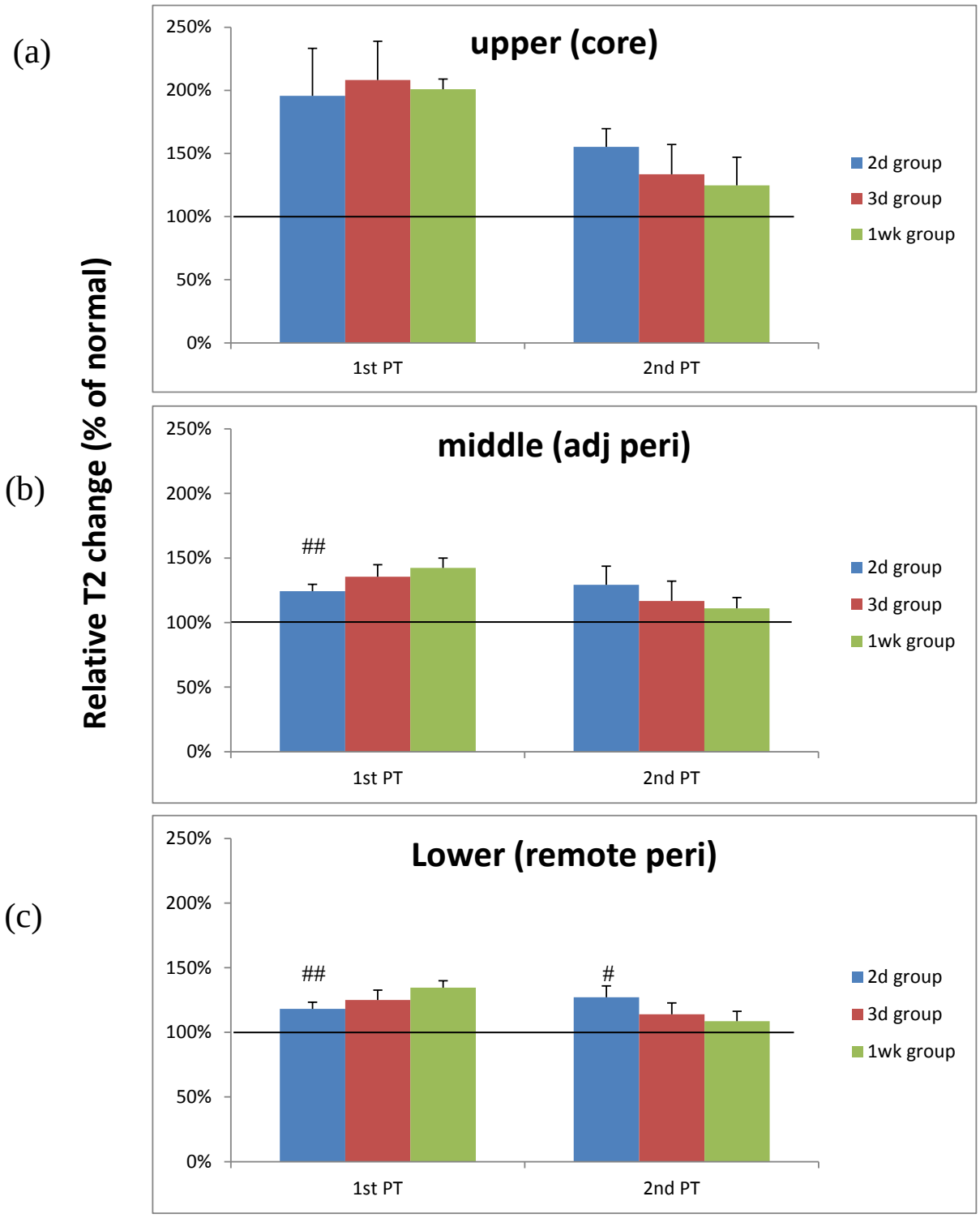

Figure 4.3.5.2 Relative T2 changes (% of normal) in the Initial-Severe Cohort (continued).

Shown are the mean±SD (n=5) T2 changes after a 1st PT and 2nd PT for regions in the upper (a), middle (b) and lower(c) layers of cortex (#p<0.05, ##p<0.01 different from 1week group, Bonferroni test).

4.3.5.3 Comparison of T2 changes in area 1 and area 3.

Similar to the results of the Initial-Mild cohort, the absolute T2 relaxation time measured in area 1 and area 3 in each interval group of the Initial-Severe cohort were similar ($p>0.05$). This indicated that there was a consistency of light conditions between the two PTs and the observed MR signatures and tissue damage were a result of repetitive ischemia.

Figure 4.3.5.3 Absolute T2 changes in area 1 and area 3 for the various time interval groups of the Initial-Severe cohort.

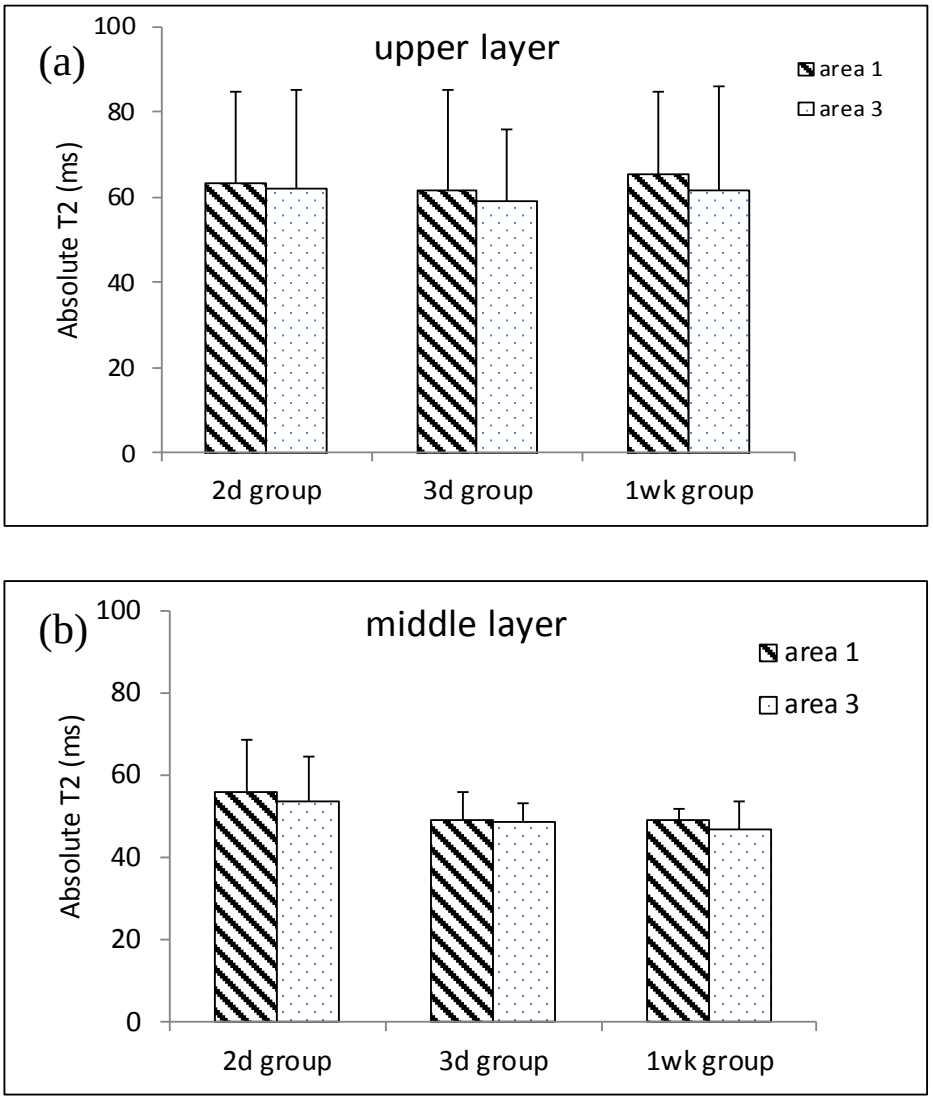

Figure 4.3.5.3 Absolute T2 changes in area 1 and area 3 for the various time interval groups of the Initial-Severe Cohort (continued).

Shown are the mean±SD T2 relaxation times measured in the regions of upper (a) and middle (b) layer of area 1 and area 3. T2 between the two areas was similar ($p>0.05$, Paired Student's t-test). Animal number: 2d group (n=4), 3d group (n=3) and 1wk group (n=5).

4.3.6 Histological score in the two cohorts

In the Initial-Mild cohort, similar to the greatest increase of T2 occurring in the upper cortical layer (see Figure 4.3.4.2), there was most extensive tissue damage as assessed using the histological score in the upper layer (a), followed by lower scores in the middle (b) and lower layers (c) (Fig 4.3.6). Histological scores in the groups with shorter intervals (1day to 3 day) significantly exceeded the group with the longer interval of 1week between insults. The differences in histological scores between the acute interval groups were not significant for all layers. These scores reflected well the corresponding T2 changes. Similarly, in the lowest cortical layers (c), where T2 increases were mild and similar between groups, so were the histological scores which ranged from 0-1. The cumulative scores (d) reflected a significant enhancement of histological deficit for the shorter interval groups (1d to 3d) compared to the 1week interval group. The comparison to the 2day interval group did not reach statistical significance ($p=0.056$) which is likely due to the large variation of score in this group.

In Initial-Severe Cohort, the 2day interval resulted in more pronounced tissue damage than for the 1week interval, as reflected in the cumulative score of all layers ($p<0.05$). In region of core (upper) where T2 relaxation decreased after 2nd PT (see Figure 4.3.4.1), the tissue had developed into infarct in all rats (e). In the region of adjacent peri-infarct (middle), the 2day interval group had a greater histological damage score than the 3day and 1week interval groups ($p<0.05$ or 0.01), corresponding to the T2 relaxation changes in this region.

In comparing scores between the two cohorts, there was no significant difference between them ($p>0.05$), despite patterns of T2 changes being different between the two.

Figure 4.3.6 Histological scores in the two cohorts.

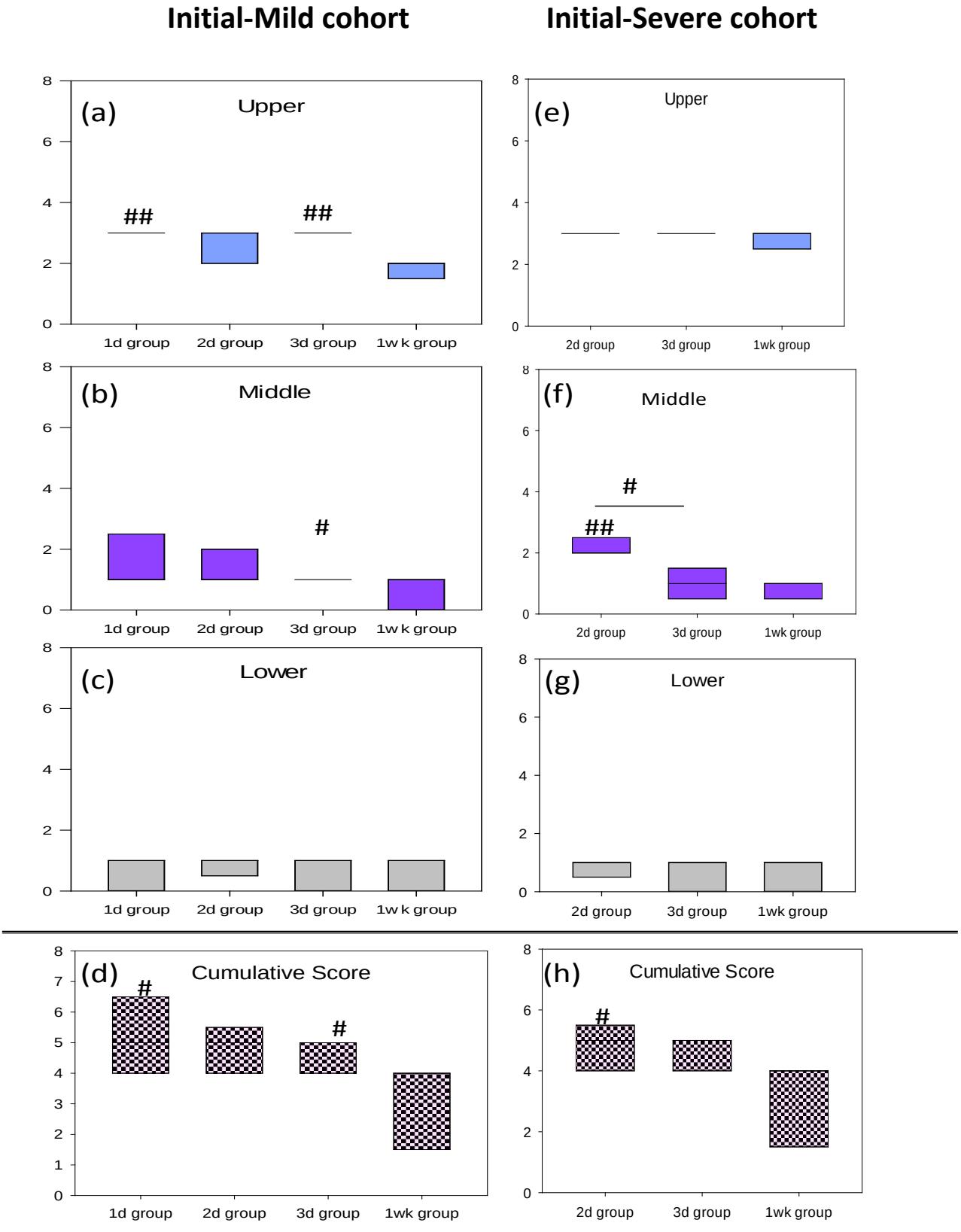

Figure 4.3.6 Histological scores in the two cohorts (continued).

Shown are whisker plots for the histological scores (n=5 per group) in the different layers of upper (a), middle (b), lower (c) for the Initial-Mild cohort. Also shown are histological scores in different layers (upper (e), middle (f) and lower (g)) for Initial-Severe cohort. The cumulative scores in Initial-Mild (d) and Initial-Severe (h) cohorts are similar (#$p<0.05$, ##$p<0.01$ different from 1wk group, Mann-Whitney test on rank sum).

4.3.7 Histological study over time following a single PT and comparisons between recurrent PTs to a single PT

The cumulative score of the three ROIs was used for a comparison of recurrent PT to single PT with a similar recovery time post-insult. Similar to the recurrent cohorts, rats with a single PT were separated into two groups - single mild and single severe with varied survial times from 1day to 1week. The former had 24h T2 signatures less than 70ms and the latter had T2 values above 80ms.

Brain tissue damage produced by PT, either mild or severe, developed over time ($p<0.05$). The severe group with higher T2 relaxation had a constant higher histological score than the mild group at subacute time points ($p<0.05$ or 0.01).

Compared with single PT, recurrent PT at acute time intervals resulted in more pronounced tissue damage. In the mild cohort, recurrent PT with 1day ($p<0.001$) to 3day ($p<0.05$) intervals significantly enhanced brain damage more than a single PT. However, cummulative ischemic damage with an interval between insults of 1week had the least enhancement and the median score was similar to a single insult ($p>0.05$). Likewise, in the severe cohort, a 1day interval between insults ($n=1$) had a highest score of 7. Recurrent ischemia with a 2d interval had a higher histlogical score than a single PT ($p<0.05$), whereas the enhancement was not significant with intervals longer than 3days between insults ($p>0.05$) (Fig 4.3.7a). Taken together, this suggested that there might have a protective mechinism or substantial recovery by 1 week reducing the additive effects of multiple insults.

Micrographs of coronal brain slice of each group (Fig 4.3.7b) revealed a big area of severe tissue deintergrity after recurrent PT with short intervals (1d to 2d). The brain

slice of 1wk interval had good preservation of tissue morphology within the illuminated cortex. This implied a close relationship between the recovery time and the final ischemic injury.

Figure 4.3.7(a) Cumulative histological score over time after a single PT and comparisons of single and recurrent PT.

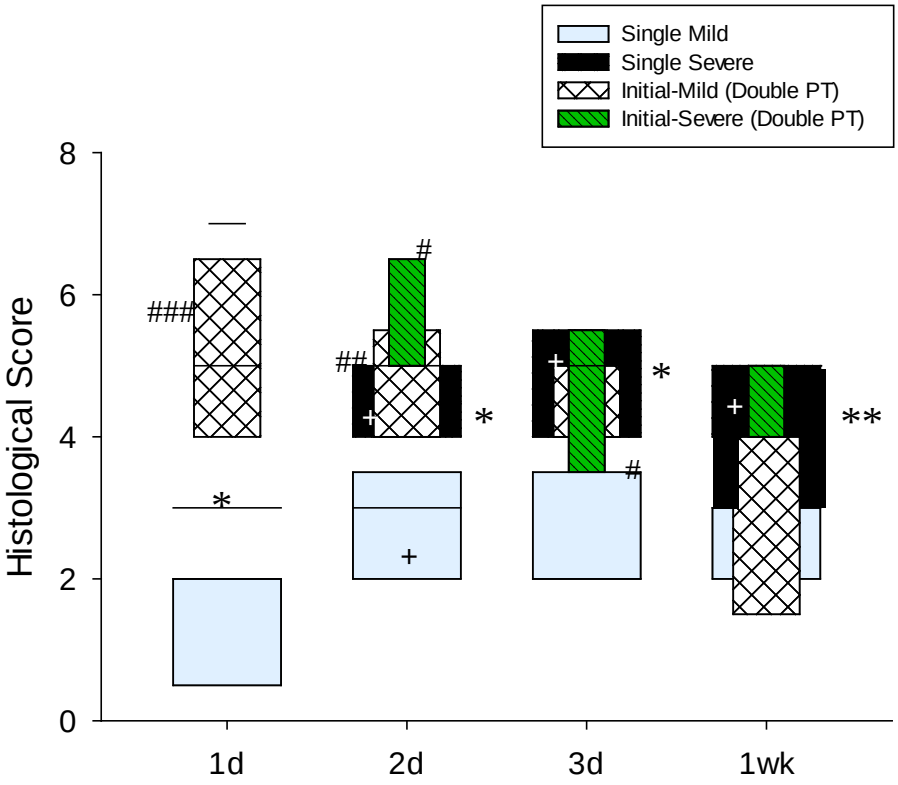

Shown are whisker plots of the histlogical scores. Sample size for the single and recurrent PT groups was 5 except for the severe single 1day and 2day groups which had 4. The 1day interval groups in the Initial-Severe cohort contained only 1 rat and was not plotted and in this graph (+$p<0.05$, score at varied time point after single PT different from day 1 score; *$p<0.05$, **$p<0.01$, single mild different from single severe; #$p<0.05$, ##$p<0.01$, ###$p<0.001$ single different from corresponding recurrent group).

Figure 4.3.7(b) Representative histological micrographs stained with Haematoxylin and Eosin.

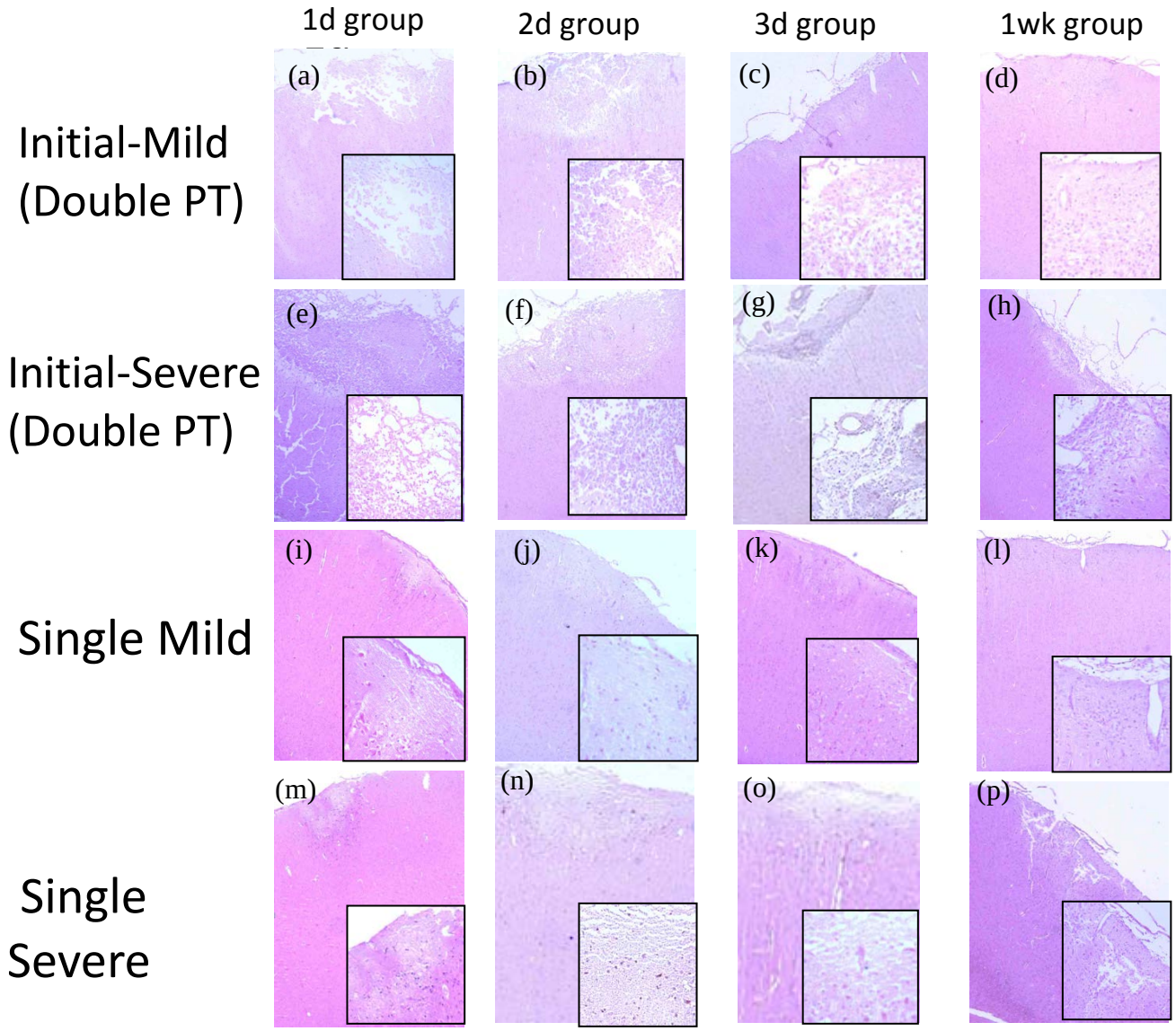

Figure 4.3.7(b) Representative histological micrographs stained with Haematoxylin and Eosin (continued).

The First two rows were representative micrographs in Initial-Mild (a to d, 1st row) and Initial-Severe (e to h, 2nd row) cohort with varied time intervals. Coronal brain slides in single mild PT (i to l) and single severe PT (m to p) at corresponding survival time are presented in the third and fourth row, respectively. The square inset (10x magnifications) in each micrograph (4x magnifications) was taken from the upper layer (core).

4.3.8 Relative PWI changes in core region following single and recurrent mild ischemia.

After a single or initial mild stroke, the 24h PWI decreased to 64% of control (n=14). Spontaneous reperfusion was observed at 2d (n=5) and 3d (n=1) following single mild stroke (Fig 4.3.8). In contrast, a recurrent ischemic insult significantly exacerbated the decrease of cerebral perfusion when the secondary ischemia occurred at an acute time point (1d and 2d, n=7 in total) following the initial mild ischemia. The perfusion measured in PWI following a 7d interval (n=5) between insults was slightly decreased as compared to values following a single PT at 24h post insult ($p>0.05$). Taken together, this suggests that a recurrent mild stroke produces greater brain damage when there is a shorter recovery time between insults.

Figure 4.3.8 Relative PWI changes in the core region following a single and recurrent mild ischemia.

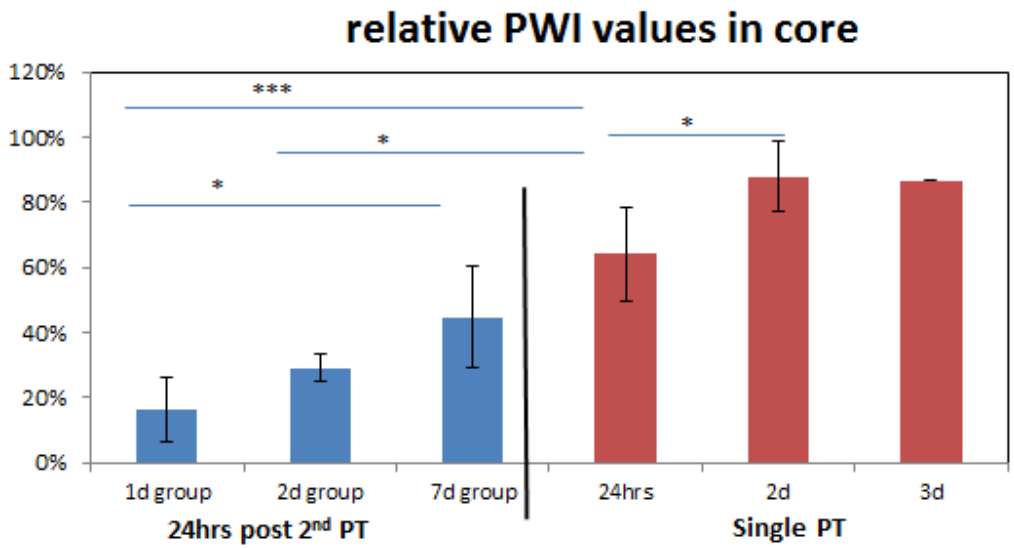

Quantification of cerebral perfusion relative to normal control regions within the core region measured at different time points after a single PT (red bar) and 24h after a

recurrent PT (blue bar) with 1d interval (n=5), 2d interval (n=2) and 1wk interval (n=5). (*p<0.05, ***p<0.001, Bonferroni t-test).

4.3.9 Summary and conclusion of Objective 2

This section of study demonstrated that two episodes of mild stroke enhanced the brain damage more than a single insult, as confirmed by histology and MRI. The enhancement was more pronounced with a shorter interval between insults (1day to 3day) than a longer interval (7days). T2 elevation was observed at 24 hr post insult and agreed with histology when the initial insult was mild, whereas it failed to distinguish the cumulative changes when the first insult was severe. When the insult was severe, T2 values tended to normalize and did not respond to the subsequent ischemic insult in the region of initial high T2 change. Quantification of PWI showed a spontaneous reperfusion in the region of mild ischemia over 3days after a single PT, whereas multiple episodes of mild stroke exacerbated the PWI deficit.

Chapter Five: Discussion

5.1 Major findings, novelty and clinical relevance

The present study examined the availability of phothothrombotic occlusion in TIA/minor stroke modeling and the cumulative brain damage in recurrent stroke with varied intervals. The major findings of this work were: 1) With modifications of PT parameters, such as light source, light intensity, illumination duration and skull preparation, we demonstrated that a mild focal ischemia could be produced in absence of a focal cortical infarct that had been reported in previous studies using PT model; 2) Using this modified PT model, we demonstrated that recurrent mild stroke led to an enhancement of brain tissue damage in a time-dependent fashion. The cumulative brain damage was more pronounced when a second ischemic episode occurred at an acute time point compared to a chronic time point post the initial one.

In this study, multiple MR sequences (T2, DWI and PWI) were used in assessment of tissue damage after a single and recurrent stroke. T2 and PWI were demonstrated to be sensitive methods and superior to DWI in detecting changes associated with mild brain injury non-invasively. MR abnormalities revealed a good correspondence with morphological changes of tissue stained with haematoxylin and eosin.

5.1.1 PT modifications in TIA/minor stroke modeling

A successful experimental model that can mimic a TIA/minor stroke is of clinical importance in studying its pathological progress and relevance to recurrent stroke. Our previous study using an MCAO model demonstrated that a short-lived brain ischemia resulted in diffuse or scattered necrosis in the occluded territory[12], referred to as a “mild

stroke". In this study, we used PT model as an alternative. We demonstrated that the traditional PT method can be modified to produce a mild stroke. The illumination parameters for a mild stroke were: illuminating upon partially thinned skull for 5min with approximate 35,000 Lux of light intensity produced by a cold halogen lamp through an optic fiber which was placed 2.5cm away from the illuminated spot. The photosensitive dye used was Rose Bengal at a concentration of 10mg/kg. The illuminated cortex showed scattered neuronal loss with preservation of neuropil. The recovery post to surgery was excellent as confirmed by body temperature measurements (Table 4.3.2).

In comparison with previous studies (i.e., Table 1.3), this current PT model produced a small cortical injury that was much milder, thereby providing a new method to model mild stroke.

5.1.2 Novelty of the recurrent stroke model

This study is the first to use a combination of two PT models to establish a recurrent stroke. The consistency of each PT can be examined by comparison of the damage in two control areas: area 1 and area 3. This is novel aspect of this model is superior to other models such as multiple mild MCAO [12] or thromboembotic injection [72, 73] methods.

5.1.3 The relevance of the mild PT model and clinical trials

Although the newest definition of TIA suggests a true TIA is one without a DWI abnormality [59], it has not been widely accepted in clinical trials. Based on the time-based definition of TIA that requires transient symptoms of less than 24h, multiple studies have shown that 25-60% of patients develop acute DWI lesions after symptom onset [110-115],

comparable to the situation of the Initial-Severe cohort in this study. The Initial-Mild cohort, on the other hand, represented a TIA without a DWI lesion.

In addition, a small infarct is most often seen [112, 115-117] in DWI-positive patients. This was also the case for both Initial-Mild and Initial-Severe cohort.

Although recovery of TIA symptoms is considered complete due to a timely restoration of cerebral blood flow, there have been few studies that examine the cerebral perfusion in TIA, surprisingly revealing a PWI deficit [111, 113, 115, 118, 119] in approximately 35% of patients within 2 days of symptom onset. In the present study, a mild PWI deficit (21% ±5% decrease of control) was also seen at 24h after a mild PT (Figure 4.2.3b).

Taken together, we believe that the current mild PT is a highly appropriate model that has relevance to treatment and understanding of recurrent TIA/minor stroke clinically. We have demonstrated that experimentally, a TIA-like insult leaves sparse necrosis in the ischemic region that has a slight progression within the first week post ischemia.

5.1.4 Implication of recurrent stroke and clinical significance

The highlight of this study was that we examined four different time intervals, varying from 1day to 1week between repetitive mild strokes, which modeled the short-term recurrence of TIA/minor stroke. We demonstrated that repetitive cerebral ischemia greatly exacerbated tissue damage within an essential time span from 1 day to 3 day, associated with a higher mortality (Table 4.3.1), implying the brain is vulnerable to a subsequent ischemic insult during this period (Figure 4.3.7). Taken together, these results indicate a crucial time window of three-day when hospitalization and medical intervention are needed for TIA patients in prevention of a major stroke. After this period,

the brain is less susceptible to a second ischemia. At 1 week after the first mild PT, the second mild PT resulted in the lowest histological score that was similar to a single mild PT developed at a corresponding time point (Figure 4.3.7). This observation is not reported in previous studies. It suggests a possible self-protective mechanism of brain against the secondary ischemia at a chronic phase,

5.2 Factors affecting severity of ischemic damage in the PT model

The current study showed that light intensity affected severity of brain damage, in line with other previous studies [79, 80, 120, 121]. The effect of illumination duration was also studied in this work. Three varied durations were examined from 5min to 15min, different from other studies that used only one duration mainly in range of 20 to 30 min (Table 1.3). By decreasing the light intensity and illumination duration, this study showed a mild cerebral injury can be produced. Under conditions examined, light intensity and illumination duration appeared linear functions of the severity of stroke. This suggests that light intensity and duration produce proportional increases in the rate of platelet adherence/aggregation and thrombi formation above the rate of disaggregation such as thrombus clearance by flowing blood.

Other potential factors that have not been studied in this model include type and dosage of photosensitive dye. A higher dosage causes more photochemical reaction and more production of thrombus per given time, resulting in a more severe damage. Different photosensitive dyes, such as Rose Bengal, Erythrosin B and flavin monoucleotide [122], may render different rates of platelet response and occlusion of cerebral microvasculature.

Despite taking care to standardize injection of Rose Bengal, light conditions and duration there was still some variability in the PT model represented as two cohorts. Considering the importance of light intensity, it is essential to make it consistent to minimize the variation of damage produced. Efforts have been made including evenly thinning the skull, measuring carefully the distance of the position of the fibre guide and positioning the optic fiber guide perpendicular to the skull. Moreover, getting a larger optic fiber to produce a highly uniform white light would likely improve consistency of damage further. Also important is to make the concentration of Rose Bengal as consistent as possible in each preparation.

5.3 Discussion on MR results

In this study, we have novel findings of MR changes with graded severities of stroke. Firstly, T2 relaxation and PWI deficit increased with an increase of light intensity. Secondly, the region of T2 change corresponded well with that of PWI abnormality. Thirdly, a mismatch between T2/PWI and DWI was present in regions of peri-infarct where T2 and PWI showed an abnormality but DWI did not.

PT had a unique T2 change of an absolute value of approximate 60ms at 24h associated with scattered necrosis observed at 2day, and approximate 80ms with incomplete infarct. In terms of regional changes, T2 had the greatest elevation in core with a lesser increase in peri-infarct, which also corresponded to the gradations of perfusion changes and histological damage.

5.3.1 Comparison with other studies using PT

The MR changes of severe stroke shown in this study are consistent with previous studies. A T2 elevation to 100ms was readily detectable at 24h after PT, in line with other reports [123-125]. Similarly, in the current study, the ADC declined to 60% of baseline in the core and was near baseline in the adjacent region [126-128]. With severe illumination, the lesion could expand to the whole illuminated cortex, which is the most common case in the photothrombotic model (Table 1.3). Pannecrosis was the pattern of cell death in the ischemic region of severe stroke.

The lesion of the PT model was mainly initiated by the endothelial leakage (blood-brain-barrier breakdown, BBB), producing the vasogenic edema [77, 129, 130] that can be detected by T2-weighted imaging. At 24h, BBB dysfunction was well developed [124, 131], which may explain the greatest increase of T2 at this time point. With the increase of light intensity, BBB damage is also enhanced; and as a result, the brain edema and water content increase and this is associated with a higher T2 relaxation.

5.3.2 Limitation of DWI/ADC measures in mild stroke produced by PT

In the novel mild stroke produced by PT, DWI had no abnormality in the peri-infarct and in this region ADC was similar to baseline, while scattered cell death was observed in association with a mild T2 increase and a PWI deficit.

Experimental and clinical evidence supports that an early ADC reduction has a transient normalization upon reperfusion or recanalization before its secondary decline [13, 132-135], occurring at varied time points based on the duration and magnitude of ischemia. This transient normalization does not indicate tissue recovery, but is a temporal marker of necrosis. Studies [13, 132] have reported that reperfusion after 10min MCAO in rat can

completely reverse the ADC change, leaving scattered necrosis. Even a severe ADC decrease to less than 50% of baseline had an ability to recover [134]. There have been studies suggesting that regions of ADC decreasing less than 80% of control do not develop into a final infarct [123, 127, 135]. These studies imply that ADC is not an accurate indicator of the final histopathology in the ischemic region and that the time point chosen for measurement is crucial. Since the very early stage of ADC change was not performed in this study, an initial decrease of ADC might occur that was masked by the spontaneous reperfusion.

Apart from reperfusion being a factor of inhomogeneous ADC change over time after stroke, the degree of CBF decrease also affects the ADC measurement. CBF must decrease to a certain level for the ADC decrease to occur [136, 137]. A CBF decrease causes ATP depletion and iron influx leading to cytotoxic edema, which has been shown to have a close relationship with the ADC decrease [127, 136]. Since ATP depletion occurs when CBF drops to 20% of baseline, beyond this an additional ADC change may not be seen. In this study, the mild ischemia had a 35% decrease of CBF measured by 24h PWI (Figure 4.3.8). The residue blood flow might be sufficient to preserve energy metabolism and caused no change of ADC, while cell death could still progress in terms of apoptosis as discussed in 1.1.2.

Taken together, although DWI and ADC provide an acute prediction of infarct [115, 138, 139] after stroke onset and have been extensively used in TIA studies, the current study implies DWI/ADC alone does not predict injury in TIA and mild stroke. There is scattered cell death not detected by DWI/ADC. T2 and PWI measures are strongly suggested to give a better prediction of brain injury.

5.3.3 Cerebral perfusion and PWI measures

The cerebral perfusion measured by 24h PWI after mild stroke had a mild decrease, followed by a spontaneous reperfusion within 3days. This delayed reperfusion was also seen in other studies using the PT model [140-142]. Gu [143] reported that the recovery of perfusion was accompanied by an over expression of vascular endothelial growth factor (VEGF), which promotes angiogenesis and reperfusion.

5.3.3.1 The discrepancy of Laser-Doppler flowmetry and Perfusion-Weighted Imaging in measurement of blood flow

Although the blood flow measured by Laser-Doppler flowmetry showed a fast recovery post to illumination, MR perfusion was usually decreased at 24h. The discrepancy was likely because of different regional measures. Laser-Doppler flowmetry measured the tissue blood flow within the local region where the probe was placed, while PWI measured the perfusion at one coronal level (p.c. level). When the stroke was mild, the cerebral perfusion deficit might be restricted in a very small area and this deficit might be masked by collateral flow that was also measured using Laser-Doppler flowmetry. In contrast, PWI measures reflected the perfusion status precisely in the affected area. Also, our PT model occludes cerebral microvessels instead of a large branch of major cerebral vessels. When the Doppler probe was placed near a non-occluded cerebral artery, there might have not been a decrease of blood flow. Another important reason for this discrepancy could be a delayed decrease in flow [142] that could be captured by 24h PWI but not by short-term Doppler measures. From all these aspects, it shows that PWI is superior to Laser-Doppler flowmetry in CBF measurement in mild stroke.

Irrespective of the extent of the flow decrease and recovery, we have Doppler and MR perfusion evidence that the damage in the peri-infarct regions are due to transient ischemia. Damage in the core may be due to permanent ischemia with some recovery of collateral flow.

5.3.4 MR performance in recurrent stroke

This study showed a greater increase of T2 after 2nd PT in short intervals than in 1week interval, associated with a more pronounce tissue damage when the initial T2 was mildly elevated. However, the 2nd T2 signatures with an initial high T2 (core) failed to predict the final histological damage. The T2 elevation decreased in the core region irrespective of another ischemic insult from 2day to 1week intervals. In the 1day group, T2 that had reached to 80ms after the 1st PT further increased to above 100ms in the 1day interval group, but the sample (n=1) size was too small to make a conclusion. MR normalization, both T2 and ADC, is a common phenomenon observed in animal and human studies, appearing normally within the first days after stroke onset [115, 123, 124, 134, 144-146]. The decrease of water content [147, 148]/alleviation of brain edema, and haemorrhagic transformation [149, 150] may be responsible for the normalization of T2 in the infarct core. The MR normalization indicates that timing of MR from stroke onset needs to be considered for its use as an accurate diagnostic tool.

It is unclear why T2 does not respond to secondary ischemia when the initial one is severe with a high T2 relaxation in core, but some reasons can be proposed. As discussed above, a high T2 indicates more severe damage of tissue. The initial severe insult triggers macrophage activation to clear the necrotic cell debris, producing a T2 decrease [146] masking the rate of T2 elevation caused by 2nd PT. In addition, as core tissue

is severely damaged, the skeleton of tissue cannot be preserved and a loose connective tissue matrix is formed along the infarct borders. Functional and electrophysiological impairments lead to a cessation of endothelial response irrespective of exposure to light, leaving no secondary vasogenic edema and elevation of T2. This finding of impaired accuracy of T2 measures in secondary ischemia may suggest a different pattern of cell injury uncoupled with vasogenic edema.

5.3.5 MR artifacts

MR has been demonstrated as an accurate and non-invasive method in detecting the ischemia-induced brain damage. However, it should be noticed that MR scanning has some potential artifacts. MR artifacts may be produced from PT surgery or imaging itself. The surgery-induced MR artifact is mainly generated by air infiltration in between the sutured skin and the thinned skull. The air can depress the superficial brain tissue, leaving darkness on the MR image. T2-weighted imaging is highly sensitive to water in presence of hyper-intensity, therefore liquid leakage post to surgery, if severe, would form a thin layer of an ischemia-like hyper-intense region above the superficial cortex. Haemorrhage, on the other hand, interferes with MR scanned brain tissue by producing a darkened spot. To avoid of this artifact, the upper ROI was drawn approximately 1mm away from the superficial edge of cortex.

The biggest system artifact originates from animal motion during the DWI scan, as a result of phase mismapping. A good DW map requires a highly static state of the rat in the magnetic coil. When the head of the imaged animal moves due to waking from insufficient anaesthesia or loose fixing within the coil, breathing motion artifact produces an appearance of replicated images overlapped with each other. To solve this problem,

MR is acquired by gating the image acquisition to a consistent state of respiration. In this study, images with movement artifacts were excluded from the ADC analysis.

In the spin-labeling perfusion imaging, the arterial blood at the level of neck must be labeled and imaged in the magnetic field as control in coding the perfusion in the brain. This required that much of the rat neck be fitted in to the 35mm coil for perfusion imaging. When the rat is too big to fit in this coil, insufficient blood is labeled and inaccurate low PWI signal occurs. For this aspect of the study, the size of experimental rat used was small (under 300g) on the imaging day if at all possible.

5.4 Potential improvement of histological assessment of brain damage

The cumulative scores after recurrent stroke with intervals between 1day to 3day were similar (Figure 4.3.6), while in haematoxylin and eosin stained coronal brain slices, the cortical neuropil of 1day was more destructed than that of 3day observed under light microscopy (Figure 4.3.7b). This may suggest some limitations of the scoring method. In this present work, four scores (0-3) were used to describe four stages of insults: no damage, scattered necrosis, incomplete infarct and complete infarct. This scoring was very brief, approximating the tissue damage by visualized difference of the morphology at only one level (approx. p.c. level). With each stage, the severity can vary significantly. For example, in the stage of scattered necrosis, the total number of selective neuronal loss varies. Improvement could be to count the amount of necrotic cells [55, 140] and give a graded score to further differentiate the brain damage in this stage. Although this scoring method may be related to the progress of “buck” cell/tissue death over time, the temporal evolution of a single cell death was also not considered as criteria for evaluation of the

cell death. The ischemia-induced neuronal death first presents swollen cells due to cytoplasmic edema, and then undergoes membrane breakdown of nucleus and cells, a failure of protein synthesis, DNA fragmentation, chromatin condensation and neuronal shrinkage providing an appearance of pyknosis. The neuron at a swollen stage may be suggestive of being less damaged than one that was pyknotic. Similarly, the phase of complete infarct experiences different morphologic changes. At the early stage when an infarct is formed, the tissue destruction is enhanced along with the number of necrotic neurons. The late phase of incomplete infarct and the early phase of complete could be very hard to distinguish, which might cause an inaccurate evaluation of scoring. At chronic times post ischemia, the necrotic cells are cleared by the activation of macrophages. The last phase of infarction is followed with tissue cavitation, scar formation, neurogenesis and vasogenesis and et al [41, 151]. These detailed changes suggest a stage of recovery which could not be differentiated with the phase of infarction using the current scoring method. Moreover, the postishemic inflammation and cytokine levels are important hallmarks to evaluate the tissue damage and their expressions can differ between different time points after single or recurrent stroke [12, 151, 152], implicating different severities of ischemic injury. However, the inflammatory response was not examined in this study. Thus, for a better evaluation of brain damage, immunochemical stains and scores might be added in future experiments. Another limitation of the scoring method lies in that the histological assessment was only determined at one level corresponding to that of MR for analysis (p.c. level). This was to study the correlation between histology and MR. However, the amount of doubled illumination region (area 2) had a length of 1.5mm (from p.c. to ant h.p. level) that contained approximately two MR

slices (0.7mm thick per slice). Thus if the tissue damage was assessed by a sum of scores of all levels of area 2, a significant difference might be revealed between 1day to 3day intervals.

The current scoring criterion is novel and first described in this present study for evaluation of the histological changes after mild stroke. It was sufficiently sensitive in detecting cell death in the stage of scattered necrosis and incomplete infarct that might be unique in mild stroke. Scoring was based on the three ROIs in MR analysis, in order to study the correlation between histology and MR changes in each ROI and to reflect the tissue damage with a sum score of all ROI. Although improvements were possible, this current scoring method successfully reflected the enhancement of tissue damage produced by recurrent mild stroke occurring at 1day and 2day post to the initial one (Figure 4.3.6). It also revealed a similar severity of tissue damage between single stroke and recurrent stroke with the 1week interval. Important was that the histological scores corresponded well with MR changes. A high T2 relaxation was associated with more pronounced tissue damage (Figure 4.2.4, 4.3.4.2 and 4.3.5). Thus the scoring system used was considered adequate for assessment of brain damage in the present study.

5.5 Potential mechanisms of enhancement of tissue damage after recurrent stroke

This present study using PT method agrees with other repetitive ischemia reports that show enhanced cumulative damage of brain tissue with bilateral CCAO (see. 1.4). Unlike the previous studies, we expanded the time interval between repetitive ischemia from minutes and hours to days. It is believed that the current intervals investigated in this study have better relevance to recurrent stroke in humans. This study revealed an

acute susceptibility of brain to secondary mild ischemia that occurred within 3day of the initial insult, contributing to an exacerbation of the tissue damage. After 1week, however, a 2nd mild stroke did not significantly enhance the damage. This time-based difference of brain susceptibility was not studied in current thesis, but potential mechanisms in underlying this difference can be postulated.

It has been reported that a repetitive 5-min ischemia of CCAO, when occurred at an acute time of a single ischemia, generates a greater release of extracellular glutamate and polyamine/spermine [104, 153]. This is believed to enhance neuronal damage by activation of NMDA receptor. The brain oedema is also exacerbated [102, 154, 155] with impaired microcirculation and brain protein synthesis.

From the cerebral flow measures, PWI showed a mild deficit at 24h after 1st mild PT, persisting until 3day (Figure 4.3.8). The cerebral protein synthesis can be suppressed for days upon reperfusion with a full recovery up to 7 days [21, 156, 157]. Although restoration of blood flow can result in recovery of energy-related metabolites, e.g. ATP, a secondary deterioration of ATP is seen that can last 3 days upon reperfusion [157, 158], a decreased glucose oxidation persists, leading to a secondary deterioration of mitochondrial malfunction which has played a big role in mediating apoptosis [25]. BBB dysfunction is most pronounced in the first days after PT [131] and tends to recover by 3days. An increase of spontaneous spreading depression is followed by BBB damage [131], which may contribute to the expansion of penumbra into infarct [159]. Brain edema and Na^+/K^+ displacement associated with BBB leakage persists 2-3 days before alleviation [81, 105, 160]. The remaining edema can lead to an increase of tissue pressure in local region and further impair cerebral perfusion. Additionally, the PT method itself produces single oxygen

species that can lead to peroxidation of the endothelial cell wall [75-77], causing secondary injury by permitting entry of neurotoxic elements to the brain. Together, these acute impairments of energy supply, protein synthesis and homeostasis likely make the brain more vulnerable to a secondary ischemic insult. At prolonged time points, these changes tend to recover to pre-occlusion levels so that the brain responds to a second insult as in healthy brain.

Apart from the normalization or clearing of detrimental changes, many other beneficial activities start to react at a later phase of ischemia as discussed in 1.1.3. After 7 days of transient MCAO, new pial arterioles begin to organize [31]. Expression of VEGF is up-regulated upon spontaneous reperfusion at 3 days in a phothorombotic "ring" model[143]. Neuronal stem cells are significantly activated to promote post-ischemic neurogenesis in subventricular zone after 7day of MCAO rat [161]. The late spontaneous reperfusion occurred at 3day after photothrombotic ring stroke [140] is associated with a decrease of lesion volume and neuronal loss [160]. As shown in 1.1.3, the late phase of ischemia is rather protective. The overexpression of neuroprotective molecules may be beneficial in the inhibition of injury produced by secondary ischemia.

The inflammatory reaction post ischemia is a robust mediator of brain damage. It can be both protective and detrimental to the brain tissue [162-164]. The acute inflammatory response may be harmful at the compromise of protein synthesis, while late inflammation can provide protection. At an early stage post ischemia, a mass generation of reactive oxygen species is produced from the intravascular compartment, triggering activation of platelet and endothelial cells. Inflammatory cytokines are secreted, causing adhesion molecule and leukocyte infiltration in the microvasculature and occlusion results. The

inflammatory mediators can alter the BBB permeability, facilitating extravasation of proteins and brain edema [124, 160]. The expression of cytokines, such as tumor necrosis factor (TNF) and interleukin (IL)-1, can elevate for days [162] and contribute to the growth of infarct. Thus, if a secondary insult occurs at such an acute time, damage may be enhanced.

In contrast, at chronic time, the expression of TNF and IL-1 normalize. Microglial/macrophage and astrocytic activation enhances at day 7 to remove the dead cell and promote tissue reconstruction [83, 84, 165]. The brain recovers and thereby may be less susceptible to another ischemia.

In summary, it is possible that exactly how the brain responds to secondary ischemic insult is dependent on the health status of brain at that time point. It should be noted that in clinic, TIA/minor patients often experience one or more complications, most reported as large-artery atherosclerosis, arterial fibrillation [62, 166] and carotid stenosis [167]. These are independent risk factors of a recurrent stroke, contributing to the deterioration of brain damage.

5.6 Summary and Conclusions

Our results demonstrate that a mild stroke with scattered necrosis can be produced with modifications of the photothrombotic occlusion method. Using this novel model, our results support the clinical observation of worsening symptoms in recurrent stroke. We further demonstrate that time intervals between the ischemic insults directly affect the severity of damage produced by subsequent ischemia. That the brain is susceptible to secondary ischemic attack at an acute phase after the initial one has clinical significance for risk factor evaluation and therapeutic determination. The proposed histological score

has been proven to be feasible for assessment of a graded mild cerebral injury. According to our findings, T2 and PWI are favored over DW in detecting cell death before an infarct grows. The T2 signature is unique in mild PT.

5.7 Future Directions

As we have shown, exacerbation of brain tissue damage after recurrent stroke varies but information is lacking regarding the mechanisms that can explain this phenomenon. This will be the main focus of future studies. Changes of the inflammatory response, free oxygen radicals, cytokine expression and energy metabolism between multiple ischemia will be pursued as factors responsible for the enhancement of tissue damage.

Considering the limited time to finish the current thesis, this study focused on only the short-term recurrence within first week, while in the clinic a recurrent stroke occurs at times that vary from days to months post the initial TIA. It would be interesting to examine the susceptibility of brain to secondary ischemia occurring at a prolonged time point, e.g. one month. Combined with the current results, such studies would offer a better understanding of brain responses to multiple ischemic insults for developing therapeutic strategies.

Prevention and treatment of recurrent stroke are important aspects clinically. In our lab, we have used a neuroprotective agent, Resveratrol, which is a compound extracted from grape seeds, to improve recovery after stroke. It will be promising to see whether it provides protection to subsequent stroke irrespective of time between insults.

In summary, future directions of recurrent stroke study will aim to further examine the brain's susceptibility to a second insult at chronic times, to seek mechanism of changes in this susceptibility over time, and to develop neuroprotective strategies.

APPENDIX A: ANIMAL PROTOCL CERTIFICATE (RENEWED)

UNIVERSITY OF CALGARY

COPY

Protocol M11017

Certification of Animal Protocol Approval

Applicant: Dr. Ursula Tuor

Faculty/Department: Physiology / Clinical Neurosciences

Project Title: Pathophysiology and Treatment of Stroke Recurrence

Sponsoring Agency(s): CIHR

Effective: 4/30/2013 Expires: 4/30/2014

The Animal Care Committee,
having examined the animal care and treatment protocol,
approves the experimental procedures proposed and certifies
with the applicant that the care and treatment of animals
used will be in accordance with the principles
outlined in the most recent policies and
"Guide to the Care and Use of Experimental Animals"
By The Canadian Council on Animal Care.

Applicant — Date: March 8, 2013

Chair of Animal Care Committee or University Veterinarian — Date: Mar 13 2013

Original - ACC File

APPENDIX B: HALOGEN LIGHT SOURCE INFORMATION AND LIGHT INTENSITY MEASUREMENTS

(a) (b) see http://www.volpiusa.com/htm/833/en_US/Onlineshop.htm?ProductId=2&Tab=3

(c) Light intensity measurements with light meters

Features and Benefits (b)

- 20V/150W and 21V/150W
- Constant Color Temperature
- Continous Intensity Adjustment
- High/Low Settings
- Filter slot
- Use of DDL or EKE Bulbs (DDL lamp included)
- Low Noise and Vibration
- Light Sources can be stacked

Technical Specifications

Rated lamp life DDL	100 / 1400 (average of continous operation)
Rated lamp life EKE	100/900 (average of continous operation)
Color temperature DDL	3280K / 3140K
Color temperature EKE	3310K / 3120K
Noise level	25 dB (A)
Housing temperature	98°F
Light adjustment	Crescent Shaped Diaphragm, 16-steps
Fuse NCL 120V	2.0AT (2 required), p/n 90045.112
Fuse NCL 230V	1.6AT (2 required), p/n 90045.114
Dimensions	4.125" x 8.625" x 8.625"
Weight	10lbs

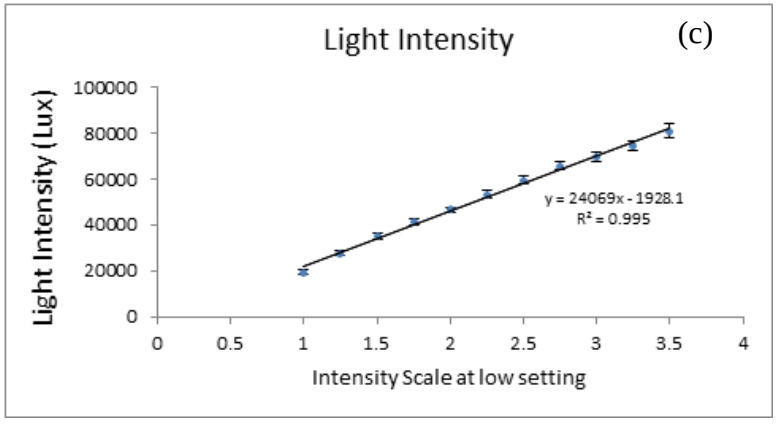

APPENDIX C: SPECTROPHOTOMETRIC MEASURES OF ROSE BENGAL DILUTIONS AT 532nm FOR DIFFERENT PREPARATIONS

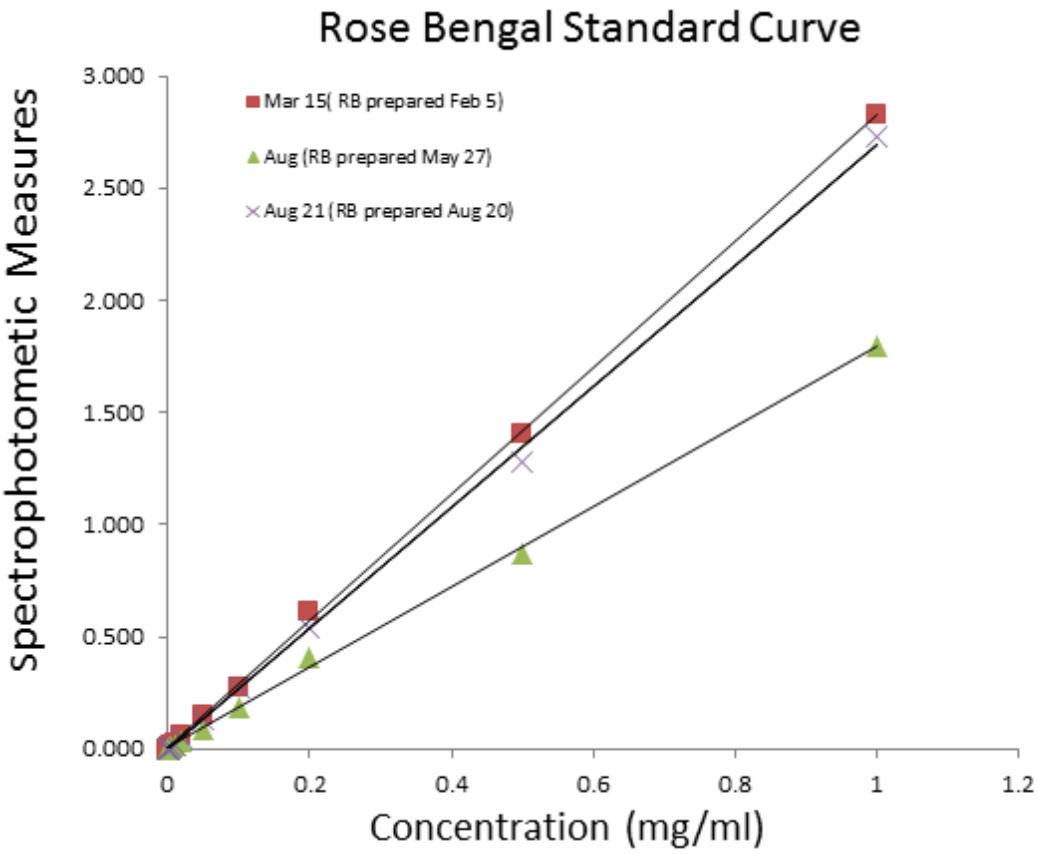

Examples of Rose Bengal (Sigma-Aldrich Company) solution in distilled H_2O showed small variations of spectrophotometric readouts from three preparations, but Rose Bengal lost efficiency (lower readouts, green triangle) overtime. (The Legend indicates analysing dates and preparation dates.)

REFERENCES

(1) Furie KL, Kasner SE, Adams RJ, Albers GW, Bush RL, Fagan SC, Halperin JL, Johnston SC, Katzan I, Kernan WN, Mitchell PH, Ovbiagele B, Palesch YY, Sacco RL, Schwamm LH, Wassertheil-Smoller S, Turan TN, Wentworth D. Guidelines for the prevention of stroke in patients with stroke or transient ischemic attack: a guideline for healthcare professionals from the american heart association/american stroke association. Stroke 2011 January;42(1):227-76.

(2) Roger VL, Go AS, Lloyd-Jones DM, Benjamin EJ, Berry JD, Borden WB, Bravata DM, Dai S, Ford ES, Fox CS, Fullerton HJ, Gillespie C, Hailpern SM, Heit JA, Howard VJ, Kissela BM, Kittner SJ, Lackland DT, Lichtman JH, Lisabeth LD, Makuc DM, Marcus GM, Marelli A, Matchar DB, Moy CS, Mozaffarian D, Mussolino ME, Nichol G, Paynter NP, Soliman EZ, Sorlie PD, Sotoodehnia N, Turan TN, Virani SS, Wong ND, Woo D, Turner MB. Heart disease and stroke statistics--2012 update: a report from the American Heart Association. Circulation 2012 January 3;125(1):e2-e220.

(3) Roach ES, Golomb MR, Adams R, Biller J, Daniels S, Deveber G, Ferriero D, Jones BV, Kirkham FJ, Scott RM, Smith ER. Management of stroke in infants and children: a scientific statement from a Special Writing Group of the American Heart Association Stroke Council and the Council on Cardiovascular Disease in the Young. Stroke 2008 September;39(9):2644-91.

(4) Zhang X, Zhang RL, Zhang ZG, Chopp M. Measurement of neuronal activity of individual neurons after stroke in the rat using a microwire electrode array. Journal of neuroscience methods 2007;162(1):91-100.

(5) Raichle ME. The pathophysiology of brain ischemia. Ann Neurol 1983 January;13(1):2-10.

(6) Lau A, Tymianski M. Glutamate receptors, neurotoxicity and neurodegeneration. PflÃ¼gers Archiv-European Journal of Physiology 2010;460(2):525-42.

(7) Szydlowska K, Tymianski M. Calcium, ischemia and excitotoxicity. Cell calcium 2010;47(2):122-9.

(8) Miller S, Kesslak JP, Romano C, Cotman CW. Roles of metabotropic glutamate receptors in brain plasticity and pathology. Ann N Y Acad Sci 1995 May 10;757:460-74.

(9) Lo EH, Dalkara T, Moskowitz MA. Mechanisms, challenges and opportunities in stroke. Nat Rev Neurosci 2003 May;4(5):399-415.

(10) Yuan J, Yankner BA. Apoptosis in the nervous system. Nature 2000 October 12;407(6805):802-9.

(11) Astrup J, Siesjo BK, Symon L. Thresholds in cerebral ischemia - the ischemic penumbra. Stroke 1981 November;12(6):723-5.

(12) Qiao M, Zhao Z, Barber PA, Foniok T, Sun S, Tuor UI. Development of a model of recurrent stroke consisting of a mild transient stroke followed by a second moderate stroke in rats. J Neurosci Methods 2009 November 15;184(2):244-50.

(13) Li F, Liu KF, Silva MD, Omae T, Sotak CH, Fenstermacher JD, Fisher M, Hsu CY, Lin W. Transient and permanent resolution of ischemic lesions on diffusion-weighted imaging after brief periods of focal ischemia in rats : correlation with histopathology. Stroke 2000 April;31(4):946-54.

(14) Jones TH, Morawetz RB, Crowell RM, Marcoux FW, FitzGibbon SJ, DeGirolami U, Ojemann RG. Thresholds of focal cerebral ischemia in awake monkeys. J Neurosurg 1981 June;54(6):773-82.

(15) Heiss WD. The ischemic penumbra: correlates in imaging and implications for treatment of ischemic stroke. Cerebrovascular Diseases 2011;32(4):307-20.

(16) Hossmann KA. Viability thresholds and the penumbra of focal ischemia. Ann Neurol 1994 October;36(4):557-65.

(17) Bandera E, Botteri M, Minelli C, Sutton A, Abrams KR, Latronico N. Cerebral blood flow threshold of ischemic penumbra and infarct core in acute ischemic stroke a systematic review. Stroke 2006;37(5):1334-9.

(18) Kulik T, Kusano Y, Aronhime S, Sandler AL, Winn HR. Regulation of cerebral vasculature in normal and ischemic brain. Neuropharmacology 2008 September;55(3):281-8.

(19) Mies G, Paschen W, Ebhardt G, Hossmann KA. Relationship between of blood flow, glucose metabolism, protein synthesis, glucose and ATP content in experimentally-induced glioma (RG1 2.2) of rat brain. J Neurooncol 1990 August;9(1):17-28.

(20) Mies G, Ishimaru S, Xie Y, Seo K, Hossmann K-A. Ischemic thresholds of cerebral protein synthesis and energy state following middle cerebral artery occlusion in rat. J Cereb Blood Flow Metab 1991;11:753-61.

(21) Dienel GA, Pulsinelli WA, Duffy TE. Regional protein synthesis in rat brain following acute hemispheric ischemia. J Neurochem 1980 November;35(5):1216-26.

(22) Leist M, Nicotera P. Apoptosis Versus Necrosis. Apoptosis: mechanisms and role in disease 1998;2:105.

(23) Kerr JF, Wyllie AH, Currie AR. Apoptosis: a basic biological phenomenon with wide-ranging implications in tissue kinetics. Br J Cancer 1972 August;26(4):239-57.

(24) Leist M, Single B, Castoldi AF, KÃ¼hnle S, Nicotera P. Intracellular adenosine triphosphate (ATP) concentration: a switch in the decision between apoptosis and necrosis. The Journal of experimental medicine 1997;185(8):1481-6.

(25) Sims NR, Muyderman H. Mitochondria, oxidative metabolism and cell death in stroke. Biochim Biophys Acta 2010 January;1802(1):80-91.

(26) Endres M, Namura S, Shimizu-Sasamata M, Waeber C, Zhang L, Gomez-Isla T, Hyman BT, Moskowitz MA. Attenuation of delayed neuronal death after mild focal ischemia in mice by inhibition of the caspase family. J Cereb Blood Flow Metab 1998 March;18(3):238-47.

(27) Gidday JM. Cerebral preconditioning and ischaemic tolerance. Nat Rev Neurosci 2006 June;7(6):437-48.

(28) Wei L, Ying DJ, Cui L, Langsdorf J, Yu SP. Necrosis, apoptosis and hybrid death in the cortex and thalamus after barrel cortex ischemia in rats. Brain Res 2004 October 1;1022(1-2):54-61.

(29) Rogers DC, Wright PW, Roberts JC, Reavill C, Rothaul AL, Hunter AJ. Photothrombotic lesions of the frontal cortex impair the performance of the delayed non-matching to position task by rats. Behav Brain Res 1992 August 10;49(2):231-5.

(30) Horinouchi K, Ikeda S, Harada K, Ohwatashi A, Kamikawa Y, Yoshida A, Nomoto Y, Etoh S, Kawahira K. Functional recovery and expression of GDNF seen in photochemically induced cerebral infarction. Int J Neurosci 2007 March;117(3):315-26.

(31) Lapi D, Vagnani S, Sapio D, Mastantuono T, Sabatino L, Paterni M, Colantuoni A. Long-term remodeling of rat pial microcirculation after transient middle cerebral artery occlusion and reperfusion. J Vasc Res 2013;50(4):332-45.

(32) Gu WG, Brannstrom T, Jiang W, Wester P. A photothrombotic ring stroke model in rats with remarkable morphological tissue recovery in the region at risk. Exp Brain Res 1999 March;125(2):171-83.

(33) Bonita R, Beaglehole R. Recovery of motor function after stroke. Stroke 1988 December;19(12):1497-500.

(34) Furlan M, Marchal G, Viader F, Derlon JM, Baron JC. Spontaneous neurological recovery after stroke and the fate of the ischemic penumbra. Ann Neurol 1996 August;40(2):216-26.

(35) Kollen B, Kwakkel G, Lindeman E. Functional recovery after stroke: a review of current developments in stroke rehabilitation research. Rev Recent Clin Trials 2006 January;1(1):75-80.

(36) Liepert J, Miltner WHR, Bauder H, Sommer M, Dettmers C, Taub E, Weiller C. Motor cortex plasticity during constraint-induced movement therapy in stroke patients. Neuroscience letters 1998;250(1):5-8.

(37) Cotman CW, Berchtold NC, Christie LA. Exercise builds brain health: key roles of growth factor cascades and inflammation. Trends in Neurosciences 2007 September;30(9):464-72.

(38) Kleihues P, Hossmann KA, Pegg AE, Kobayashi K, Zimmermann V. Resuscitation of the monkey brain after one hour complete ischemia. III. Indications of metabolic recovery. Brain Res 1975 September 12;95(1):61-73.

(39) Cross AJ, Jones JA, Snares M, Jostell KG, Bredberg U, Green AR. The protective action of chlormethiazole against ischaemia- induced neurodegeneration in gerbils when infused at doses having little sedative or anticonvulsant activity. Br J Pharmacol 1995;114:1625-30.

(40) Green AR, Hainsworth AH, Jackson DM. GABA potentiation: a logical pharmacological approach for the treatment of acute ischaemic stroke. Neuropharmacology 2000 July 10;39(9):1483-94.

(41) Dirnagl U, Simon RP, Hallenbeck JM. Ischemic tolerance and endogenous neuroprotection. Trends Neurosci 2003 May;26(5):248-54.

(42) Anderson KM, Ells G, Bonomi P, Harris JE. Free radical spin traps as adjuncts for the prevention and treatment of disease. Med Hypotheses 1999 January;52(1):53-7.

(43) Lapchak PA, Chapman DF, Zivin JA. Pharmacological effects of the spin trap agents N-t-butyl-phenylnitrone (PBN) and 2,2,6, 6-tetramethylpiperidine-N-oxyl (TEMPO) in a rabbit thromboembolic stroke model: combination studies with the thrombolytic tissue plasminogen activator. Stroke 2001 January;32(1):147-53.

(44) Tureyen K, Vemuganti R, Sailor KA, Bowen KK, Dempsey RJ. Transient focal cerebral ischemia-induced neurogenesis in the dentate gyrus of the adult mouse. J Neurosurg 2004 November;101(5):799-805.

(45) Thored P, Arvidsson A, Cacci E, Ahlenius H, Kallur T, Darsalia V, Ekdahl CT, Kokaia Z, Lindvall O. Persistent production of neurons from adult brain stem cells during recovery after stroke. Stem cells 2006;24(3):739-47.

(46) Carmichael ST. Plasticity of cortical projections after stroke. Neuroscientist 2003 February;9(1):64-75.

(47) Wang L, Zhang Z, Wang Y, Zhang R, Chopp M. Treatment of stroke with erythropoietin enhances neurogenesis and angiogenesis and improves neurological function in rats. Stroke 2004;35(7):1732-7.

(48) Greenberg DA, Jin K. Growth factors and stroke. NeuroRx 2006 October;3(4):458-65.

(49) Wang Y, Galvan V, Gorostiza O, Ataie M, Jin K, Greenberg DA. Vascular endothelial growth factor improves recovery of sensorimotor and cognitive deficits after focal cerebral ischemia in the rat. Brain Res 2006 October 18;1115(1):186-93.

(50) Dempsey RJ, Sailor KA, Bowen KK, Tureyen K, Vemuganti R. Stroke-induced progenitor cell proliferation in adult spontaneously hypertensive rat brain: effect of exogenous IGF-1 and GDNF. J Neurochem 2003 November;87(3):586-97.

(51) Kolb B, Morshead C, Gonzalez C, Kim M, Gregg C, Shingo T, Weiss S. Growth factor-stimulated generation of new cortical tissue and functional recovery after stroke damage to the motor cortex of rats. J Cereb Blood Flow Metab 2007 May;27(5):983-97.

(52) Jaquet K, Krause K, Tawakol-Khodai M, Geidel S, Kuck KH. Erythropoietin and VEGF Exhibit Equal Angiogenic Potential. Microvascular Research 2002 September;64(2):326-33.

(53) Sun Y, Jin K, Xie L, Childs J, Mao XO, Logvinova A, Greenberg DA. VEGF-induced neuroprotection, neurogenesis, and angiogenesis after focal cerebral ischemia. Journal of Clinical Investigation 2003;111(12):1843-51.

(54) Garcia JH, Liu KF, Ye ZR, Gutierrez JA. Incomplete infarct and delayed neuronal death after transient middle cerebral artery occlusion in rats. Stroke 1997 November;28(11):2303-9.

(55) Garcia JH, Wagner S, Liu KF, Hu XJ. Neurological deficit and extent of neuronal necrosis attributable to middle cerebral artery occlusion in rats. Statistical validation. Stroke 1995 April;26(4):627-34.

(56) Katsman D, Zheng J, Spinelli K, Carmichael ST. Tissue microenvironments within functional cortical subdivisions adjacent to focal stroke. J Cereb Blood Flow Metab 2003 September;23(9):997-1009.

(57) Prado R, Dietrich WD, Watson BD, Ginsberg MD, Green BA. Photochemically induced graded spinal cord infarction. Behavioral, electrophysiological, and morphological correlates. J Neurosurg 1987 November;67(5):745-53.

(58) Yao H, Yoshii N, Akira T, Nakahara T. Reperfusion-induced temporary appearance of therapeutic window in penumbra after 2 h of photothrombotic middle cerebral artery occlusion in rats. J Cereb Blood Flow Metab 2009 March;29(3):565-74.

(59) Easton JD, Saver JL, Albers GW, Alberts MJ, Chaturvedi S, Feldmann E, Hatsukami TS, Higashida RT, Johnston SC, Kidwell CS, Lutsep HL, Miller E, Sacco RL. Definition and evaluation of transient ischemic attack: a scientific statement for healthcare professionals from the American Heart Association/American Stroke Association Stroke Council; Council on Cardiovascular Surgery and Anesthesia; Council on Cardiovascular Radiology and Intervention; Council on Cardiovascular Nursing; and the Interdisciplinary Council

on Peripheral Vascular Disease. The American Academy of Neurology affirms the value of this statement as an educational tool for neurologists. Stroke 2009 June;40(6):2276-93.

(60) Hill MD, Yiannakoulias N, Jeerakathil T, Tu JV, Svenson LW, Schopflocher DP. The high risk of stroke immediately after transient ischemic attack: a population-based study. Neurology 2004 June 8;62:2015-20.

(61) Cancelli I, Janes F, Gigli GL, Perelli A, Zanchettin B, Canal G, D'Anna L, Russo V, Barbone F, Valente M. Incidence of transient ischemic attack and early stroke risk: validation of the ABCD2 score in an Italian population-based study. Stroke 2011 October;42(10):2751-7.

(62) Purroy F, Jimenez Caballero PE, Gorospe A, Torres MJ, Alvarez-Sabin J, Santamarina E, Martinez-Sanchez P, Canovas D, Freijo MM, Egido JA, Giron JM, Ramirez-Moreno JM, Alonso A, Rodriguez-Campello A, Casado I, Delgado-Medeiros R, Marti-Fabregas J, Fuentes B, Silva Y, Quesada H, Cardona P, Morales A, de la Ossa N, Garcia-Pastor A, Arenillas JF, Segura T, Jimenez C, Masjuan J. Prediction of early stroke recurrence in transient ischemic attack patients from the PROMAPA study: a comparison of prognostic risk scores. Cerebrovasc Dis 2012;33(2):182-9.

(63) Arsava EM, Furie KL, Schwamm LH, Sorensen AG, Ay H. Prediction of early stroke risk in transient symptoms with infarction: relevance to the new tissue-based definition. Stroke 2011 August;42(8):2186-90.

(64) Giles MF, Albers GW, Amarenco P, Arsava EM, Asimos AW, Ay H, Calvet D, Coutts SB, Cucchiara BL, Demchuk AM, Johnston SC, Kelly PJ, Kim AS, Labreuche J, Lavallee PC, Mas JL, Merwick A, Olivot JM, Purroy F, Rosamond WD, Sciolla R, Rothwell PM. Early stroke risk and ABCD2 score performance in tissue- vs time-defined TIA: a multicenter study. Neurology 2011 September 27;77(13):1222-8.

(65) Delgado P, Chacon P, Penalba A, Pelegri D, Garcia-Berrocoso T, Giralt D, Santamarina E, Ribo M, Maisterra O, Alvarez-Sabin J, Rosell A, Montaner J. Lipoprotein-associated phospholipase A(2) activity is associated with large-artery atherosclerotic etiology and recurrent stroke in TIA patients. Cerebrovasc Dis 2012;33(2):150-8.

(66) Ay H, Gungor L, Arsava EM, Rosand J, Vangel M, Benner T, Schwamm LH, Furie KL, Koroshetz WJ, Sorensen AG. A score to predict early risk of recurrence after ischemic stroke. Neurology 2010 January 12;74(2):128-35.

(67) Engelter ST, Amort M, Jax F, Weisskopf F, Katan M, Burow A, Bonati LH, Hatz F, Wetzel SG, Fluri F, Lyrer PA. Optimizing the risk estimation after a transient ischaemic attack - the ABCDE plus sign in circle score. Eur J Neurol 2012 January;19(1):55-61.

(68) Alexandrov AV, Demchuk AM, Felberg RA, Christou I, Barber PA, Burgin WS, Malkoff M, Wojner AW, Grotta JC. High rate of complete recanalization and dramatic clinical recovery during tPA infusion when continuously monitored with 2-MHz transcranial doppler monitoring. Stroke 2000 March;31(3):610-4.

(69) Chandratheva A, Geraghty OC, Luengo-Fernandez R, Rothwell PM. ABCD2 score predicts severity rather than risk of early recurrent events after transient ischemic attack. Stroke 2010 May;41(5):851-6.

(70) Asdaghi N, Hameed B, Saini M, Jeerakathil T, Emery D, Butcher K. Acute perfusion and diffusion abnormalities predict early new MRI lesions 1 week after minor stroke and transient ischemic attack. Stroke 2011 August;42(8):2191-5.

(71) Longa EZ, Weinstein PR, Carlson S, Cummins R. Reversible middle cerebral artery occlusion without craniectomy in rats. Stroke 1989 January;20(1):84-91.

(72) Kaneko D, Nakamura N, Ogawa T. Cerebral infarction in rats using homologous blood emboli: development of a new experimental model. Stroke 1985 January;16(1):76-84.

(73) Kudo M, Aoyama A, Ichimori S, Fukunaga N. An animal model of cerebral infarction. Homologous blood clot emboli in rats. Stroke 1982 July;13(4):505-8.

(74) Watson BD, Dietrich WD, Busto R, Wachtel MS, Ginsberg MD. Induction of reproducible brain infarction by photochemically initiated thrombosis. Ann Neurol 1985 May;17(5):497-504.

(75) Gajkowska B, Frontczak-Baniewicz M, Gadamski R, Barskov I. Photochemically-induced vascular damage in brain cortex. Transmission and scanning electron microscopy study. Acta Neurobiol Exp (Wars) 1997;57(3):203-8.

(76) Frontczak-Baniewicz M. Focal ischemia in the cerebral cortex has an effect on the neurohypophysis. I. Ultrastructural changes in capillary vessels of the

neurohypophysis after focal ischemia of the cerebral cortex. Neuro Endocrinol Lett 2001 April;22(2):81-6.

(77) Dietrich WD, Watson BD, Busto R, Ginsberg MD, Bethea JR. Photochemically induced cerebral infarction. I. Early microvascular alterations. Acta Neuropathol 1987;72(4):315-25.

(78) Strom JO, Ingberg E, Theodorsson A, Theodorsson E. Method parameters' impact on mortality and variability in rat stroke experiments: a meta-analysis. BMC Neurosci 2013;14:41.

(79) Boquillon M, Boquillon JP, Bralet J. Photochemically induced, graded cerebral infarction in the mouse by laser irradiation evolution of brain edema. J Pharmacol Toxicol Methods 1992 March;27(1):1-6.

(80) Alaverdashvili M, Moon SK, Beckman CD, Virag A, Whishaw IQ. Acute but not chronic differences in skilled reaching for food following motor cortex devascularization vs. photothrombotic stroke in the rat. Neuroscience 2008 November 19;157(2):297-308.

(81) Pevsner PH, Eichenbaum JW, Miller DC, Pivawer G, Eichenbaum KD, Stern A, Zakian KL, Koutcher JA. A photothrombotic model of small early ischemic infarcts in the rat brain with histologic and MRI correlation. J Pharmacol Toxicol Methods 2001 May;45(3):227-33.

(82) Grome JJ, Gojowczyk G, Hofmann W, Graham DI. Quantitation of photochemically induced focal cerebral ischemia in the rat. J Cereb Blood Flow Metab 1988 February;8(1):89-95.

(83) Schroeter M, Franke C, Stoll G, Hoehn M. Dynamic changes of magnetic resonance imaging abnormalities in relation to inflammation and glial responses after photothrombotic cerebral infarction in the rat brain. Acta Neuropathol 2001 February;101(2):114-22.

(84) Nowicka D, Rogozinska K, Aleksy M, Witte OW, Skangiel-Kramska J. Spatiotemporal dynamics of astroglial and microglial responses after photothrombotic stroke in the rat brain. Acta Neurobiol Exp (Wars) 2008;68(2):155-68.

(85) Jin Z, Wu J, Oh SY, Kim KW, Shin BS. The effect of stress on stroke recovery in a photothrombotic stroke animal model. Brain research 2010;1363:191-7.

(86) Ikeda S, Ohwatashi A, Harada K, Kamikawa Y, Yoshida A. Expected for acquisition movement exercise is more effective for functional recovery than simple exercise in a rat model of hemiplegia. Springerplus 2013;2:517.

(87) Dietrich WD, Feng ZC, Leistra H, Watson BD, Rosenthal M. Photothrombotic infarction triggers multiple episodes of cortical spreading depression in distant brain regions. J Cereb Blood Flow Metab 1994 January;14(1):20-8.

(88) Mullins PG, Reid DG, Hockings PD, Hadingham SJ, Campbell CA, Chalk JB, Doddrell DM. Ischaemic preconditioning in the rat brain: a longitudinal magnetic resonance imaging (MRI) study. NMR Biomed 2001 May;14(3):204-9.

(89) Nakamura M, Nakakimura K, Matsumoto M, Sakabe T. Rapid tolerance to focal cerebral ischemia in rats is attenuated by adenosine A1 receptor antagonist. J Cereb Blood Flow Metab 2002 February;22(2):161-70.

(90) Abe H, Nowak TS, Jr. Induced hippocampal neuron protection in an optimized gerbil ischemia model: insult thresholds for tolerance induction and altered gene expression defined by ischemic depolarization. J Cereb Blood Flow Metab 2004 January;24(1):84-97.

(91) Tanaka H, Calderone A, Jover T, Grooms SY, Yokota H, Zukin RS, Bennett MV. Ischemic preconditioning acts upstream of GluR2 down-regulation to afford neuroprotection in the hippocampal CA1. Proc Natl Acad Sci U S A 2002 February 19;99(4):2362-7.

(92) Kawahara N, Wang Y, Mukasa A, Furuya K, Shimizu T, Hamakubo T, Aburatani H, Kodama T, Kirino T. Genome-wide gene expression analysis for induced ischemic tolerance and delayed neuronal death following transient global ischemia in rats. J Cereb Blood Flow Metab 2004 February;24(2):212-23.

(93) Gao X, Zhang H, Steinberg G, Zhao H. The Akt Pathway Is Involved in Rapid Ischemic Tolerance in Focal Ischemia in Rats. Transl Stroke Res 2010;1(3):202-9.

(94) Danton GH, Prado R, Watson BD, Dietrich WD. Temporal profile of enhanced vulnerability of the postthrombotic brain to secondary embolic events. Stroke 2002 April;33:1113-9.

(95) Dietrich WD, Danton G, Hopkins AC, Prado R. Thromboembolic events predispose the brain to widespread cerebral infarction after delayed transient global ischemia in rats. Stroke 1999 April;30:855-61.

(96) Lin WY, Chang YC, Lee HT, Huang CC. CREB activation in the rapid, intermediate, and delayed ischemic preconditioning against hypoxicG€“ischemia in neonatal rat. Journal of Neurochemistry 2009 February 1;108(4):847-59.

(97) Steiger HJ, Hanggi D. Ischaemic preconditioning of the brain, mechanisms and applications. Acta Neurochir (Wien) 2007 January;149:1-10.

(98) O'duffy AE, Bordelon YM, McLaughlin B, 't Hart BA. Killer proteases and little strokes-how the things that do not kill you make you stronger. J Cereb Blood Flow Metab 2006 August 9;.27:655-68.

(99) Gidday JM. Cerebral preconditioning and ischaemic tolerance. Nat Rev Neurosci 2006 June;7:437-48.

(100) Lehotsky J, Burda J, Danielisova V, Gottlieb M, Kaplan P, Saniova B. Ischemic tolerance: the mechanisms of neuroprotective strategy. Anat Rec (Hoboken) 2009 December;292(12):2002-12.

(101) Mrsulja BB, Lust WD, Mrsulja BJ, Passonneau JV. Effect of repeated cerebral ischemia on metabolites and metabolic rate in gerbil cortex. Brain Res 1977 January 7;119(2):480-6.

(102) Vass K, Tomida S, Hossmann KA, Nowak TS, Jr., Klatzo I. Microvascular disturbances and edema formation after repetitive ischemia of gerbil brain. Acta Neuropathol 1988;75(3):288-94.

(103) Tomida S, Nowak TS, Jr., Vass K, Lohr JM, Klatzo I. Experimental model for repetitive ischemic attacks in the gerbil: the cumulative effect of repeated ischemic insults. J Cereb Blood Flow Metab 1987 December;7(6):773-82.

(104) Paschen W, Widmann R, Weber C. Changes in regional polyamine profiles in rat brains after transient cerebral ischemia (single versus repetitive ischemia): evidence for release of polyamines from injured neurons. Neurosci Lett 1992 January 20;135(1):121-4.

(105) Deluga KS, Plotz FB, Betz AL. Effect of indomethacin on edema following single and repetitive cerebral ischemia in the gerbil. Stroke 1991 October;22(10):1259-64.

(106) Hanyu S, Ito U, Hakamata Y, Yoshida M. Repeated unilateral carotid occlusion in Mongolian gerbils: quantitative analysis of cortical neuronal loss. Acta Neuropathol 1993;86(1):16-20.

(107) Hossmann KA, Hoehn-Berlage M. Diffusion and perfusion MR imaging of cerebral ischemia. Cerebrovasc Brain Metab Rev 1995;7(3):187-217.

(108) Calamante F, Thomas DL, Pell GS, Wiersma J, Turner R. Measuring cerebral blood flow using magnetic resonance imaging techniques. J Cereb Blood Flow Metab 1999 July;19(7):701-35.

(109) Paxinos G, Watson C. The rat brain in stereotaxic coordinates: hard cover edition. Access Online via Elsevier; 2006.

(110) Kidwell CS, Alger JR, Di SF, Starkman S, Villablanca P, Bentson J, Saver JL. Diffusion MRI in patients with transient ischemic attacks. Stroke 1999 June;30(6):1174-80.

(111) Zaharchuk G, Olivot JM, Fischbein NJ, Bammer R, Straka M, Kleinman JT, Albers GW. Arterial spin labeling imaging findings in transient ischemic attack patients: comparison with diffusion- and bolus perfusion-weighted imaging. Cerebrovasc Dis 2012;34(3):221-8.

(112) Fazekas F, Fazekas G, Schmidt R, Kapeller P, Offenbacher H. Magnetic resonance imaging correlates of transient cerebral ischemic attacks. Stroke 1996 April;27(4):607-11.

(113) Mlynash M, Olivot JM, Tong DC, Lansberg MG, Eyngorn I, Kemp S, Moseley ME, Albers GW. Yield of combined perfusion and diffusion MR imaging in hemispheric TIA. Neurology 2009 March 31;72(13):1127-33.

(114) Sylaja PN, Coutts SB, Subramaniam S, Hill MD, Eliasziw M, Demchuk AM. Acute ischemic lesions of varying ages predict risk of ischemic events in stroke/TIA patients. Neurology 2007 February 6;68(6):415-9.

(115) Asdaghi N, Campbell BC, Butcher KS, Coulter JI, Modi J, Qazi A, Goyal M, Demchuk AM, Coutts SB. DWI Reversal Is Associated with Small Infarct Volume in Patients with TIA and Minor Stroke. AJNR Am J Neuroradiol 2013 December 12.

(116) Gass A, Ay H, Szabo K, Koroshetz WJ. Diffusion-weighted MRI for the "small stuff": the details of acute cerebral ischaemia. Lancet Neurol 2004 January;3(1):39-45.

(117) Koudstaal PJ, van GJ, Frenken CW, Hijdra A, Lodder J, Vermeulen M, Bulens C, Franke CL. TIA, RIND, minor stroke: a continuum, or different subgroups? Dutch TIA Study Group. J Neurol Neurosurg Psychiatry 1992 February;55(2):95-7.

(118) Krol AL, Coutts SB, Simon JE, Hill MD, Sohn CH, Demchuk AM. Perfusion MRI abnormalities in speech or motor transient ischemic attack patients. Stroke 2005 November;36(11):2487-9.

(119) Restrepo L, Jacobs MA, Barker PB, Wityk RJ. Assessment of transient ischemic attack with diffusion- and perfusion-weighted imaging. AJNR Am J Neuroradiol 2004 November;25(10):1645-52.

(120) Hu X, Wester P, Brannstrom T, Watson BD, Gu W. Progressive and reproducible focal cortical ischemia with or without late spontaneous reperfusion generated by a ring-shaped, laser-driven photothrombotic lesion in rats. Brain Res Brain Res Protoc 2001 April;7(1):76-85.

(121) Hu X, Brannstrom T, Gu W, Wester P. A photothrombotic ring stroke model in rats with or without late spontaneous reperfusion in the region at risk. Brain Res 1999 December 4;849(1-2):175-86.

(122) Watson BD, Dietrich WD, Prado R, Nakayama H, Kanemitsu H, Futrell N, Yao H, Markgraf CG, Wester P. Concepts and techniques of experimental stroke induced by cerebrovascular photothrombosis. Central Nervous System Trauma: Research Techniques 1995;169-94.

(123) Lee VM, Burdett NG, Carpenter TA, Hall LD, Pambakian PS, Patel S, Wood NI, James MF. Evolution of Photochemically Induced Focal Cerebral Ischemia in the Rat Magnetic Resonance Imaging and Histology. Stroke 1996;27(11):2110-9.

(124) van BN, Cullen BM, King MD, Doran M, Williams SR, Gadian DG, Cremer JE. T2- and diffusion-weighted magnetic resonance imaging of a focal ischemic lesion in rat brain. Stroke 1992 April;23(4):576-82.

(125) Kleinschnitz C, SchÃ¼tz A, NÃ¶lte I, Horn T, Frank M, Solymosi L, Stoll G, Bendszus M. In vivo detection of developing vessel occlusion in photothrombotic ischemic brain lesions in the rat by iron particle enhanced MRI. Journal of Cerebral Blood Flow & Metabolism 2005;25(11):1548-55.

(126) Robertson CA, McCabe C, Gallagher L, Lopez-Gonzalez MR, Holmes WM, Condon B, Muir KW, Santosh C, Macrae IM. Stroke penumbra defined by an MRI-based oxygen challenge technique: 2. Validation based on the consequences of reperfusion. J Cereb Blood Flow Metab 2011 August;31(8):1788-98.

(127) Olah L, Wecker S, Hoehn M. Relation of apparent diffusion coefficient changes and metabolic disturbances after 1 hour of focal cerebral ischemia and at different reperfusion phases in rats. J Cereb Blood Flow Metab 2001 April;21(4):430-9.

(128) Liu Y, Karonen JO, Vanninen RL, Ostergaard L, Roivainen R, Nuutinen J, Perkio J, Kononen M, Hamalainen A, Vanninen EJ, Soimakallio S, Kuikka JT, Aronen HJ. Cerebral hemodynamics in human acute ischemic stroke: a study with diffusion- and perfusion-weighted magnetic resonance imaging and SPECT. J Cereb Blood Flow Metab 2000 June;20(6):910-20.

(129) Verlooy J, Van RJ, Peersman G, Van d, V, Van DB, Borgers M, Selosse P. Photochemically-induced cerebral infarction in the rat: comparison of NMR imaging and histologic changes. Acta Neurochir (Wien) 1993;122(3-4):250-6.

(130) Dietrich WD, Busto R, Watson BD, Scheinberg P, Ginsberg MD. Photochemically induced cerebral infarction. II. Edema and blood-brain barrier disruption. Acta Neuropathol 1987;72(4):326-34.

(131) Lapilover EG, Lippmann K, Salar S, Maslarova A, Dreier JP, Heinemann U, Friedman A. Peri-infarct bloodG€“brain barrier dysfunction facilitates induction of spreading depolarization associated with epileptiform discharges. Neurobiology of Disease 2012 December;48(3):495-506.

(132) Li F, Silva MD, Liu KF, Helmer KG, Omae T, Fenstermacher JD, Sotak CH, Fisher M. Secondary decline in apparent diffusion coefficient and neurological outcomes after a short period of focal brain ischemia in rats. Ann Neurol 2000 August;48(2):236-44.

(133) Neumann-Haefelin T, Kastrup A, De Crespigny A, Yenari MA, Ringer T, Sun GH, Moseley ME. Serial MRI after transient focal cerebral ischemia in rats dynamics of tissue injury, blood-brain barrier damage, and edema formation. Stroke 2000;31(8):1965-73.

(134) Fiehler J, Foth M, Kucinski T, Knab R, von BM, Weiller C, Zeumer H, Rother J. Severe ADC decreases do not predict irreversible tissue damage in humans. Stroke 2002 January;33(1):79-86.

(135) Olah L, Wecker S, Hoehn M. Secondary deterioration of apparent diffusion coefficient after 1-hour transient focal cerebral ischemia in rats. J Cereb Blood Flow Metab 2000 October;20(10):1474-82.

(136) Busza AL, Allen KL, King MD, van BN, Williams SR, Gadian DG. Diffusion-weighted imaging studies of cerebral ischemia in gerbils. Potential relevance to energy failure. Stroke 1992 November;23(11):1602-12.

(137) Yushmanov VE, Kharlamov A, Simplaceanu E, Williams DS, Jones SC. Differences between arterial occlusive and cortical photothrombosis stroke models with magnetic resonance imaging and microtubule-associated protein-2 immunoreactivity. Magn Reson Imaging 2006 October;24(8):1087-93.

(138) Moseley ME, Cohen Y, Mintorovitch J, Chileuitt L, Shimizu H, Kucharczyk J, Wendland MF, Weinstein PR. Early detection of regional cerebral ischemia in cats: comparison of diffusion- and T2-weighted MRI and spectroscopy. Magn Reson Med 1990 May;14(2):330-46.

(139) Yoneda Y, Tokui K, Hanihara T, Kitagaki H, Tabuchi M, Mori E. Diffusion-weighted magnetic resonance imaging: detection of ischemic injury 39 minutes after onset in a stroke patient. Ann Neurol 1999 June;45(6):794-7.

(140) Gu WG, Brannstrom T, Jiang W, Wester P. A photothrombotic ring stroke model in rats with remarkable morphological tissue recovery in the region at risk. Exp Brain Res 1999 March;125(2):171-83.

(141) Gu WG, Jiang W, Brannstrom T, Wester P. Long-term cortical CBF recording by laser-Doppler flowmetry in awake freely moving rats subjected to reversible photothrombotic stroke. J Neurosci Methods 1999 August 1;90(1):23-32.

(142) Chen F, Suzuki Y, Nagai N, Sun X, Coudyzer W, Yu J, Marchal G, Ni Y. Delayed perfusion phenomenon in a rat stroke model at 1.5T MR: An imaging sign parallel to spontaneous reperfusion and ischemic penumbra? European journal of radiology 2007 January;61(1):70-8.

(143) Gu W, Brannstrom T, Jiang W, Bergh A, Wester P. Vascular endothelial growth factor-A and -C protein up-regulation and early angiogenesis in a rat photothrombotic ring stroke model with spontaneous reperfusion. Acta Neuropathol 2001 September;102(3):216-26.

(144) Qiao M, Malisza KL, Del Bigio MR, Tuor UI. Transient hypoxia-ischemia in rats: changes in diffusion-sensitive MR imaging findings, extracellular space, and Na+-K+ -adenosine triphosphatase and cytochrome oxidase activity. Radiology 2002 April;223:65-75.

(145) Chen F, Suzuki Y, Nagai N, Jin L, Yu J, Wang H, Marchal G, Ni Y. Rodent stroke induced by photochemical occlusion of proximal middle cerebral artery: Evolution monitored with MR imaging and histopathology. European journal of radiology 2007 July;63(1):68-75.

(146) Wagner DC, Deten A, Hartig W, Boltze J, Kranz A. Changes in T2 relaxation time after stroke reflect clearing processes. Neuroimage 2012 July 16;61(4):780-5.

(147) Lin SP, Song SK, Miller JP, Ackerman JJ, Neil JJ. Direct, longitudinal comparison of (1)H and (23)Na MRI after transient focal cerebral ischemia. Stroke 2001 April;32(4):925-32.

(148) Lin SP, Schmidt RE, McKinstry RC, Ackerman JJ, Neil JJ. Investigation of mechanisms underlying transient T2 normalization in longitudinal studies of ischemic stroke. J Magn Reson Imaging 2002 February;15(2):130-6.

(149) Alvarez-Sabin J, Maisterra O, Santamarina E, Kase CS. Factors influencing haemorrhagic transformation in ischaemic stroke. Lancet Neurol 2013 July;12(7):689-705.

(150) Simard JM, Kent TA, Chen M, Tarasov KV, Gerzanich V. Brain oedema in focal ischaemia: molecular pathophysiology and theoretical implications. Lancet Neurol 2007 March;6(3):258-68.

(151) Wegener S, Weber R, Ramos-Cabrer P, Uhlenkueken U, Sprenger C, Wiedermann D, Villringer A, Hoehn M. Temporal profile of T2-weighted MRI

distinguishes between pannecrosis and selective neuronal death after transient focal cerebral ischemia in the rat. J Cereb Blood Flow Metab 2006 January;26(1):38-47.

(152) Qiao M, Meng S, Foniok T, Tuor UI. Mild cerebral hypoxia-ischemia produces a sub-acute transient inflammatory response that is less selective and prolonged after a substantial insult. Int J Dev Neurosci 2009 November;27(7):691-700.

(153) Lee GJ, Choi SK, Eo YH, Kang SW, Choi S, Park JH, Lim JE, Hong KW, Jin HS, Oh BS, Park HK. The effect of extracellular glutamate release on repetitive transient ischemic injury in global ischemia model. Korean J Physiol Pharmacol 2009 February;13(1):23-6.

(154) Nowak TS, Jr., Tomida S, Pluta R, Xu S, Kozuka M, Vass K, Wagner HG, Klatzo I. Cumulative effect of repeated ischemia on brain edema in the gerbil. Biochemical and physiological correlates of repeated ischemic insults. Adv Neurol 1990;52:1-9.

(155) Masaoka H, Klatzo I, Tomida S, Vass K, Wagner HG, Nowak TS, Jr. Role of circulatory disturbances in the development of post-ischemic brain edema. Neurochem Pathol 1988 July;9:21-9.

(156) Bergstedt K, Hu BR, Wieloch T. Postischaemic changes in protein synthesis in the rat brain: effects of hypothermia. Exp Brain Res 1993;95(1):91-9.

(157) Hata R, Maeda K, Hermann D, Mies G, Hossmann KA. Evolution of brain infarction after transient focal cerebral ischemia in mice. J Cereb Blood Flow Metab 2000 June;20(6):937-46.

(158) Mies G, Paschen W, Hossmann KA. Cerebral blood flow, glucose utilization, regional glucose, and ATP content during the maturation period of delayed ischemic injury in gerbil brain. J Cereb Blood Flow Metab 1990 September;10(5):638-45.

(159) Dreier JP. The role of spreading depression, spreading depolarization and spreading ischemia in neurological disease. Nat Med 2011 April;17(4):439-47.

(160) Gu W, Jiang W, Wester P. A photothrombotic ring stroke model in rats with sustained hypoperfusion followed by late spontaneous reperfusion in the region at risk. Exp Brain Res 1999 March;125(2):163-70.

(161) Zhang R, Zhang Z, Wang L, Wang Y, Gousev A, Zhang L, Ho KL, Morshead C, Chopp M. Activated neural stem cells contribute to stroke-induced neurogenesis and neuroblast migration toward the infarct boundary in adult rats. Journal of Cerebral Blood Flow & Metabolism 2004;24(4):441-8.

(162) Lambertsen KL, Biber K, Finsen B. Inflammatory cytokines in experimental and human stroke. J Cereb Blood Flow Metab 2012 September;32(9):1677-98.

(163) del Zoppo GJ, Becker KJ, Hallenbeck JM. Inflammation after stroke: is it harmful? Arch Neurol 2001 April;58(4):669-72.

(164) Barone FC, Feuerstein GZ. Inflammatory mediators and stroke: new opportunities for novel therapeutics. J Cereb Blood Flow Metab 1999 August;19(8):819-34.

(165) Schroeter M, Jander S, Stoll G. Non-invasive induction of focal cerebral ischemia in mice by photothrombosis of cortical microvessels: characterization of inflammatory responses. J Neurosci Methods 2002 May 30;117(1):43-9.

(166) Calvet D, Touze E, Oppenheim C, Turc G, Meder JF, Mas JL. DWI lesions and TIA etiology improve the prediction of stroke after TIA. Stroke 2009 January;40(1):187-92.

(167) Sheehan OC, Kyne L, Kelly LA, Hannon N, Marnane M, Merwick A, McCormack PM, Duggan J, Moore A, Moroney J, Daly L, Harris D, Horgan G, Williams EB, Kelly PJ. Population-based study of ABCD2 score, carotid stenosis, and atrial fibrillation for early stroke prediction after transient ischemic attack: the North Dublin TIA study. Stroke 2010 May;41(5):844-50.